2001

A Lumped Parameter Model for the Filling of an Automotive Fuel Tank

Shelagh Fackrell
University of Windsor

A LUMPED PARAMETER MODEL FOR THE FILLING OF AN AUTOMOTIVE FUEL TANK

BY

SHELAGH A. FACKRELL

FACULTY OF GRADUATE STUDIES AND RESEARCH
UNIVERSITY OF WINDSOR
2001

A LUMPED PARAMETER MODEL FOR THE FILLING OF AN AUTOMOTIVE FUEL TANK

By

Shelagh A. Fackrell

A Thesis
Submitted to the Faculty of Graduate Studies and Research
Through Mechanical, Automotive and Materials Engineering
in partial fulfilment of the requirements for
the Degree of Master of Applied Science at the
University of Windsor

Windsor, Ontario, Canada

2001

Approved and recommended for acceptance as a thesis in partial fulfilment of the requirements for the Degree of Master of Applied Science.

Approved by:

Dr. G.W. Rankin, Advisor
Mechanical, Automotive and Materials Engineering Department,
University of Windsor.

Dr. N. Zamani, Internal Department Reader
Mechanical, Automotive and Materials Engineering Department
and Mathematics and Statistics,
University of Windsor.

Dr. P. F. Henshaw, External Department Reader,
Civil and Environmental Engineering Department,
University of Windsor.

Dr. R. Gaspar, Chair of the Committee
Mechanical, Automotive and Materials Engineering Department,
University of Windsor.

ABSTRACT

One of the problems facing automotive fuel tank designers today is that of premature shut-off during the filling process. Premature shut-off occurs when the fuel dispensing nozzle stops before the automotive fuel tank is completely full.

A simplified lumped parameter model has been developed in order to predict the pressures and flow rates associated with fuel tank filling. These are used to predict the occurrence of premature shut-off. The entire fuel tank system, including a closed rectangular tank with a filler tube, rollover valve and a vent tube that connects the filler tube to the tank, was divided into several control volumes and connecting valves. Continuity equations were written for each of the control volumes and energy equations were written for each of the connecting valves. The model includes the effects of the fuel tank system geometry, fuel nozzle dispensing rate, fuel volatility, multi-phase, multi-component flow through the filler tube, air/fuel vapour in the tank dome, vapour generation and choking in the vent tube and the rollover valve.

This mathematical model consists of seven non-linear, integral equations. A commercial numerical solver (Simulink) was used to solve these equations.

The model was used to determine sensitivity of the model output to changes in the values of important model parameters. The parameters listed in order of most to least sensitive are; effective diameter of vent area around the fuel nozzle, fuel dispensing flow rate, fuel volatility, rollover valve diameter, vent tube diameter, void fraction, filler tube diameter and mass transfer coefficient.

The simplified model was also used to generate results to compare with existing experimental results. It was capable of predicting the nature of the shut-off for all of the

corresponding sets of experimental data. Prediction of the magnitudes of the tank dome pressure and the filler tube pressure were in fair agreement with the experimental values.

Dedicated to:

Mom, Dad

and

Linton

ACKNOWLEDGMENTS

I would like to take this opportunity to thank my advisor, Dr. Gary W. Rankin, for his support, knowledge and guidance. His understanding and patience are greatly appreciated.

I would also like to thank Kautex Textron for their support, specifically Luigi Savoni and Maurizio Mastroianni.

Financial support was provided by Kautex Textron and the Natural Sciences and Engineering Research Council of Canada through Collaborative Research Development Grant, number CRD 227033/99.

TABLE OF CONTENTS

List of Figures

Nomenclature

A= empirical constant for fuel

A_i = cross-sectional area of control volume

A_j = cross sectional area of valve

A_N = cross sectional area of the nozzle

A_{vt} = cross sectional area of the vent tube

C_{is} = constant defined in equation 3.2

$C_{is,a}$ = constant for air defined in equation 3.55

$C_{is,v}$ = constant for fuel vapour defined in equation 3.65

c_{mix} = speed of acoustic sound for the air/fuel vapour mixture

D_i = diameter

D_j = diameter

D_N = diameter of the nozzle

D_{vt} = diameter of the vent tube

f_j = friction factor

g = gravitational constant

h_2 = height of the liquid in the filler tube (defined in Figure 3.1)

h_3 = height of the liquid in the tank (defined in Figure 3.1)

h_f = height from bottom of the tank to bottom of the filler tube (defined in Figure 3.1)

h_{ft} = height from bottom of the filler tube to bottom of the nozzle (defined in Figure 3.1)

h_N = height of filler tube (defined in Figure 3.1)

K_{exit} = exit losses

K_{ent} = entrance losses

$K_{f\text{-}h}$= transition loss

k = ratio of specific heats

L_j = effective length

m_i = mass of control volume

$\dot{m}_i$ = mass flow rate

Ma = Mach number

MM = molecular mass

MM_{air} = molecular mass of air

MM_{vap} = molecular mass of gasoline vapour

N_{air} = mole number of air

N_{mix} = mole number of the air/fuel vapour mixture

N_{vap} = mole number of the fuel vapour

P = pressure

P_{STP} = standard atmospheric pressure = 101.3 kPa

$P_{v,4\_eq}$ = equilibrium vapour pressure

P_{foc} = focal pressure

$P_{4,v}$ = partial pressure in the vapour space due to the fuel vapour

$P_{4,a}$ = partial pressure in the vapour space due to air

P_i = pressure in the control volume

P_{atm} = atmospheric pressure

Q_g = volume flow rate of the gas

Q_L = volume flow rate of the liquid

Q_T = volume flow rate of the homogeneous mixture

Q_{1-2} = volume flow rate of homogeneous mixture into CV 2

Q_{2-3} = volume flow rate of homogeneous mixture from the filler tube to tank

R = gas constant

Re = Reynold's number

Ru = universal gas constant = 8314 Pa m^3/kmol K

RVP = Reid Vapour Pressure

r_{v0} = radius of valve 0

r_N = radius of the nozzle

T_{STP} = standard atmospheric temperature = 300 K

T = temperature of the system

T_{foc} = focal temperature

T_{RVP} = temperature at which the RVP was measured

$\overline{V_i}$ = volume

V_i = velocity for control volume

V_j = velocity for valves

V/L = ratio of volume of vapour to volume of liquid

Z_{ltov} = mass fraction of liquid that has turned to vapour

Z_{RVP} = mass fraction for constant V/L ratio

Z_1 = mass fraction of fuel vapour in the filler tube (Control Volume 1)

Z_4 = mass fraction of fuel vapour in the vapour space (Control Volume 4)

Greek Symbols

α = void fraction

ρ_i = density in control volume

ρ_j = density through valve

ρ_{STP} = density at standard temperature and pressure =1.1765 kg/m^3

ρ_L = density of the liquid fuel

ρ_h = density of the homogeneous mixture

γ_L = specific weight of liquid fuel

γ_h =specific weight of homogeneous mixture

Subscripts

i = 1,2,3,4 for the control volume 1,..,4

j = v0, v1, v2, v3, for valve 0,…, 3

CHAPTER 1: INTRODUCTION

1.1. INTRODUCTION/BACKGROUND

One of the major sets of components in an automobile is the fuel system, which is shown schematically in Figure 1.1 [1].

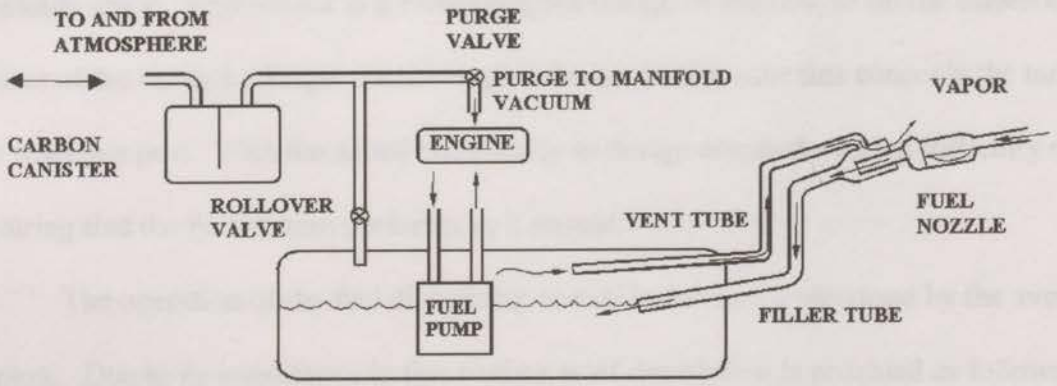

Figure 1.1: Schematic of Fuel Tank System

A typical automobile fuel system consists of five major components: the filler tube, the fuel tank, the vent tube and the rollover valve. The filler tube is the pipe that provides a passage from the fuel nozzle to the fuel tank, which is the storage area for the fuel. Both liquid fuel and an air/fuel vapour mixture are stored in the tank. The vent tube has an orifice that protrudes into the tank through the top of the tank. The vent tube runs along the filler tube and exits near the mouth of the filler tube. The rollover valve is meant to prevent any liquid escaping from the fuel tank in the event of an accident (the car rolls over). The gaseous mixture of fuel vapour and air in the tank can exit through both the vent tube and the rollover valve during the filling process. The carbon canister is another environmental safety device, designed to adsorb the hydrocarbons that are

released from the tank through the rollover valve. When the engine is running, atmospheric fresh air is dawn in through the carbon canister which causes the hydrocarbons to be desorbed.

Due to current consumer safety demands, the fuel tank is required to be outside the crash zone and the competitive market requires that the tank design efficiently use the available space. This results in a more complex design of the tank to fill the underbody spaces of the car and a longer more complex design for the tube that connects the tank to the refueling port. With the added complexity in design comes the added difficulty of ensuring that the fuel system performs as it should.

The operation of the fuel dispensing nozzle is not well understood by the average person. Due to its importance in this study a brief description is provided as follows which refers to the diagram of a fuel dispensing nozzle shown in Figure 1.2 [2].

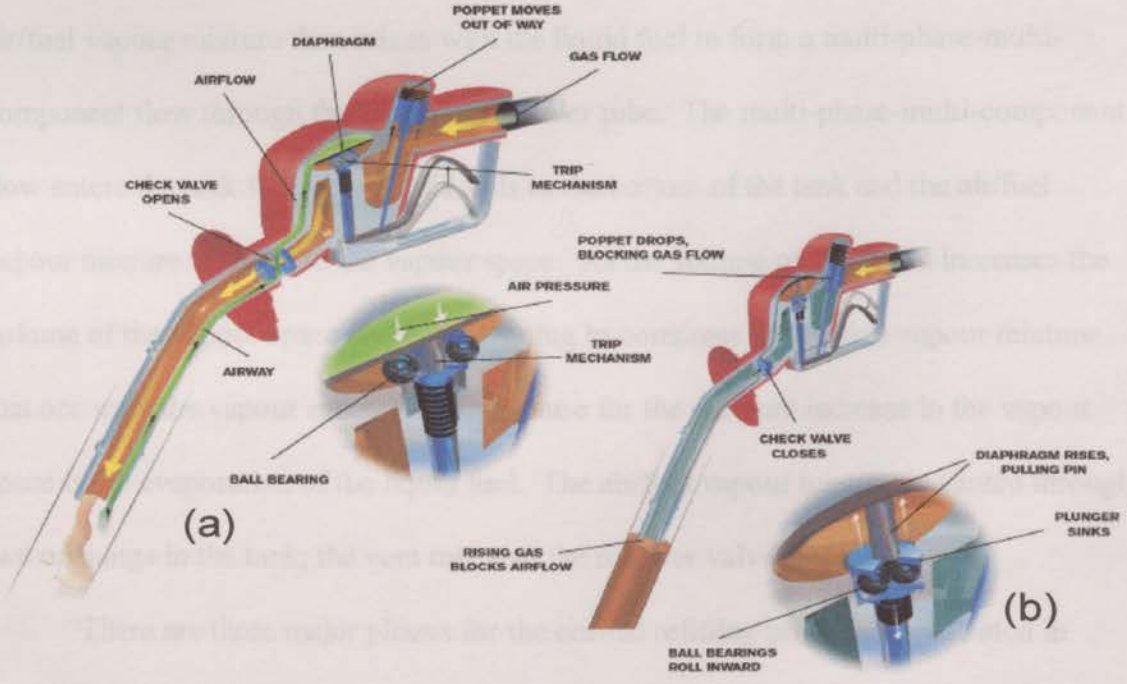

Figure 1.2: Diagram of Fuel Dispensing Nozzle a) On position, b) Off Position [2]

When the dispensing nozzle handle is raised, as indicated in Figure 1.2a, the fuel passes through a check valve in the nozzle, which creates a low-pressure area. This low-pressure area then causes air and fuel vapour to be sucked in through a small hole at the end of the nozzle. When the level of the liquid in the filler tube is high enough to cover the air hole, the pressure on the diaphragm decreases allowing the diaphragm to rise. This diaphragm is attached to a pin, which releases the handle to its original position, causing the flow of fuel to stop as indicated in Figure 1.2b.

The liquid fuel that is dispensed from the filling station nozzle into the filler tube flows into the tank. In some vehicles there is a back-check valve between the filler tube and the tank which prevents any of the fuel from reentering the filler tube after entering the tank. The air that is drawn in by the nozzle (5% to 15% air/fuel by volume [3]) along with atmospheric air, mixes with the fuel vapour to create a multi-component gas. The air/fuel vapour mixture then mixes with the liquid fuel to form a multi-phase-multi-component flow through the length of the filler tube. The multi-phase-multi-component flow enters the tank where the liquid falls to the bottom of the tank and the air/fuel vapour mixture is added to the vapour space. As the volume of the liquid increases the volume of the vapour space decreases tending to compress the air/fuel vapour mixture that occupies the vapour space. Another cause for the pressure increase in the vapour space is the evaporation of the liquid fuel. The air/fuel vapour mixture is vented through two openings in the tank; the vent tube and the rollover valve.

There are three major phases for the normal refilling process, as indicated in Figure 1.3 which is a graph of the tank gauge pressure versus time.

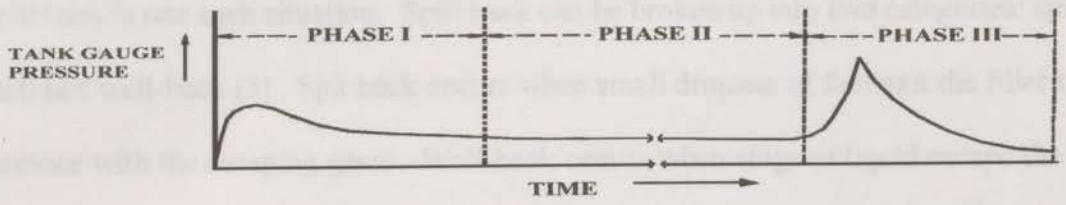

Figure 1.3: Pressure-Time Relationship Depicting Different Phases During Normal Tank Filling Process.

During the first phase of the filling process the sudden decrease in the vapour space combined with the additional mass entering the vapour space causes the gases with in the vapour space to compress. The compression causes the vapour space pressure to increase. There is some evidence [1] that significant compression waves occur within the vent tube and rollover valve tubing. This decreases the flow of gas through these tubes. The pressure in the vapour space lowers as the exiting gas flow rate increases. During the second phase of a normal refilling process the tank gauge pressure remains almost constant. This phase constitutes most of the refilling process. During the third phase of the refilling process the liquid in the tank covers the vent tube port. This decreases the venting area to only the rollover valve area. This sudden decrease in venting area causes a sudden increase in the vapour space pressure. Due to the high back pressure, the liquid in the filler tube backs up and the liquid in the vent tube rises. Either situation will eventually lead to the sensing port in the fuel nozzle being covered thus stopping the fuel flow. With no more flow into the system the rollover valve quickly vents the excess air, reducing the pressure in the vapour space until it reaches equilibrium with the surroundings.

Certain situations occur where the filling process is considered to be unsuccessful. Spill back is one such situation. Spill back can be broken up into two categories: spit-back and well-back [3]. Spit back occurs when small droplets of fuel exit the filler tube entrance with the escaping gases. Well-back occurs when slugs of liquid escape the filler tube entrance. Another unsuccessful filling situation is premature shut-off. In this case the fuel nozzle shuts off before the tank is full.

Possible causes for premature shut-off are now considered. In the first case, a misalignment of the filler nozzle with the filler tube would cause the liquid fuel to bounce of the wall of the filler tube back towards the nozzle. If the liquid covers up the fuel dispensing nozzle sensing port the nozzle shuts off. In the second case, as liquid fuel enters the tank it causes a wave behaviour on the surface of the liquid in the tank which bounces off the far side of the tank. Improper positioning of the vent tube orifice could allow a slug of liquid to enter the vent tube. As the pressure in the vapour space rises, this slug of liquid could be pushed along the vent tube to the opening of the filler tube, covering the sensor port in the fuel nozzle thus shutting off the fuel flow. In the third case, high back pressure in the vapour space of the tank can cause the liquid in the filler tube to back up and cover the sensor port of the nozzle thus shutting off the fuel flow. Some filler tubes are equipped with a valve that prevents the back flow of fuel from the tank. A fourth cause for premature shut-off is too much restriction by this valve which causes the liquid to fill the filler tube before it fills the tank. Once the liquid in the filler tube reaches the nozzle it will cover the sensor port and shut the flow off.

The tank vapour space pressure depends upon the amount of enclosed mass. There are three factors that contribute to the amount of mass of air and fuel vapour within

the vapour space; entrained air/fuel vapour, air dissolved in the inflow of fuel and evaporation of the fuel into fuel vapours. The air/fuel vapour mixture is entrained in the liquid flow at the mouth of the filler nozzle. This is where the vent tube from the vapour space exits. It is the entrained air/vapour mixture that Stoneman [3] predicts should be between 5% and 15% of the total flow into the filler pipe. Once the multi-phase-multi-component flow reaches the tank, the air/fuel vapour no longer remains entrained in the liquid, since it can enter the vapour space. During the flow through the filler pipe air may dissolve in the liquid fuel. Once the fluid reaches the tank the dissolved air will be added to the vapour space. The effect of dissolved air, however, is expected to be small and therefore not considered in this work. The third factor that will contribute mass to the vapour space is the evaporation of the liquid gasoline. This evaporation is very dependent upon the liquid gas interface within the tank and filler tube.

1.2 PURPOSE OF THE STUDY

The purpose of this study is to develop a numerical tool that can be used during the design phase to predict the fuel filling performance of automotive fuel systems. Specifically, the objective is to develop a simplified lumped parameter model that describes the process of refueling an automotive fuel tank in order to predict premature shut-off. The results of the model will also be compared with available experimental data. The sensitivity of the results to changes in the problem parameters will also be investigated

CHAPTER 2 - LITERATURE REVIEW

There has been previous research conducted on the fuel tank system and its associated components and this chapter will review the relevant articles. The chapter begins with articles that are related directly to the automotive fuel tank filling process and the associated problems. Papers which are concerned with the automotive fuel tanks in general but are not specific to the refueling process are then considered followed by papers that deal with the tank filling process in general. Finally, papers which deal with particular phenomena that are important to the refueling process are discussed. This includes methods of modeling two-phase flow, compressible flow effects in the tubes, and methods for predicting vapour generation.

The literature, which describes the general process of the filling of a fuel tank has already been referred to in the introduction and will not be repeated here.

2.1 AUTOMOTIVE FUEL TANK FILLING

There are two different approaches to determining the complex dynamics involved in automotive fuel tank filling; experimental, and computational. Very little experimental data exists for the filling of tanks with fuel.

The thesis by Mastroianni [4] contains a great deal of useful experimental data. Mastroianni conducted a set of experiments that indicated how certain parameters affect premature shut-off. For these experiments, a simple rectangular tank was fitted with a standard filler pipe. The simplified tank had a vent tube and a rollover valve. Mastroianni changed the volume flow rate of the fuel, the RVP of the fuel and the diameter of the vent tube. The tank dome pressure and filler tube pressure were

measured using pressure transducers. This data was presented in a dimensionless form. The most important aspect of this data is that it is used as a basis for comparison with the simplified lumped parameter model presented in this thesis.

Numerical approaches to fuel tank filling prediction involve the use of Computational Fluid Dynamic (CFD) methods; although no complete CFD solution of the entire fuel tank system exists.

The paper by Banerjee et al. [5] made use of a commercial Computational Fluid Dynamics package (Fluent), in order to gain a better understanding of such phenomena as well-back and premature shut-off. They found that, in the case of the fuel tank filling, it is impractical to model the entire system in a single computational domain. There are varying time and geometric scales. Their model, therefore, includes only the filling nozzle inserted into the filler tube and the detailed filler tube geometry which opens into a large space. Turbulence and multi-phase flow models were used. However, they did not consider mass transfer in the multi-phase model and focused on the flow in the filler pipe only.

The paper by Sinha et al. [1] also used CFD in order to describe the flow during refueling. Due to the difficulty of conducting a CFD simulation of the entire system Sinha et al. broke the system up into several carefully designed key sub-processes. These sub-processes were then studied separately and various conclusions derived. The sub-processes considered were flow through the vent pipe, multi-phase flow, choking at the vent tube entrance due to the low acoustic speed in multi-phase media, and frictional effects along the vent tube.

The article by Stoneman [3] used a commercial computational fluid dynamics package to simulate the filler pipe for the purpose of predicting the occurrence of spill back.

Rodriguez et al.[6] presented results of one and three dimensional models in order to predict vapour generation due to diurnal, hot soak, running losses and refueling losses. They assumed the mass transfer to be diffusive for the one dimensional model. They used a commercial CFD package (PHOENIX 1.6 version).

2.2 AUTOMOTIVE FUEL TANKS

Several papers have been written concerning automotive fuel tanks that were not explicitly about the filling process. They include, however, certain phenomenon involved in the fuel tank filling process. One of these phenomenon is vapour generation due to the evaporation of liquid fuel. There is a considerable amount of information relating to air pollution caused by evaporative fuel emissions. Several studies have been reported which attempt to accurately predict the amount of vapour generated in a fuel tank under a variety of conditions.

The model developed by Lavoie et al. [7] predicts the amount of evaporative emissions. The model includes the fuel tank, fuel pump, filler tube, liquid supply and return lines, fuel rail, vent valves, vent line, carbon canister and purge lines. The model took into consideration the relationship between vapour generation and heat transfer from the heat generated under the hood and under the car body. The relationship between vapour generation and vapour pressure changes were also considered. The main cause of vapour generation throughout the normal driving cycle is the heat transferred from the

surrounding systems to the liquid fuel. Since there is only a limited time for evaporation, the fuel vapour pressure is not usually equal to the equilibrium vapour pressure.

Lockhart [8] presented three models for vapour generation from a tank in general. They included a model based on theoretical principles, a semi empirical model and a model that was entirely empirical. The theoretical model is based on thermodynamic relationships and requires knowledge of the properties of the different pure substances of which gasoline is composed. The empirical model is only applicable to a limited range of fuel types and conditions. The models were applied to vapour emitted from a fuel tank and then compared to experimental data collected by Lockhart. The experiments consisted of trapping the hydrocarbons that escaped the fuel tank and measuring the amount collected. The objective was to determine the vapour generated within tanks for the purposes of designing On-board Refueling Vapour Recovery (RVR) devices. These are environmental safety features for the purpose of reducing the amount of hydrocarbons entering the atmosphere during the refueling process.

Kunimitsu et al. [9] provide methods of predicting vapour generation over a wide range of fuel temperatures (including extremely high temperatures). The results are then compared with available experimental tests on vehicles operating at higher temperatures over longer drive periods. This model can be used for predicting evaporative emissions and running losses. The driving force of this model of vapour generation is the change in temperature of the fuel.

Parra et al. [10] used a three dimensional commercial CFD package (PHOENICS version 2.0) to model the evaporative emissions from a fuel tank and then compared the results with simple experiments. The article describes the method used to model the two

phase flow and includes a model for mass transfer, free surface flows (the two phases at the interface were treated as a single phase), and heat transfer at the free surface. Their experimental work includes limited data on the amount of gasoline mass evaporated.

2.3 TANK FILLING

Several papers have been published which deal with the general problem of tank filling [11,12]. Although the liquid used is not gasoline, these papers include information that can be informative when dealing with the case of an automotive fuel tank.

Vaughan and Schmidt [11] developed a computational model that was able to predict the pressure history in a no-vent filling process. The entire system was divided into seven key sub-systems and the continuity and energy equations written for each. The model included interfacial mass transfer and was concerned with cryogenic liquids which have unique thermodynamic properties.

Whalley [12] conducted a series of experiments to examine the occurrence of flooding in connection with the emptying and filling times of bottles. Flooding is the term used to describe the limit of counter-current flow (where the gas phase is flowing upwards and the liquid phase is flowing down) which occurs when the upward flowing gas phase prevents the liquid phase from flowing down. In his experiments he explored the link between flooding and slugging by examining a number of parameters that might affect the flow of multi-phase fluids. Whalley performed a number of other experiments on the filling time of bottles including the effects of the depth below the surface of the liquid, and the geometry and positioning of the neck of the bottle. Various types and

sizes of bottles were immersed in water and the time for each bottle to fill was measured. The filling time is much more dependant on these parameters than the emptying time.

2.4 MULTI-PHASE, MULTI-COMPONENT

One of the difficulties in modeling the refueling process is accurately describing the multi-phase, multi-component flow through the filler tube. There is a great deal of literature which considers multi-phase, multi-component flow in various situations. The book by Whalley [13] contains a chapter on homogeneous mixtures and also a chapter on acoustic speed. The acoustic speed in a multi-phase medium was found to be of great importance to fuel tank filling by Sinha et al [1]. By having a large number of very small droplets in a gaseous medium the speed of sound decreases to values much lower than that in each of the constituents, creating a situation where choking may occur in the vent tube and rollover valve.

2.5 VAPOUR GENERATION

The articles that deal with vapour generation in a fuel tank have been mentioned above, however there have been several articles that deal with vapour generation in general terms [14,15,16].

Reddy [14] developed a correlation relating the amount of vapour generated and the volatility of the fuel. Separate relationships for diurnal and hot soak emissions were developed then combined to create the correlation. The results were then compared with available experimental data.

Bardon and Rao [15] developed a procedure to calculate the instantaneous properties (such as vapour pressure, molecular weight and enthalpy) of vaporizing fuel. This required distillation curve information, the specific gravity of the fuel and knowledge of the species properties of the fuel.

Lavoie and Smith [16] developed a model which linked the pressure within the fuel tank dome, the temperature and the mass of liquid that evaporated into vapour. They performed experiments to determine the vapour pressure and equilibrium distillation information used in their model. This model can be used to determine the vapour generation due to temperature changes of the fuel over longer periods of time (i.e. a long drive), flammability limits, pressure rise in the tank as well as evaporative vapour generation.

CHAPTER 3: MODEL OF FUEL TANK FILLING

The mathematical model developed in this section is based on a simplified fuel tank geometry as indicated in Figure 3.1. When the fuel nozzle is inserted into the filler tube there is only a small opening at the filler tube entrance to allow air to flow from the atmosphere to the filler tube and air/fuel vapour to flow from the filler tube to the atmosphere. The liquid is assumed to flow in a column down the centre of the filler tube thus creating an annular space around it (Control Volume 1). This region will also increase in pressure since it is connected to the tank. The flow of air/fuel vapour is assumed to mix with the liquid gasoline exiting the fuel nozzle and begins to collect in the filler tube as the pressure in the tank vapour space increases. This homogeneous mixture of liquid gasoline and air/fuel vapour forms Control Volume 2. The liquid level sensing port is assumed to be located at the bottom of flow nozzle, therefore, when the height of this column reaches the nozzle the flow of liquid from it stops. A valve (Valve 1) is used to account for the frictional effects of the walls of the filler tube and any minor energy losses that occur in the fluid as it flows from the filler tube into the tank. The tank itself contains liquid and air/fuel vapour, which have separated with the liquid at the bottom (Control Volume 3) and the air/fuel vapour mixture at the top (Control Volume 4). The liquid level of the tank will steadily increase, decreasing the amount of space available for the air/fuel vapour mixture. As the pressure in the vapour space increases the gases will exit through the vent tube and the rollover valve. The vent tube is connected to the filler tube and the rollover valve is vented to the atmosphere. Valves are used to account for frictional effects and minor losses in the vent tube (Valve 2) and the rollover valve (Valve 3).

In the following pages each control volume and valve is considered individually and the model equations developed.

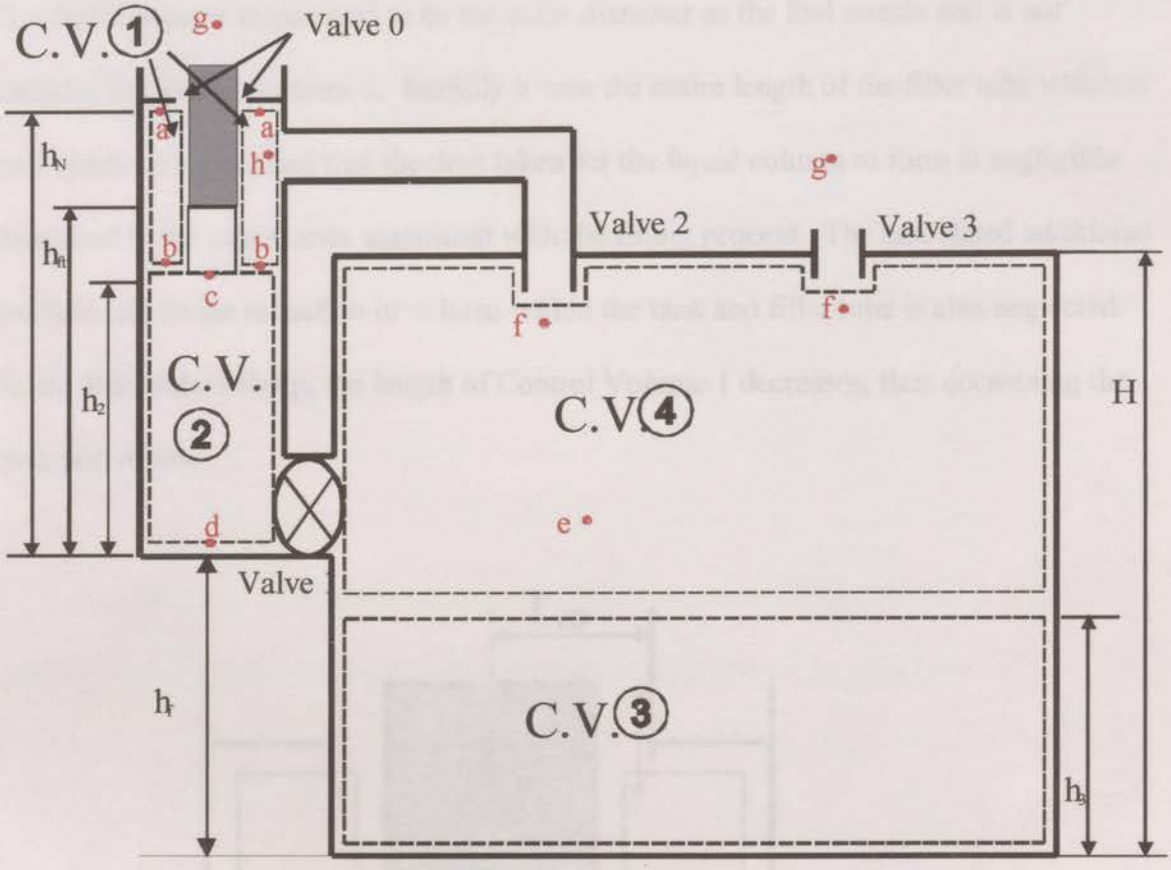

Figure 3.1: Schematic Diagram of the Simple Fuel Tank System Showing Various Control Volumes

3.1 CONTROL VOLUME 1

Control Volume 1 represents the annular space in the filler tube (see Figure 3.2). The liquid column is assumed to be the same diameter as the fuel nozzle and is not included in Control Volume 1. Initially it runs the entire length of the filler tube which is consistent with assuming that the time taken for the liquid column to form is negligible compared to the other times associated with the filling process. The associated additional pressure due to the reduction in volume within the tank and filler tube is also neglected. As the filler tube fills up, the length of Control Volume 1 decreases, thus decreasing the enclosed volume.

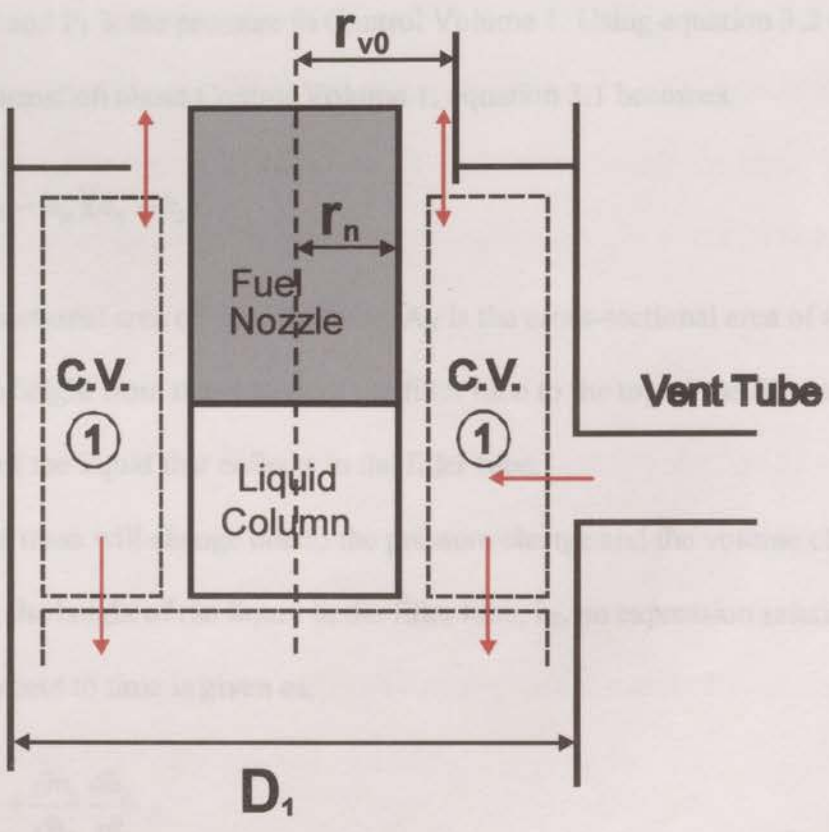

Figure 3.2: Schematic Diagram of Control Volume 1.

An expression for the mass of air/fuel vapour that is contained in Control Volume 1 is,

$$m_1 = \rho_1 \overline{V}_1 , \tag{3.1}$$

where m_1 is the mass of air/fuel vapour, ρ_1 is the density and $\overline{V}_1$ is the volume of Control Volume 1.

The gases in Control Volume 1 are assumed to be compressible and the temperature for the system is assumed to remain constant, therefore from the perfect gas law an expression for the density can be written as,

$$\rho_1 = \frac{P_1}{C_{is}} = \frac{P_1}{RT_1} \tag{3.2}$$

C_{is} is a constant and P_1 is the pressure in Control Volume 1. Using equation 3.2 and geometrical information about Control Volume 1, equation 3.1 becomes,

$$m_1 = \left(\frac{P_1}{C_{is}}\right)(A_2 - A_N)(h_N - h_2). \tag{3.3}$$

A_2 is the cross-sectional area of the filler tube, A_N is the cross-sectional area of the fuel nozzle, h_N is the height from the bottom of the filler tube to the top of the filler tube and h_2 is the height of the liquid that collects in the filler tube.

Since the mass will change due to the pressure change and the volume change due to the change in the height of the liquid in the filler tube, h_2, an expression relating the changes with respect to time is given as,

$$\frac{dm_1}{dt} = \frac{\partial m_1}{\partial P_1}\frac{dP_1}{dt} + \frac{\partial m_1}{\partial h_2}\frac{dh_2}{dt} . \tag{3.4}$$

Taking the partial differential of m_1 with respect to P_1 and h_2 and substituting into equation 3.4 yields,

$$\frac{dm_1}{dt} = \frac{(A_2 - A_N)(h_N - h_2)}{C_{is}} \frac{dP_1}{dt} - (A_2 - A_N)\left(\frac{P_1}{C_{is}}\right)\frac{dh_2}{dt} \tag{3.5}$$

Applying the conservation of mass principle to Control Volume 1 yields,

$$\frac{dm_1}{dt} = \dot{m}_{in,1} - \dot{m}_{out,1} \quad . \tag{3.6}$$

Mass can enter or leave Control Volume 1 through the vent tube and the small opening around the nozzle. Since the pressure in the tank (Control Volume 4) is assumed to always be greater than the pressure in the filler tube (Control Volume1) the flow of gases through the vent tube will only be from the tank to the filler tube. The density of the gas flowing through the vent tube is, therefore, the density of the fluid in the tank. The flow through the small opening around the filler nozzle can be either in or out. The direction is determined by knowing the difference in pressure between the atmosphere and that in the filler tube. If the pressure in the filler tube is greater than atmospheric pressure then the flow of gas will be from the filler tube to the atmosphere hence the density of the gases flowing through valve 0, ρ_{v0},will be that of the filler tube ($\rho_{v0}=\rho_1$). If the pressure in the filler tube is lower than atmospheric, the flow will be from the atmosphere to the filler tube and the density through valve 0 will be that of air at standard conditions ($\rho_{v0}=\rho_a$). The equation for the net inflow rate of mass is given by,

$$\dot{m}_{in,1} = [\rho_{v0} A_{v0} V_{v0}] + [\rho_4 A_{vt} V_{vt}] \quad . \tag{3.7}$$

A_{v0} is the cross-sectional area of the space around the nozzle at the opening of the filler tube which is assumed to be constant, V_{v0} is the velocity of the fluid through A_{v0}, ρ_4 is the density of the fluid flowing through the vent tube from the tank which is assumed to go only from the tank to the filler tube, A_{vt} is the cross-sectional area of the tube connecting the tank to the filler tube which is assumed to be constant and V_{vt} is the velocity of the fluid through the vent tube that is attached to the filler tube.

Air/fuel vapour mixture from Control Volume 1 is mixed with the liquid fuel exiting the fuel nozzle due to the action of the fuel nozzle shut-off sensor (see Section 1.1). In the current model, the assumption is made that the flow is multi-phase when exiting Control Volume 1 and entering Control Volume 2.

One of the simpler models for multi-component, multi-phase flow is the homogeneous model. This model assumes that the two phases are dispersed uniformly and the two phases travel at the same velocity. The homogeneous density and viscosity [17] are given by,

$$\rho_h = \rho_g \alpha + \rho_L (1-\alpha) \quad \text{and} \tag{3.8}$$

$$\mu_h = \mu_g \alpha + \mu_L (1-\alpha)(1+2.5\alpha) \tag{3.9}$$

The void fraction is the fraction of the multi-phase flow that is gas. Using the homogenous assumptions an expression relating the void fraction and the volume flow rates of both the liquid and gaseous phases can be developed.

$$\alpha = \frac{Q_g}{Q_T} = \frac{Q_g}{Q_g + Q_L} \tag{3.10}$$

where Q_g is the volume flow rate of air/fuel vapour and Q_T is the total volume flow rate of both the liquid and the gas.

The flow rate of liquid exiting the fuel nozzle, Q_{inL}, is assumed to be given in the current problem. It was also assumed that the void fraction remains constant throughout the filler tube and therefore the volume flow rate for the air/fuel vapour phase is,

$$Q_g = \frac{\alpha}{1-\alpha} Q_L \quad . \tag{3.11}$$

The flow rate of the multi-phase mixture from Control Volume 1 to Control Volume 2 can be expressed in terms of the liquid volume flow rate as,

$$Q_{1-2} = \frac{Q_L}{1-\alpha} \quad . \tag{3.12}$$

The mass flow rate for the air/fuel vapour is given by,

$$\dot{m}_{out,1} = \rho_1 \frac{\alpha}{1-\alpha} Q_L . \tag{3.13}$$

Substituting equation 3.5, equation 3.7 and equation 3.13 into equation 3.6, yields,

$$\frac{(A_2 - A_N)(h_N - h_2)}{C_{is}} \frac{dP_1}{dt} - \left(\frac{P_1}{C_{is}}\right)(A_1 - A_N)\frac{dh_2}{dt}$$
$$= (\rho_{v0} A_{v0} V_{v0}) + (\rho_4 A_{vt} V_{vt}) - \rho_1 \frac{\alpha}{1-\alpha} Q_L \quad . \tag{3.14}$$

Integrating and rearranging equation 3.14, gives

$$P_1 = \int \frac{C_{is}}{(A_2 - A_N)(h_N - h_2)} \left\{ \left[(A_2 - A_N)\rho_1 \frac{dh_2}{dt} \right] + [\rho_{v0} A_{v0} V_{v0}] + [\rho_4 A_{vt} V_{vt}] - \left[\rho_1 \frac{\alpha}{1-\alpha} Q_L \right] \right\} dt \quad . \tag{3.15}$$

where V_{v0} is discussed in the following section and V_{vt} is discussed later.

3.1.1 VELOCITY THROUGH VALVE 0

The modified Bernoulli's equation between point g and a (see Figure 3.1) is given by,

$$\frac{P_g}{\gamma_g}+z_g+\frac{V_g^2}{2g}=\frac{P_a}{\gamma_a}+z_a+\frac{V_a^2}{2g}+h_{L_{atm-1}}, \tag{3.16}$$

where,

$$P_g = P_{atm}, \tag{3.17}$$

$$P_a = P_1, \tag{3.18}$$

$$z_g \approx z_a, \tag{3.19}$$

$$V_g = V_a \approx 0, \tag{3.20}$$

$$h_{L_{atm-1}} = \frac{f_{v0}L_{v0}}{D_{v0}}\frac{V_{v0}^2}{2g}+K_{exit}+K_{ent}\ . \tag{3.21}$$

Substituting equation 3.17-3.21 into equation 3.16 and rearranging,

$$V_{v0}=\sqrt{\left[\frac{(P_{atm}-P_1)}{\rho_{P1}}\right]\left[\frac{2}{\left(\frac{f_{v0}L_{v0}}{D_{v0}}+K_{ent}+K_{exit}\right)}\right]}\ . \tag{3.22}$$

Where f_{v0} is the friction factor for valve 0 (see section Valve 1), L_{v0} is the effective length of valve 0 and D_{v0} is the diameter of valve 0.

3.2 CONTROL VOLUME 2

As the pressure in the tank rises, the flow of fluid out of the filler tube slows while the flow into the filler tube remains constant. This causes the fluid to collect in the filler tube. This collection of fluid in the filler tube is contained in Control Volume 2.

Applying the conservation of mass to Control Volume 2,

$$\frac{dm_2}{dt} = \frac{d}{dt}\left(\int_{C.V.} \rho_2 d\overline{V}_2\right) = \rho_{in,2} A_{in,2} V_{in,2} - \rho_{out,2} A_{out,2} V_{out,2} \,. \tag{3.23}$$

Since $\overline{V}_2 = A_2 h_2$,

$$\frac{d}{dt}(\rho_2 A_2 h_2) = \rho_{in,2} A_{in,2} V_{in,2} - \rho_{out,2} A_{out,2} V_{out,2} \,. \tag{3.24}$$

The homogeneous mixture in the filler tube is assumed to be incompressible which means that the air/fuel vapour in the filler tube is also assumed to be incompressible. The density, therefore, remains constant $(\rho_2 = \rho_{in,2} = \rho_{out,2})$ and A_2 is also constant. The conservation of mass then becomes,

$$A_2 \frac{dh_2}{dt} = A_{in,2} V_{in,2} - A_{out,2} V_{out,2} \,. \tag{3.25}$$

Since $Q_2 = A_2 V_2$,

$$A_2 \frac{dh_2}{dt} = Q_{in,2} - Q_{out,2} \,, \tag{3.26}$$

where

$$Q_{in,2} = Q_{1\text{-}2} = Q_L + Q_g = \frac{1}{1-\alpha} Q_L \,, \tag{3.27}$$

and

$$Q_{out,2} = Q_{2\text{-}3} \,. \tag{3.28}$$

Integrating and rearranging equation 3.25, yields

$$h_2 = \frac{1}{A_2} \int (Q_{1\text{-}2} - Q_{2\text{-}3}) dt \,. \tag{3.29}$$

3.2.1 VALVE 1

The losses for the flow in the filler tube are accounted for in Valve 1.

The modified Bernoulli's equation between points d and e (see Figure 3.1) is given by,

$$\frac{P_d}{\gamma_d}+z_d+\frac{V_d^2}{2g}=\frac{P_e}{\gamma_e}+z_e+\frac{V_e^2}{2g}+h_{l_{2-3}} \quad . \tag{3.30}$$

It is also assumed that hydrostatic conditions apply at point d, the difference in height between point d and e is negligible, the velocity at point e is approximately zero, and the fluid remains a homogeneous mixture until it reaches point e, which results in the following equations,

$$P_d = P_1+\gamma_h h_2 \,, \tag{3.31}$$

$$z_d \approx z_e \,, \tag{3.32}$$

$$V_e \approx 0 \,, \tag{3.33}$$

$$V_d = \frac{Q_{2-3}}{A_2} \,, \tag{3.34}$$

$$h_{l_{2-3}} = K\frac{V_{2-3}^2}{2g}=\left(\frac{f_{v1}L_{v1}}{D_{v1}}+K_{exit}+K_{ent}\right)\left(\frac{Q_{2-3}^2}{2gA_2^2}\right). \tag{3.35}$$

γ_h is the specific weight of the homogeneous mixture, g is the gravitational constant, V_{2-3} is the velocity of the flow from the filler tube to the tank, f_{v1} is the friction factor associated with valve 1, L_{v1} is the effective length of the valve which is assumed to be equal to the length of the filler tube, D_{v1} is the diameter of the filler tube, K_{exit} is the exit loss for valve 1 and K_{ent} is the entrance loss for valve 1.

The friction factor for laminar flow (Re<2300) is taken to be

$$f_{v1}=\frac{64}{\mathrm{Re}_{v1}} \tag{3.36}$$

The Blasius equation was used to determine the friction factor for the case of turbulent flow (Re>2300), and is given by

$$f_{v1} = \frac{0.3146}{\mathrm{Re}_{v1}^{1/4}}, \tag{3.37}$$

where the Reynold's number for pipe flow is defined as,

$$\mathrm{Re}_{v1} = \frac{\rho_{v1} V_{v1} D_{v1}}{\mu_{v1}}. \tag{3.38}$$

If the level of the liquid in the tank, h_3, is below the point where the filler tube joins the tank, h_f, then

$$P_e = P_4, \tag{3.39}$$

where P_4 is the pressure in the tank, otherwise hydrostatic conditions apply, as given by

$$P_e = P_4 + \gamma_L (h_3 - h_f). \tag{3.40}$$

Substituting equations 3.31-3.35 and equation 3.39 into equation 3.30 for the case where the liquid height in the tank is lower than the entrance to the filler pipe, the modified Bernoulli equation becomes

$$\frac{P_1 + \gamma_h h_2}{\gamma_h} + \frac{Q_{2-3}^2}{2gA_2^2} = \frac{P_4}{\gamma_h} + \left(\frac{f_{v1} L_{v1}}{D_{v1}} + K_{exit} + K_{ent} \right) \frac{Q_{2-3}^2}{2gA_2^2}. \tag{3.41}$$

Rearranging equation 3.41, yields,

$$Q_{2-3} = \sqrt{\left[\frac{P_1 - P_4}{\gamma_h} + h_2 \right] \left[\frac{1}{\left(\frac{f_{v1} L_{v1}}{D_{v1}} + K_{exit} + K_{ent} \right) \frac{1}{2gA_2^2} - \frac{1}{2gA_2^2}} \right]}. \tag{3.42}$$

Substituting equations 3.31-3.35 and equation 3.40 into equation 3.30 for the liquid height of the tank is greater than the entrance to the filler pipe yields,

$$\frac{P_1+\gamma_h h_2}{\gamma_h}+\frac{Q_{2-3}^2}{2gA_2^2}=\frac{P_4+\gamma_L\left(h_3-h_f\right)}{\gamma_h}+\left(\frac{f_1L_1}{D_1}+K_{exit}+K_{ent}\right)\frac{Q_{2-3}^2}{2gA_2^2} \quad , \tag{3.43}$$

and after rearranging yields,

$$Q_{2-3}=\sqrt{\left[\frac{P_1-P_4\gamma_L\left(h_3-h_f\right)}{\gamma_h}+h_2\right]\left[\frac{1}{\left(\frac{f_{v1}L_{v1}}{D_{v1}}+K_{exit}+K_{ent}\right)\frac{1}{2gA_2^2}-\frac{1}{2gA_2^2}}\right]} \quad . \tag{3.44}$$

3.3 CONTROL VOLUME 3

After the fluid reaches point e it is assumed that the liquid and gases separate with liquid falling to the bottom of the tank and the gases rising to the top of the tank. Control Volume 3 is the collection of the liquid fuel in the tank. It is assumed that initially there is a small amount of fuel in the tank.

Applying the conservation of mass to Control Volume 3 yields,

$$\frac{dm_3}{dt}=\frac{d}{dt}\left(\int_{C.V.}\rho_3 d\overline{V}_3\right)=\rho_{in,3}A_{in,3}V_{in,3}-\rho_{out,3}A_{out,3}V_{out,3} \quad . \tag{3.45}$$

Since $\overline{V}_3 = A_3h_3$ equation 3.45 becomes,

$$\frac{d}{dt}\left(\rho_3A_3h_3\right)=\rho_{in,3}A_{in,3}V_{in,3}-\rho_{out,3}A_{out,3}V_{out,3} \quad . \tag{3.46}$$

where ρ_3 is the density of the liquid fuel, A_3 is the cross-sectional area of the tank and h_3 is the height of the liquid in the tank.

Since A_3 is assumed to be constant and $\dot{m}_3=\rho_3A_3V_3$,

$$\rho_3A_3\frac{dh_3}{dt}=\rho_{in,3}A_{in,3}V_{in,3}-\dot{m}_{out,3} \tag{3.47}$$

Rearranging equation 3.47 gives,

$$A_3 \frac{dh_3}{dt} = A_{in,3} V_{in,3} - \frac{\dot{m}_{out,3}}{\rho_3} \quad . \tag{3.48}$$

From the article by Lavoie et al. [7] the mass flow rate of the fuel that is evaporating, hence leaving the control volume, can be expressed as,

$$\dot{m}_{out,3} = h_d \frac{MM_{vap}}{RuT} A_{liq} \left(P_{4,v\_eq} - P_{4,v} \right) \quad . \tag{3.49}$$

In the above equation h_d is the mass transfer coefficient, MM_{vap} is the molecular weight of the vapour, Ru is the universal gas constant, T is the constant temperature of the fluid, A_{liq} is the surface area of the liquid interface, P_{4,v_eq} is the equilibrium vapour pressure and $P_{4,v}$ is the vapour partial pressure in the tank.

Substituting equation 3.49 into equation 3.48 and after integrating and rearranging gives,

$$h_3 = \frac{1}{A_3} \int \left\{ Q_{2-3} - h_d \frac{MM_{vap}}{RuT} A_{liq} \left(P_{4,v\_eq} - P_{4,v} \right) \right\} dt \quad . \tag{3.50}$$

3.4 CONTROL VOLUME 4

Control Volume 4 represents the air and fuel vapour mixture that is collected in the tank.

Applying the Law of Partial Pressures to Control Volume 4 for air and fuel vapour,

$$P_4 = P_{4,v} + P_{4,a} \quad . \tag{3.51}$$

There are two sources that will add mass to the tank vapour space; the air/fuel vapour that enters through the filler tube, $\dot{m}_{in,a}$, and the fuel vapour that evaporates from the liquid fuel, $\dot{m}_{in,v}$. There are two exit ports for the gases; the vent tube which is connected to the filler tube and the rollover valve. As air and fuel vapour collect in the tank, the tank pressure rises, causing the liquid in the filler tube to backup.

Applying the conservation of mass to Control Volume 4 for air and fuel vapour separately yields,

$$\frac{dm_{4,a}}{dt} = \frac{d}{dt}\left(\int_{C.V.} \rho_{4,a} d\overline{V}_4\right) = \dot{m}_{in,a} - \dot{m}_{out,a}, \tag{3.52}$$

and

$$\frac{dm_{4,v}}{dt} = \frac{d}{dt}\left(\int_{C.V.} \rho_{4,v} d\overline{V}_4\right) = \dot{m}_{in,v} - \dot{m}_{out,v}. \tag{3.53}$$

Each of the terms in the above equations is now considered separately, beginning with the equation for air in the vapour space.

An expression for the mass of air mixture that is contained in Control Volume 4 is given by,

$$m_{4,a} = \rho_{4,a}\overline{V}_4, \tag{3.54}$$

where $m_{4,a}$ is the mass of air in the tank vapour space, $\rho_{4,a}$ is the density of the air in Control Volume 4 and $\overline{V}_4$ is the volume of the vapour space.

Assuming that the cross-sectional area of the tank is constant and the air in the vapour space is compressible,

$$m_{4,a} = \left(\frac{P_{4,a}}{C_{is,a}}\right) A_4 (H - h_3). \tag{3.55}$$

where $P_{4,a}$ is the partial pressure of the air in the vapour space, $C_{is,a}$ is a constant, A_4 is the cross-sectional area of the tank and H is the height of the tank.

Since the mass will change due to the pressure change and the volume change due to the change in the height of the liquid in the tank, it can be stated that,

$$\frac{dm_{4,a}}{dt} = \frac{\partial m_{4,a}}{\partial P_{4,a}} \frac{dP_{4,a}}{dt} + \frac{\partial m_{4,a}}{\partial h_3} \frac{dh_3}{dt} . \tag{3.56}$$

Taking the partial differential of equation 3.55 with respect to the height of the liquid in the tank and that with respect to the pressure in the tank, and substituting into equation 3.56 yields,

$$\frac{dm_{4,a}}{dt} = \frac{A_4(H-h_3)}{C_{is,a}} \frac{dP_{4,a}}{dt} - \left(\frac{P_{4,a}}{C_{is,a}}\right) A_4 \frac{dh_3}{dt} . \tag{3.57}$$

The mass flow rates of air are determined as follows.

$$\dot{m}_{in,a} = (1-Z_1)\alpha\rho_1 Q_{2-3} , \tag{3.58}$$

and

$$\dot{m}_{out,a} = (1-Z_4)\left(\dot{m}_{v2,out} + \dot{m}_{v3,out}\right) . \tag{3.59}$$

where,

$$\dot{m}_{v2,out} = \rho_4 A_{v2} V_{v2}, \tag{3.60}$$

and

$$\dot{m}_{v3,out} = \rho_4 A_{v3} V_{v3} . \tag{3.61}$$

Z_4 and Z_1 are described later.

Substituting equation 3.57, equation 3.58 and equation 3.59 into equation 3.52, yields,

$$\frac{A_4(H-h_3)}{C_{is,a}} \frac{dP_{4,a}}{dt} - \left(\frac{P_{4,a}}{C_{is,a}}\right) A_4 \frac{dh_3}{dt} = (1-Z_1)\alpha\rho_1 Q_{2-3} - (1-Z_4)\left(\dot{m}_{v2,out} + \dot{m}_{v3,out}\right) . \tag{3.62}$$

Integrating and rearranging equation 3.62, gives,

$$P_{4,a} = \int \frac{C_{is,a}}{A_4(H-h_3)} \left\{ \rho_{4,a} A_4 \frac{dh_3}{dt} - (1-Z_4)\left(\dot{m}_{v2,out} + \dot{m}_{v3,out}\right) + (1-Z_1)\alpha\rho_1 Q_{2-3} \right\} dt , \tag{3.63}$$

An expression for the mass of fuel vapour mixture that is contained in Control Volume 4 is given by,

$$m_{4,v} = \rho_{4,v}\overline{V}_4 \,, \tag{3.64}$$

where $m_{4,v}$ is the mass of fuel vapour in the tank vapour space, $\rho_{4,v}$ is the density of the fuel vapour mixture in Control Volume 4 and $\overline{V}_4$ is the volume of the vapour space. Assuming that the cross-sectional area of the tank is constant and the fuel vapour in the vapour space is compressible,

$$m_{4,v} = \left(\frac{P_{4,v}}{C_{is,v}}\right) A_4 (H - h_3). \tag{3.65}$$

where $P_{4,v}$ is the partial pressure of the air in the vapour space, $C_{is,v}$ is a constant, A_4 is the cross-sectional area of the tank and H is the height of the tank.

Since the mass will change due to the pressure change and the volume change due to the change in the height of the liquid in the tank, it can be stated that,

$$\frac{dm_{4,v}}{dt} = \frac{\partial m_{4,v}}{\partial P_{4,v}} \frac{dP_{4,v}}{dt} + \frac{\partial m_{4,v}}{\partial h_3} \frac{dh_3}{dt} \,. \tag{3.66}$$

Taking the partial differential of equation 3.65 with respect to the height of the liquid in the tank and that with respect to the pressure in the tank, and substituting into equation 3.66 yields,

$$\frac{dm}{dt} = \frac{A_4 (H - h_3)}{C_{is,v}} \frac{dP_{4,v}}{dt} - \left(\frac{P_{4,v}}{C_{is,v}}\right) A_4 \frac{dh_3}{dt} \,. \tag{3.67}$$

The equation developed by Lavoie et al. [7] was used to predict the mass flow rate of evaporating fuel as indicated below.

The mass flow rates of fuel vapour are determined as follows.

$$\dot{m}_{in,v} = Z_1 \alpha \rho_1 Q_{2-3} + h_d \frac{MM_{vap}}{RuT} A_{liq}\left(P_{4,v\_eq} - P_{4,v}\right), \tag{3.68}$$

$$\dot{m}_{out,v} = Z_4\left(\dot{m}_{v2,out} + \dot{m}_{v3,out}\right). \tag{3.69}$$

where Z_4, Z_1, and P_{4,v_eq} are described in the sub-sections at the end of this section.

Substituting equation 3.67, equation 3.68, and equation 3.69 into equation 3.53, gives,

$$\frac{A_4(H-h_3)}{C_{is,v}}\frac{dP_{4,v}}{dt} - \left(\frac{P_{4,v}}{C_{is,v}}\right)A_4\frac{dh_3}{dt}$$
$$= h_d \frac{MM_{vap}}{RuT} A_{liq}\left(P_{4,v\_ep} - P_{4,v}\right) - Z_4\left(\dot{m}_{v2,out} + \dot{m}_{v3,out}\right) + Z_1\alpha\rho_1 Q_{2-3} \quad . \tag{3.70}$$

Integrating and rearranging equation 3.70 gives,

$$P_{4,v} = \int \frac{C_{ic,v}}{A_4(H-h_3)} \begin{Bmatrix} h_d \frac{MM_{vap}}{RuT} A_{liq}\left(P_{4,v\_eq} - P_{4,v}\right) + \rho_{4,v} A_4 \frac{dh_3}{dt} \\ - Z_4\left(\dot{m}_{v2,out} + \dot{m}_{v3,out}\right) + Z_1\alpha\rho_1 Q_{2-3} \end{Bmatrix} dt \quad . \tag{3.71}$$

3.4.1 MASS FRACTION

Z_4 is the mass fraction of fuel vapour in the vapour space and Z_1 is the mass fraction of fuel vapour in the filler tube (Control Volume 1). Expressions for these quantities are developed in this section.

In order to determine the mass fraction for the vapour space, Gibbs-Dalton law for perfect gas mixtures as found in Hasanein et al. [18] was used. This yields,

$$Z_4 = \frac{MM_{mix}}{MM_{vap}}\frac{P_{vap}}{P_{mix}} \quad , \tag{3.72}$$

where,

$$MM_{mix} = \frac{m_{mix}}{N_{mix}} = \frac{m_{air} + m_{vap}}{N_{air} + N_{vap}} \quad . \tag{3.73}$$

Since,

$$N_{air} = MM_{air} m_{air}\,, \tag{3.74}$$

$$N_{vap} = MM_{vap} m_{vap} \tag{3.75}$$

then,

$$MM_{mix} = \frac{1 + m_{vap}/m_{air}}{MM_{air} + MM_{vap}\left(m_{vap}/m_{air}\right)}\,. \tag{3.76}$$

From the Ideal Gas Law

$$m = \frac{P\bar{V}MM}{RuT}\,, \tag{3.77}$$

hence

$$\frac{m_{vap}}{m_{air}} = \frac{\dfrac{P_{vap} MM_{vap} V}{RuT}}{\dfrac{P_{air} MM_{air} V}{RuT}} = \frac{P_{vap}}{P_{air}} \frac{MM_{vap}}{MM_{air}} = \frac{P_{vap}}{\left(P_{mix} - P_{vap}\right)} \frac{MM_{vap}}{MM_{air}}\,, \tag{3.78}$$

and

$$MM_{mix} = \frac{MM_{vap}^2 P_{vap} + \left(P_{mix} - P_{vap}\right) MM_{air}^2}{P_{vap} MM_{vap} + \left(P_{mix} - P_{vap}\right) MM_{air}}, \tag{3.79}$$

which gives,

$$Z_4 = \frac{1}{MM_{vap}} \left[\frac{MM_{vap}{}^2 P_{vap} + \left(P_{mix} - P_{vap}\right) MM_{air}^2}{P_{vap} MM_{vap} + \left(P_{mix} - P_{vap}\right) MM_{air}} \right] \frac{P_{vap}}{P_{mix}}$$

$$= \frac{1}{MM_{vap}} \left[\frac{MM_{vap}{}^2 P_{4,v} + \left(P_4 - P_{4,v}\right) MM_{air}^2}{P_{4,v} MM_{vap} + \left(P_4 - P_{4,v}\right) MM_{air}} \right] \frac{P_{4,v}}{P_4}. \tag{3.80}$$

To determine the mass fraction of fuel vapour in Control Volume 1,

$$Z_1 = \frac{m_{v,1}}{m_1}\,, \tag{3.81}$$

where $m_{v,1}$ is the mass of the fuel vapour in Control Volume 1 and m_1 is the mass of air and fuel vapour in Control Volume 1.

$$m_{v,1} = \int \{Z_4 \rho_4 A_{v2} V_{v2} + Z_{v0} \rho_{v0} A_{v0} V_{v0} - Z_1 \rho_1 Q_g\} dt + initial \quad value \quad of \quad m_{v,1} \tag{3.82}$$

where Z_{v0}, ρ_{v0} and V_{vo} depend on the difference between atmospheric pressure and the pressure in Control Volume 1.

The total mass in Control Volume 1 is given by,

$$m_1 = \int \{\rho_4 A_{v2} V_{v2} + \rho_{v0} A_{v0} V_{v0} - \rho_1 Q_g\} dt + initial \quad value \quad of \quad m_1 . \tag{3.83}$$

3.4.2 EQUILIBRIUM VAPOUR PRESSURE

From the article by Lavoie et al. [7] the equilibrium vapour pressure can be expressed as,

$$P_{f\_eq}(RVP, T, Z_{ltov}) = P_{foc} \exp\left\{ \frac{\ln\left(\frac{RVP}{P_{foc}}\right)\left(\frac{1}{T} - \frac{1}{T_{foc}}\right)}{\frac{1}{T_{RVP} + A(Z_{ltov} - Z_{RVP})} - \frac{1}{T_{foc}}} \right\} . \tag{3.84}$$

where Z_{ltov} is the mass fraction of liquid that evaporates to vapour given by,

$$Z_{ltov} = \frac{1}{1 + \frac{\rho_L RuT}{(V/L) P_{f\_eq} MM_{vap}}} = \frac{1}{1 + \frac{\rho_L RuT}{((H/h_3) - 1) P_{f\_eq} MM_{vap}}} \tag{3.85}$$

and Z_{RVP} is the mass fraction for the conditions used to determine RVP,

$$Z_{RVP} = \frac{1}{1 + \frac{\rho_L RuT}{4 \cdot RVP \cdot MM_{vap}}} . \tag{3.86}$$

3.4.3 VALVE 2

The vent tube and the vent tube valve were arranged as indicated in Figure 3.3.

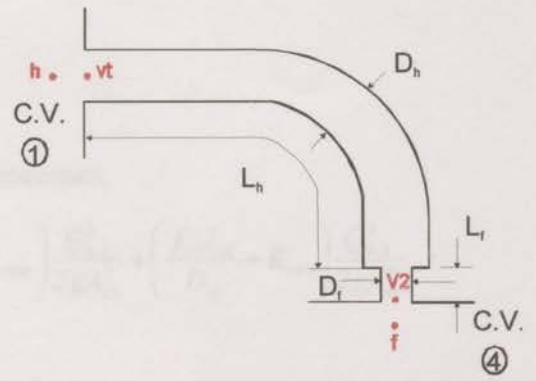

Figure 3.3- Diagram of the Vent Tube.

It is assumed that the losses for the vent tube are accounted for in Valve 2.

The modified Bernoulli's equation between point f and h (see Figure 3.3) is given by,

$$\frac{P_f}{\gamma_f}+z_f+\frac{V_f^2}{2g}=\frac{P_h}{\gamma_h}+z_h+\frac{V_h^2}{2g}+h_{L_{4-1}}, \tag{3.87}$$

where,

$$P_f = P_4, \tag{3.88}$$

$$P_h = P_1 \ , \tag{3.89}$$

$$z_f \approx z_h \ , \tag{3.90}$$

$$V_f \approx 0 \ , \tag{3.91}$$

$$V_h \approx 0 \ , \tag{3.92}$$

$$h_{L_{4-1}} = K_f + K_h = \left(\frac{f_{v2}L_{v2}}{D_{v2}}+K_{f-h}+K_{reent}\right)\frac{V_{v2}^2}{2g}+\left(\frac{f_{vt}L_{vt}}{D_{vt}}+K_{exit}\right)\frac{V_{vt}^2}{2g} \ . \tag{3.93}$$

but,

$$V_{v2}=\frac{Q_{4-1}}{A_{v2}}, \quad \text{and} \tag{3.94}$$

$$V_{vt} = \frac{Q_{4-1}}{A_{vt}} \quad . \tag{3.95}$$

Therefore equation 3.93 becomes,

$$h_{L_{4-1}} = \left(\frac{f_{v2} L_{v2}}{D_{v2}} + K_{f-h} + K_{reent} \right) \frac{Q_{4-1}^2}{2gA_{v2}^2} + \left(\frac{f_{v2} L_{vt}}{D_{vt}} + K_{exit} \right) \frac{Q_{4-1}^2}{2gA_{vt}^2} \quad . \tag{3.96}$$

where f_{v2} is the friction factor for vent tube valve and f_{vt} is the friction factor for the vent tube (assumed equal to f_{v2}), handled in a similar fashion as for Valve 1, L_{v2} is the effective length of the vent tube valve, D_{v2} is the diameter of the vent tube valve, K_{f-h} is the transition loss coefficient [18], K_{exit} is the exit loss, K_{reent} is the reentrance loss coefficient [19], L_{vt} is the effective length of the tube connecting the vent tube valve to the filler tube and D_{vt} is the diameter of that connecting tube.

Substituting equations 3.88-3.92 and equation 3.96 into equation 3.87 and rearranging,

$$Q_{4-1} = \sqrt{\left[\frac{(P_4 - P_1)}{\rho_4} \right] \left[\frac{1}{\left\{ \begin{array}{l} \frac{1}{2A_{vt}^2} - \frac{1}{2A_{v2}^2} + \left(\frac{f_{v2} L_{v2}}{D_{v2}} + K_{f-h} + K_{reent} \right) \frac{1}{2A_{v2}^2} \\ + \left(\frac{f_{v2} L_{vt}}{D_{vt}} + K_{exit} \right) \frac{1}{2A_{vt}^2} \end{array} \right\}} \right]} \quad . \tag{3.97}$$

3.4.4 VALVE 3

It is assumed that the losses for the rollover valve are accounted for in Valve 3. The modified Bernoulli's equation between point f and g (see Figure 3.1) is given by,

$$\frac{P_f}{\gamma_f}+z_f+\frac{V_f^2}{2g}=\frac{P_g}{\gamma_g}+z_g+\frac{V_g^2}{2g}+h_{L_{4-atm}} \quad , \tag{3.98}$$

where,

$$P_f = P_4 \quad , \tag{3.99}$$

$$P_g = P_{atm}, \tag{3.100}$$

$$z_f \approx z_g, \tag{3.101}$$

$$V_f = V_g = 0, \tag{3.102}$$

$$h_{L_{4-atm}} = \frac{f_{v3}L_{v3}}{D_{v3}}\frac{V_{v3}^2}{2g}+K_{exit}+K_{ent}. \tag{3.103}$$

Substituting equations 3.99-3.103 into equation 3.98 and rearranging gives,

$$V_{v3}=\sqrt{\left[\frac{(P_4-P_{atm})}{\rho_4}\right]\left[\frac{1}{\frac{1}{2}\left(\frac{f_{v3}L_{v3}}{D_{v3}}+K_{ent}+K_{exit}\right)}\right]} \quad . \tag{3.104}$$

where f_{v3} is the friction factor for Valve 3, handled in a similar fashion as valve 1, L_{v3} is the effective length of the rollover valve, D_{v3} is the diameter of the rollover valve, K_{ent} is the entrance loss and K_{exit} is the exit loss.

3.4.5 CHOKING

The flow through the rollover valve and vent tube have been determined in previous sections assuming incompressible flow. In this section, the conditions required for the flows in the vent tube and rollover valve to experience choking are developed. The article by Sinha et al. [1] describes the effect of small droplets in the vapour which has the effect of lowering the speed of sound. By lower the speed of sound the

occurrence of choking is more likely to occur. Therefore the mass flow leaving the vapour space via the vent tube and the rollover valve is subject to choking.

To determine the tank pressure at which choking will occur isentropic choking will be assumed. According to Wallis [17], if the density of the gas phase, ρ_g, is much less than the density of the liquid phase, ρ_L, and the speed of sound in the gas, c_g, is less than the speed of sound in the liquid, c_L, the speed of sound in the mixture can be given by,

$$c_{mix} = \sqrt{\frac{c_g^2 \rho_g}{\rho_L Y(1-Y)}} \,. \tag{3.105}$$

where Y is the percentage by mass of liquid droplets in the gas.

The lowest value of c_{mix} occurs at Y=0.5 and is given by,

$$c_{mix_{min}} = 2c_g \left(\frac{\rho_g}{\rho_L}\right)^{1/2} \,. \tag{3.106}$$

Using the numerical values in equation 3.106 gives the minimum speed of sound in the mixture to be 26.85 m/s.

To find the equivalent ratio of specific heats for the mixture, k_{mix},

$$c_{mix} = \sqrt{k_{mix} R_{mix} T} \,. \tag{3.107}$$

Therefore,

$$k_{mix} = \frac{c_{mix}^2}{R_{mix} T} = \frac{c_{mix}^2 MM_{mix}}{RuT} \,, \tag{3.108}$$

where

$$MM_{mix} = Y(MM_L) + (1-Y)(MM_g) \,, \tag{3.109}$$

The numerical value for k_{mix}, for this case, is 0.01921.

In general, for the isentropic flow of a perfect gas, the ratio of static to total pressure is given as [20],

$$\frac{P}{P_O} = \frac{1}{\left[1+\frac{k_{mix}-1}{2}(Ma)\right]^{k_{mix}/k_{mix}-1}}. \tag{3.110}$$

where P is the static pressure, P_o is the total pressure, Ma is the Mach number and k_{mix} is the ratio of specific heats.

Since choking occurs at Ma=1, equation 3.110 becomes,

$$\frac{P^*}{P_O} = \left[\frac{2}{1+k_{mix}}\right]^{k_{mix}/k_{mix}-1} = 0.98688 \tag{3.111}$$

where P^* is the critical pressure. Under this condition, the dimensionless mass flow rate becomes

$$\frac{\dot{m}\sqrt{RT_o}}{AP_o} = \sqrt{k_{mix}\left(\frac{2}{k_{mix}+1}\right)^{k_{mix}+1/k_{mix}-1}} \tag{3.112}$$

For the rollover valve P^* is atmospheric pressure and P_o is the vapour space pressure. Therefore, there will be choking if,

$$P_4 \; \rangle \; \frac{101.3}{0.98688} = 102.6 \quad kPa_{absolute} = 1346 \quad Pa_{gauge}. \tag{3.113}$$

Therefore, if P_4 >1346.3 Pa_{gauge} the mass flow rate can be obtained by substituting numerical values into equation 3.112 and rearranging as follows,

$$\dot{m}_{v3,out} = \frac{A_{v3}P_4}{\sqrt{R_{mix}T_O}}0.097644 = \frac{A_{v3}P_4}{\sqrt{\frac{Ru}{MM_{mix}}T}}0.097644 \; . \tag{3.114}$$

For the vent tube, P^* is the pressure in the filler tube, P_1, and P_o is the tank dome pressure,P_4. Therefore, there will be choking if,

$$P_4 \rangle \frac{P_1}{0.98688}. \tag{3.115}$$

and again using equation 3.112, the mass flow rate in the vent tube becomes;

$$\dot{m}_{v2,out} = \frac{A_{v2}P_4}{\sqrt{R_{mix}T_O}}0.097644 = \frac{A_{v2}P_4}{\sqrt{\frac{Ru}{MM_{mix}}T}}0.097644 \tag{3.116}$$

CHAPTER 4 - SOLUTION OF MODEL EQUATIONS

In order to solve the ordinary differential equations presented in Chapter 3, Simulink was used. Simulink is part of the Matlab software package, which uses a graphical interface to model, solve and analyse dynamic systems. Matlab version 5.3.1.29215a (R11.1) was used to solve these model equations on an IBM compatible PC, with an 800 MHz AMD Athlon processor and 640 MB of RAM memory.

Due to the excessive computational times to achieve a solotion with an extremely small step size [21], the model was considered stiff. For stiff problems, implicit methods perform much better than explicit ones. The solver used was ode23s which is a modified implicit Rosenbrock method of orders 2 and 3 with error control for stiff systems [21]. This is a variable step size solver, a maximum step size of 0.01 was used with an initial step size of 0.001.

A copy of the Simulink .mat file and the .m file that contains the parameter constants used with the .mat file, are available in the Mechanical, Automotive and Materials Engineering Department office.

CHAPTER 5 - RESULTS

5.1 MODEL PARAMETERS

The model equations were solved as described in Chapter 4 using common parameters as indicated below. Only the symbols are used in what follows in an effort to conserve space. The symbols are, however, defined in the nomenclature. The values given below are in the units required by the Simulink .m file.

The parameters associated with the geometry of the tank are as follows:

D_{v0}= 0.02486 m, D_1 = 0.0318 m, D_{v3} =0.0025 m, D_N = 0.0245 m, D_{vt} = 0.0095 m, A_3 = 0.2787 m^2, $A_4 = A_3$, h_N = 0.55 m, h_{ft} =0.5 m, h_f = 0.2286 m, H = 0.315 m, H_v = 0.305 m, L_{v0} = 0.001 m, L_{v1} = 0.5 m, L_{v2} = 0.05 m, L_{v3} = 0.029 m and L_{vt}= 0.95 m.

The liquid fuel properties are:ρ_L = 787 kg/m^3, ν_L = 4x 10^{-7} m^2/s and γ_L = 7.7205 x 10^3 kg/$m^2 \cdot s^2$.

The properties associated with atmospheric air at 300 K are: MM = 28.97 kg/kmol, ρ_{air} = 1.176538 kg/m^3, ν_{air} =1.82669960879 x10^{-5} m^2/s and γ_{air} = 11.5418 kg/$m^2 \cdot s^2$.

The properties associated with fuel vapour are: MM_{vap} = 65 kg/kmol and ρ_{vap} = 2.639 kg/m^3.

The properties associated with homogeneous fluid flow are: α= 0.15

The properties associated with vapour generation are: h_d=1 m/s, P_{foc} = 1.38 x 10^7 Pa, T_{foc} = 703 K, T_{RVP} = 311 K and A = 150 °C/(mass fraction evaporated).

The general properties of the model are: π= 3.14159, g=9.81 m/s^2, Ru = 8314 Pa m^3/kmol k, T_1 = 300 K, P_{atm} = 101300 Pa, $P_{choking,v3}$ = 102646 Pa, $Q_{in,a}$ = 1.1132 x 10^{-4} m^3/s, K_{exit} = 1.0, K_{reent} = 1.0, $K_{entrance}$ = 0.5

The initial conditions associated with the model are: h_{2_init} = 0, h_{3_init} = 0.01 m, P_{4,v_init} = is determined by solving equation 3.82 using Simulink and taking the steady state value, $P_{4,a\_init} = P_{atm} - P_{4,v\_init}$, $P_{1\_init} = P_{atm}$,

$$Z_{4\_init} = \frac{1}{MM_{vap}}\left(\frac{MM_{vap}^2 P_{4,v\_init} + \left(P_{atm} - P_{4,v\_init}\right)MM^2}{MM_{vap} P_{4,v\_init} + \left(P_{atm} - P_{4,v\_init}\right)MM}\right)\frac{P_{4,v\_init}}{P_{atm}} \quad ,$$

$$\rho_{mix,init} = \frac{P_{atm}\left(\left(1 - Z_{4\_init}\right)MM + Z_{4\_init} MM_{vap}\right)}{RuT} \quad ,$$

$$m_{1,init} = \frac{P_{atm}\left(\left(1 - Z_{4\_init}\right)MM + Z_{4\_init} MM_{vap}\right)h_N\left(A_2 - A_N\right)}{RuT} \quad .$$

Parameters that change for the different cases that are considered in the thesis are;

RVP= 7 kPa - 88 kPa

D_{v2} = 3.2 mm, 6.4 mm or 9.5 mm

for D_{v2} = 3.2 mm , $K_{f\text{-}h}$ = 0.3

for D_{v2} = 6.4 mm , $K_{f\text{-}h}$ = 0.8

for D_{v2} = 9.5 mm , $K_{f\text{-}h}$ = 0

Q_{inL} = 10 GPM = 38 L/min

or

Q_{inL} = 12 GPM = 45 L/min

5.2 EXAMPLES OF NORMAL AND PREMATURE SHUT-OFF

This section demonstrates that the model is capable of predicting the important features of Normal Shut-Off (NSO) and Premature Shut-Off (PSO). Included in this section are typical examples of a NSO and a PSO tank filling situation. It should be recalled that the volume flow rate of the liquid fuel dispensed by the fuel nozzle remains constant throughout the process until shut-off where it drops instantly.

For the NSO filling situation the parameter values are RVP = 55 kPa, D_{v2} = 6.4 mm and Q_{inL} = 45 L/min. The height of the liquid in the tank, tank dome pressure, the height of the liquid in the filler tube and the flow rate into the tank are plotted versus time in Figure 5.1, 5.2, 5.3 and 5.4 respectively. The height of the liquid in the tank is set to 0.01 m initially. It is seen to increase almost linearly until it reaches the bottom of the vent tube, which is 0.305 m in this case. This is the beginning of the shut-off process and occurs at a time indicated by the left vertical line in each figure. The liquid level continues to rise due to the fact that the shut-off sensor has not yet stopped the fuel dispensing nozzle.

At the start of the filling process the pressure in the tank dome rises to a peak (Phase I) and then drops to an equilibrium pressure for most of the filling process (Phase II). At the beginning of the shut-off process air/fuel vapour can only exit the tank dome through the rollover valve. The liquid is still evaporating and there is still liquid coming into the tank, therefore the pressure in the tank rapidly rises. The magnitude of this rise, however, seems to be excessive compared to what is observed experimentally.

The difference may be due to flexible nature of the tank used in the experiments and the rigid assumption made in the simplified model. The liquid level in the filler tube follows the same trend; it shoots up to a peak and then drops to an equilibrium level, at approximately the same time that the tank dome pressure does. The liquid level is noticed to begin to rise linearly at about 80 seconds and continues until shut-off. The beginning of the rise coincides with the liquid in the tank covering the entrance of the filler tube into the tank. At the beginning of shut-off the liquid level in the filler tube rapidly rises and as the tank pressure reaches its Phase III maximum the liquid level in the filler tube reaches the shut-off point which is 0.5 m in this case. This shuts off the liquid flow from the nozzle which is the end of the shut-off process. The flow rate into the tank is seen to increase initially, however, it remains nearly constant for most of the filling process. At the beginning of the shut-off process the flow rate decreases but ,in some cases exhibits a spike at the end of shut-off. This spike is abnormally large and is thought to be related to the solution procedure.

For the PSO filling situation the parameter values are RVP= 58 kPa, D_{v2} = 3.2 mm and Q_{inL} = 45 L/min. The height of the liquid in the tank, tank dome pressure, the height of the liquid in the filler tube and the flow rate into the tank are plotted versus time in Figure 5.5, 5.6, 5.7 and 5.8 respectively. In the case of PSO the liquid level in the tank never reaches the bottom of the vent tube. During the filling process the tank dome pressure rises quickly. The liquid level in the filler tube follows the same trend until it reaches the shut-off point. This shuts off the flow of liquid from the fuel dispensing nozzle, even though the tank is not full. The flow rate into the tank is seen to rise slightly

as the filler tube liquid level increases. A spike in this quantity, similar to that observed at the end of the filling process is also observed.

In both the NSO and PSO cases the model is not capable of accurately predicting the events that occur after the homogeneous mixture level in the filler tube reaches the shut-off point.

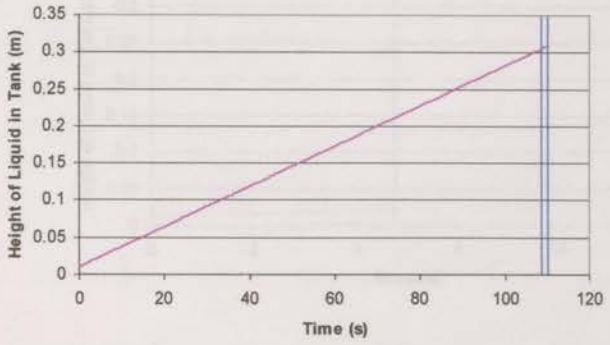

Figure 5.1- Height of Liquid in the Tank (h_3) for Normal Shut-Off

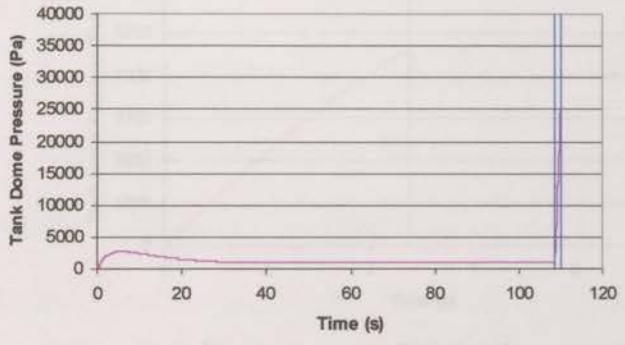

Figure 5.2- Tank Pressure (P_4) for Normal Shut-Off

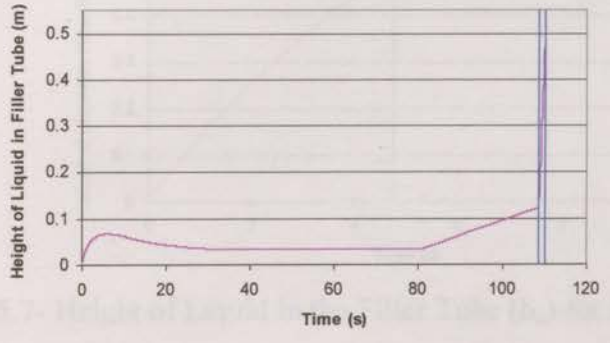

Figure 5.3- Height of Liquid in the Filler Tube (h_2) for Normal Shut-Off

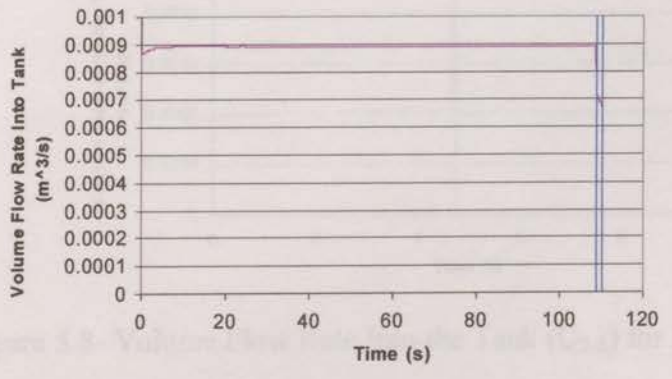

Figure 5.4- Volume Flow Rate Into the Tank ($Q_{2\text{-}3}$) for Normal Shut-Off

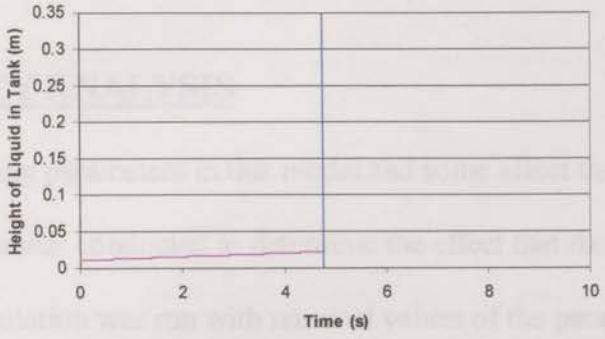

Figure 5.5- Height of Liquid in the Tank (h_3) for Premature Shut-Off

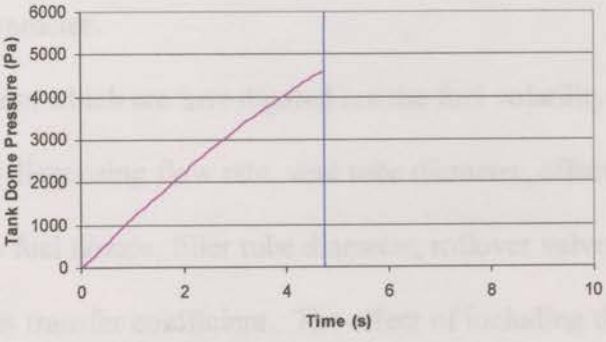

Figure 5.6- Tank Pressure (P_4) for Premature Shut-Off

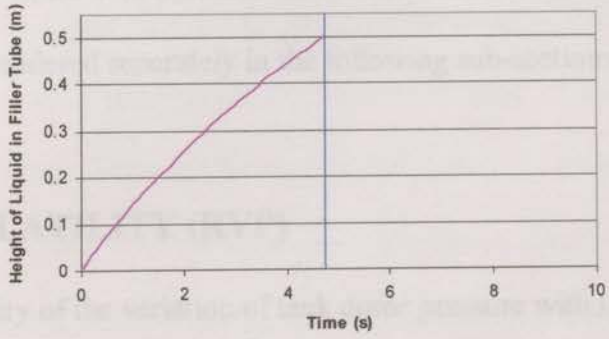

Figure 5.7- Height of Liquid in the Filler Tube (h_2) for Premature Shut-Off

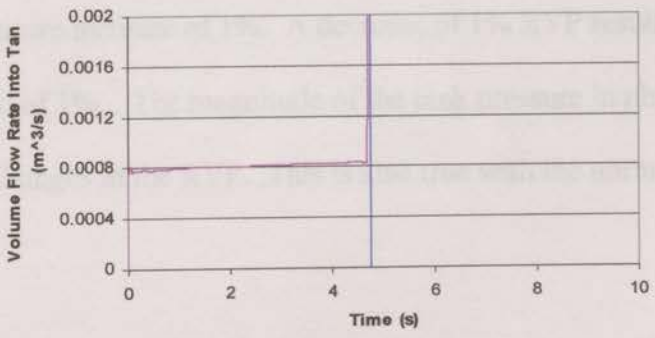

Figure 5.8- Volume Flow Rate Into the Tank ($Q_{2\text{-}3}$) for Premature Shut-Off

5.3 SENSITIVITY ANALYSIS

There are many parameters in this model and some affect the results more than others. This analysis was conducted to determine the effect that the parameters have on the results. The simulation was run with nominal values of the parameters (D_{v2}=6.4 mm, Q_{inL}=45 L/min, RVP = 55 kPa) then at values of ±10%, ±1% or ±0.2%, depending on the sensitivity of the parameter.

The parameters which are investigated are the fuel volatility as indicated by the RVP, the liquid fuel dispensing flow rate, vent tube diameter, effective diameter of the vent area around the fuel nozzle, filler tube diameter, rollover valve diameter, void fraction and the mass transfer coefficient. The effect of including the assumption of a "choking condition" in the vent tube and the rollover valve is also included in this section. Each is considered separately in the following sub-sections.

5.3.1 FUEL VOLATILITY (RVP)

The sensitivity of the variation of tank dome pressure with time to changes in the RVP is presented in Figure 5.9. It can be seen that an increase in RVP of 1% results in a phase I peak pressure increase of 1%. A decrease of 1% RVP results in a phase I peak pressure decrease of 1%. The magnitude of the tank pressure in phase II of the filling is not affected by changes in the RVP. This is also true with the normal shut-off time.

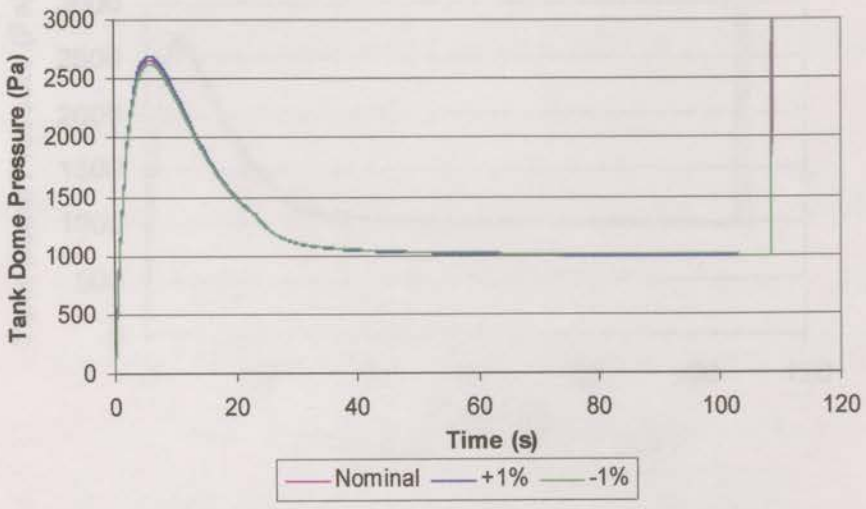

Figure 5.9-Tank Dome Pressure for RVP ±1%

5.3.2 FUEL DISPENSING FLOW RATE (Q_{inL})

The sensitivity of the variation of tank dome pressure with time to changes in the fuel dispensing flow rate is presented in Figure 5.10. With a 1% increase in the fuel dispensing flow rate there was a 1% increase in the phase I peak pressure while with a 1% decrease in the volume flow rate there was a 1% decrease in the phase I peak pressure. Increasing the fuel dispensing flow rate is seen to increase the magnitude of the tank dome pressure during phase II of tank filling by 2% and also increase the nominal shut-off time by 1%. Decreasing the fuel dispensing flow rate is seen to decrease the magnitude of the tank dome pressure during phase II of tank filling by 2% and also increase the nominal shut-off time by 1%.

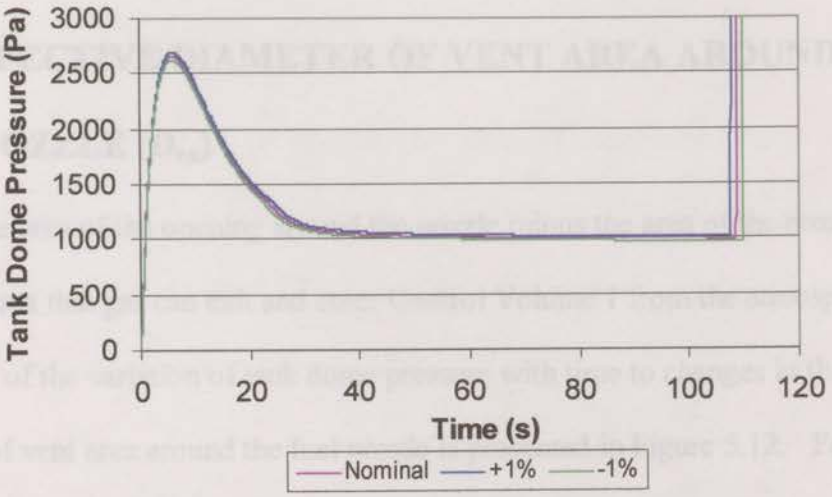

Figure 5.10- Tank Dome Pressure for Volume Flow Rate into the System ± 1%

5.3.3 VENT TUBE DIAMETER (D_{v2})

The sensitivity of the variation of tank dome pressure with time to changes in the vent tube diameter is presented in Figure 5.11. For an increase of 10% in the diameter of the vent tube there was no significant change in the phase I peak pressure. For a decrease of 10% in the vent tube diameter there was no significant change in the phase I peak pressure. This was also true for the tank dome pressure in phase II of filling and for normal shut-off time.

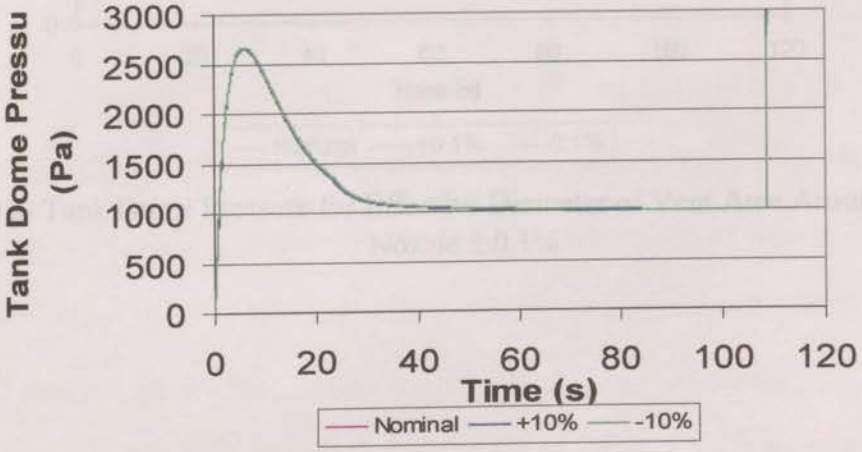

Figure 5.11- Tank Dome Pressure for Vent Tube Diameter ± 10%

5.3.4 EFFECTIVE DIAMETER OF VENT AREA AROUND THE FUEL NOZZLE (D_{ea})

The area of the opening around the nozzle minus the area of the nozzle gives the effective area that gas can exit and enter Control Volume 1 from the atmosphere. The sensitivity of the variation of tank dome pressure with time to changes in the effective diameter of vent area around the fuel nozzle is presented in Figure 5.12. For an increase of 0.1% in the diameter there was an 5% decrease in the phase I peak pressure and a 8% decrease in the phase II pressure magnitude. For a decrease of 0.1% in the diameter there was a 6% increase in the phase I peak pressure and a 9% increase in the phase II pressure magnitude. There was no effect on the value of the normal shut-off time.

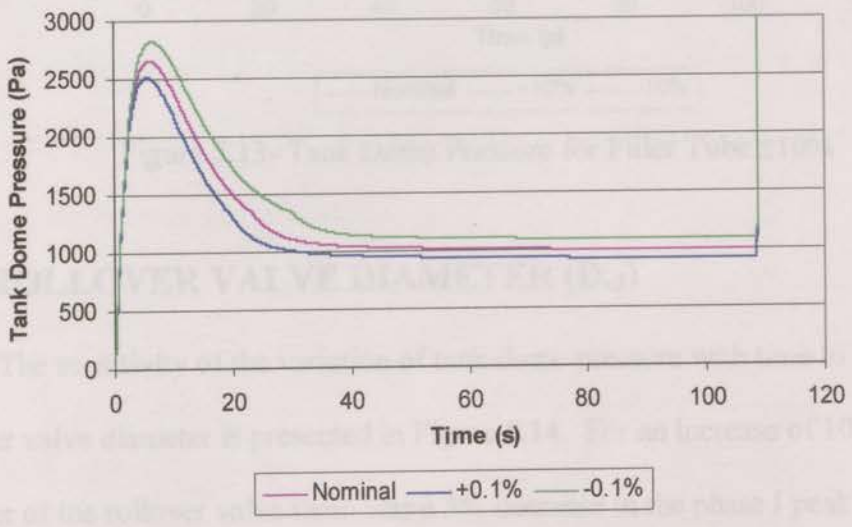

Figure 5.12- Tank Dome Pressure for Effective Diameter of Vent Area Around the Fuel Nozzle ± 0.1%

5.3.5 FILLER TUBE DIAMETER (D_1)

The sensitivity of the variation of tank dome pressure with time to changes in the filler tube is presented in Figure 5.13. For a change of ±10% in the diameter of the filler tube there was no significant change in the phase I peak pressure, tank dome pressure during phase II or the normal shut-off time.

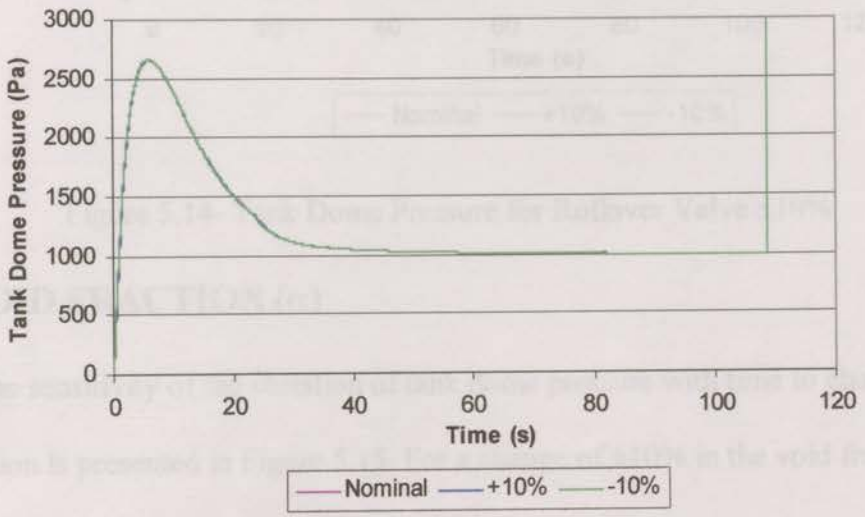

Figure 5.13- Tank Dome Pressure for Filler Tube ±10%

5.3.6 ROLLOVER VALVE DIAMETER (D_{v3})

The sensitivity of the variation of tank dome pressure with time to changes in the Rollover valve diameter is presented in Figure 5.14. For an increase of 10% in the diameter of the rollover valve there was a 5% decrease in the phase I peak pressure and a 11% decrease in the phase II pressure magnitude. For a decrease of 10% in the rollover valve diameter there was 4% increase in the phase I peak pressure and a 11 % increase in the phase II pressure magnitude. There was no effect on the normal shut-off time.

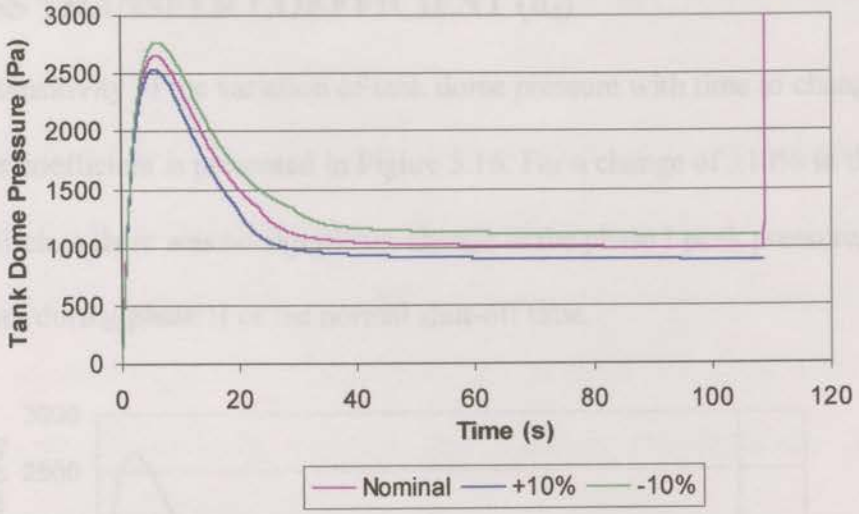

Figure 5.14- Tank Dome Pressure for Rollover Valve ±10%

5.3.7 VOID FRACTION (α)

The sensitivity of the variation of tank dome pressure with time to changes in the void fraction is presented in Figure 5.15. For a change of ±10% in the void fraction there was no significant change in the phase I peak pressure, the tank dome pressure during phase II or the normal shut-off time.

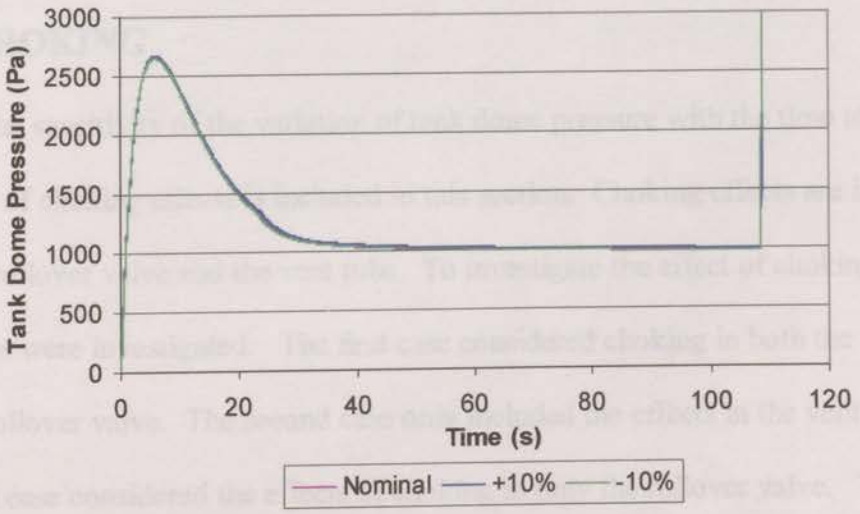

Figure 5.15- Tank Dome Pressure for Void Fraction ± 10%

5.3.8 MASS TRANSFER COEFFICIENT (h_d)

The sensitivity of the variation of tank dome pressure with time to changes in the mass transfer coefficient is presented in Figure 5.16. For a change of ±10% in the mass transfer coefficient there was no significant change in the phase I peak pressure, the tank dome pressure during phase II or the normal shut-off time.

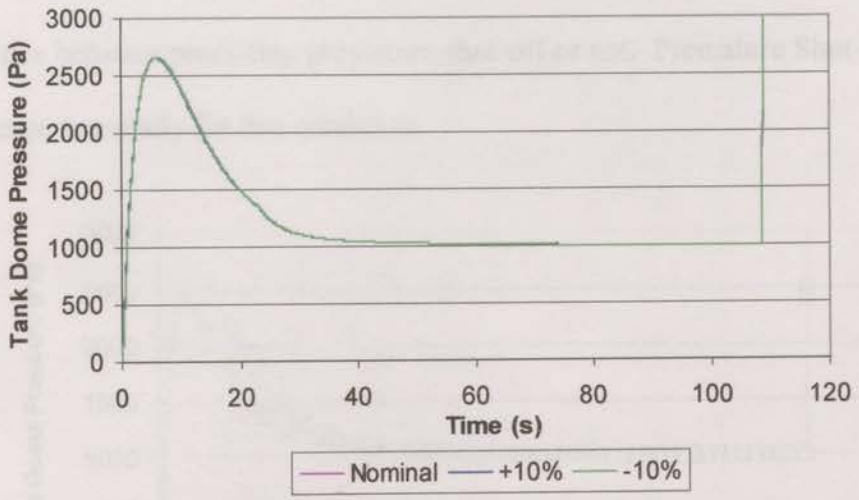

Figure 5.16- Tank Dome Pressure for Mass Transfer Coefficient ±10%

5.3.9 CHOKING

The sensitivity of the variation of tank dome pressure with the time to the inclusion of choking effects is included in this section. Choking effects are included in both the rollover valve and the vent tube. To investigate the effect of choking four conditions were investigated. The first case considered choking in both the vent tube and the rollover valve. The second case only included the effects in the vent tube valve. The third case considered the effects of choking in only the rollover valve. The fourth case neglected choking effects completely. The results are presented in Figure 5.17. Choking in the rollover valve has the effect of increasing the maximum phase I peak

pressure, however it does not affect the tank dome pressure during phase II of filling, nor the normal shut-off time.

Increasing the maximum phase I peak tank pressure can lead to premature shut-off. The variation of tank dome pressure with time for the case of a 3.2 mm diameter vent tube is shown in Figure 5.18. The choking (in both vent tube and rollover valve) and no choking cases are included. In this case, the inclusion of choking effects makes the difference between predicting premature shut-off or not. Premature Shut-Off was observed experimentally for this condition.

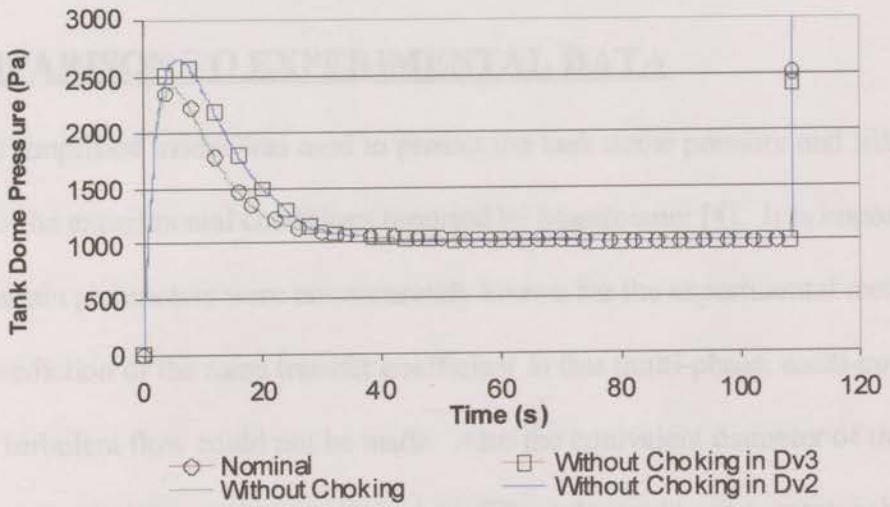

Figure 5.17-Tank Dome Pressure With/Without Choking

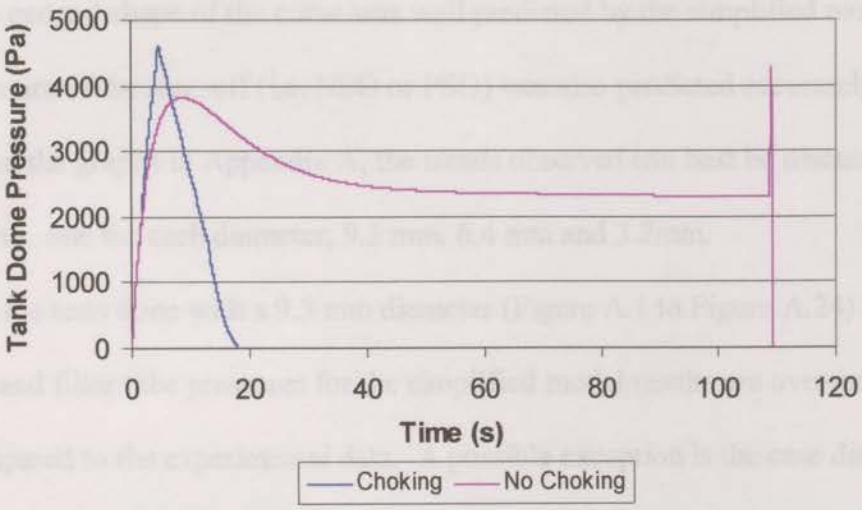

Figure 5.18- Tank Dome Pressure With/Without Choking for D_{v2}=3.2 mm

5.4 COMPARISON TO EXPERIMENTAL DATA

The simplified model was used to predict the tank dome pressure and filler tube pressure for the experimental conditions reported by Mastroianni [4]. It is important to note that certain parameters were not accurately known for the experimental method. Accurate prediction of the mass transfer coefficient in this multi-phase, multi-component and highly turbulent flow could not be made. Also the equivalent diameter of the vent area between the fuel dispensing nozzle and the filler tube could not accurately be determined. It should be noted that the filling performance is extremely sensitive to this value. It, therefore, was decided to take a value of the mass transfer coefficient of 1 m/s and adjust the effective vent area until the peak tank dome pressure agreed with the experimental results for the case of 6.4 mm vent tube diameter, 45 L/min liquid fuel flow rate, and 55 kPa RVP. These values were then kept constant for the remainder of the predictions made in this thesis. The results for the 31 experimental cases are included in Appendix A. Study of these curves leads to the observations which are included below.

The general shape of the curve was well predicted by the simplified model. In all cases the nature of the shut-off (i.e. NSO or PSO) was also predicted accurately.

From the graphs in Appendix A, the trends observed can best be discussed in three sections, one for each diameter, 9.5 mm, 6.4 mm and 3.2mm.

For the tests done with a 9.5 mm diameter (Figure A.1 to Figure A.24) the peak tank dome and filler tube pressures for the simplified model results are over-predicted results compared to the experimental data. A possible exception is the case displayed in Figure A.1. The experimental data for this case has a similar peak pressure as the case Figure A.3, however the first case had an RVP of 61 kPa while the second case had an RVP of 88 kPa.

Considering Phase II for the 9.5 mm case, the simplified model agreed very well, in magnitude, to the experimental data for the tank dome pressure but slightly over-predicted the filler tube pressure. The shut-off time (NSO) was accurately predicted for the 9.5 mm diameter cases.

Small discontinuities are observed at the same time as those which occur in the simplified model during unchoking in a number of the graphs. This tends to occur at pressures of about 800 Pa. It is difficult to say whether this is a physical representation for the choking or just coincidence.

For the 6.4 mm diameter cases (Figure A.25 to Figure A.48) the phase I peak tank dome pressure predicted by the simplified model tends to under-predict or be approximately the same as the experimental data. The filler tube phase I peak pressure tended to be greater than the experimental values. Considering the pressure during phase II, the tank dome pressure was consistently under-predicted, while the filler tube pressure

was consistently over-predicted. The times to reach the phase I peak pressure for the experimental data are usually longer than those predicted by the simplified model.

For both 9.5 mm and 6.4 mm diameter, there was a greater difference between experimental and model phase I peak pressure for the higher RVP range (83 kPa) than the lower RVP range (55 kPa), except for the case in Figure A.25. For Figure A.25 there was a peak pressure of 3500 Pa for an RVP of 52 kPa, while the peak pressure was 2000 Pa for an RVP of 51 kPa and just under 2000 Pa for an RVP of 50 kPa for the same conditions. This illustrates the variability of the experimental results for this case. A similar trend was noticed for Q_{inL}. The difference was greater for 38 L/min than for that of 45 L/min. This, however, is believed to be related to the fact that one test was used to calibrate the simplified model. Since the calibration model was the intermediate diameter (6.4 mm), a mid range RVP (55 kPa) and the higher Q_{inL} (45 L/min), the models that have parameters closer to those parameters are in better agreement with the experiments.

For the 3.2 mm diameter cases (see Figure A.49 to Figure A.58) the simplified model does not consistently over-predict or under-predict the peak tank dome pressure compared to that found experimentally. The simplified model, however, predicts a shut-off at around 4500 kPa for all test cases, regardless of the RVP. The model also does not consistently over-predict or under-predict the shut-off time (PSO). It is difficult to make a comparison with the filler tube pressure due to irregularities in the experimental results.

For the case of the Stoddard fluid at the higher fuel nozzle flow rate (Figure A.59) both the simplified model and the experimental results showed PSO. The simplified model predicted the shape of the curve to a reasonable degree of accuracy. For the case of Stoddard fluid at the lower fuel nozzle flow rate (Figure A.61) the experimental results

showed PSO, however, this was after a considerable amount of the tank had been filled. The simplified model accurately predicted the nature of the flow (PSO), however it did not accurately predict the degree of tank filling.

CHAPTER 6 - CONCLUSIONS

A simplified lumped parameter model that reasonably describes the process of refuelling an automotive fuel tank in order to predict premature shut-off has been developed.

The sensitivity of the results to changes in the problem parameters was investigated:

- the results were very sensitive to changes in the effective diameter of the vent area around the fuel nozzle, liquid fuel volume flow rate and fuel volatility
- the results were sensitive to the rollover valve diameter
- the results were not sensitive to changes in the vent tube diameter, mass transfer coefficient, void fraction and filler tube diameter
- including the effect of choking has a significant affect on the prediction of Phase I peak pressure and is important for accurately predicting the nature of the shut-off (i.e. PSO or NSO)

The results of the model were also compared with available experimental data with the following observations.

For 9.5 mm vent tube diameter;

- the model over-predicted the phase I peak pressure
- the phase II magnitude was predicted reasonably closely
- the shut-off time was predicted reasonably closely

For 6.4 mm vent tube diameter;

- the model under-predicted the peak pressure, but there was less of a difference than for the 9.5 mm diameter
- the phase II magnitude was also under-predicted
- the shut-off time was predicted reasonably closely

For 3.2 mm vent tube diameter;

- the model did not consistently over-predict or under-predict the peak pressure
- shut-off time was not closely predicted on a percentage basis
- model shuts off at around 4500 Pa for all cases

For the 9.5 mm and 6.4 mm vent tube diameters;

- higher RVP caused a greater difference between the model and experimental peak tank dome pressure
- a lower liquid level fuel flow rate had a greater difference between the model and the experimental peak pressure.

CHAPTER 7 - RECOMMENDATIONS

This simplified model developed in this work is restricted to a rectangular tank. Modifications could easily be made to accommodate variable cross sectional tanks. This would involve specifying the change of volume of the liquid in the tank with respect to time.

The carbon canister that is attached to the rollover valve could also be easily included in the model by determining an equivalent frictional resistance and adding it to the rollover valve resistance.

A model to account for the bubble growth throughout the multi-phase, multi-component flow in the filler tube should also be considered for future models.

A future model that accounts for the dissolved air/fuel vapour in the liquid fuel that flows through the filler tube and into the tank should also be considered.

A model that can be used for different tank geometries would not be difficult to add as long as the change in volume with respect to the change in liquid is known.

REFERENCES

[1] Sinha, N., Thompson, R., and Harrigan, M., *Computational Simulation of Fuel Shut-Off During Refueling*, SAE Technical Paper Series, Paper 981377, International Spring Fuels & Lubricants Meeting & Exposition, Dearborn, Michigan, May 4-6, 1998.

[2] Holloway, M., *Fill 'Er Up*, Scientific America, New York, NY, May 2000, pp. 92-93.

[3] Stoneman, S., *On the Design of Automotive Fuel Filler Pipes*, Automotive Engineer, Vol. 22, No. 1, Feb 1997.

[4] Mastroianni, M., *Experimental Investigation of Automotive Fuel Tank Filling*, M.A.Sc. Thesis, Mechanical, Automotive and Material Engineering Department, University of Windsor, Windsor, Ontario, 2000.

[5] Banerjee, R., Isaac, K.M., Oliver, L., and Breig, W., *A Numerical Study of Automotive Gas Tank Filler Pipe Two Phase Flow*, SAE Technical Paper Series 2001-01-0732, Society of Automotive Engineers, Detroit Michigan, March 5-8, 2001.

[6] Rodriguez, M.A., Parra, M.T., and Castro, F., *Vehicle Evaporative Emission Models*, ECCEMEI 1994 Proceedings.

[7] Lavoie, G.A., Imai, Y.A., and Johnson, P.J., *A Fuel Vapour Model (FVSMOD) for Evaporative Emissions System Design and Analysis*, SAE Technical Paper Series, Paper 982644, Society of Automotive Engineers, International Fall Fuels and Lubricant Meeting and Exposition, San Francisco, California, October 19-22, 1998

[8] Lockhart, M.C., *Predicting Tank Vapor Mass for On-Board Refueling Vapor Recovery*, SAE Technical Paper Series, Paper 970308, Society of Automotive Engineers, International Congress and Exposition, Detroit, Michigan, February 24-27, 1997.

[9] Kunimitsu, M., Mori, K., and Muragushi, T., *Prediction of Gasoline Vapor Generation from a Vehicle Fuel Tank at High Temperature*, JSAE Review, Vol. 14, No. 4, October 1993

[10] Parra, M.T., Rodriquez, M.A., and Castro, F., and Villafruela, J.M., *Three-Dimensional Evaporative Emission Model*, IMechE, C496/005/95, 1995.

[11] Vaughan, D.A., and Schmidt, G.R., *Analytical Modeling of No-Vent Fill Process, Journal of Spacecraft an Rockets*, Vol. 28, No. 5, September 1991.

[12] Whalley, P.B., *Two-Phase Flow During Filling and Emptying of Bottles*, International Journal of Multi-phase Flow, Vol. 17, No. 1, January/February 1991.

[13] Whalley, P.B., Boiling, *Condensation and Gas-Liquid Flow*, Oxford University Press, New York, NY, 1987.

[14] Reddy, S.R., *A New Correlation for Predicting Average Vehicle Evaporative Emissions as a Function of Fuel Volatility*, SAE Technical Paper Series, Paper 881592, Society of Automotive Engineers, 1988.

[15] Bardon, M.F., and Rao, V.K., *Estimating Instantaneous Properties of Vaporizing Light Petroleum Fractions*, Combustion and Flame, Vol. 84, 427-431, 1991.

[16] Lavoie, G.A., and Smith, C.S., *Vapor Pressure Equations for Characterizing Automotive Fuel Behavior Under Hot Fuel Handling Conditions*, SAE Technical

Paper Series, Paper 971650, Society of Automotive Engineers, International Spring Fuels & Lubricants Meeting Dearborn, Michigan, May 5-8, 1997.

[17] Wallis, G.B., *One-Dimensional Two-Phase Flow*, McGraw Hill Inc., New York, NY, 1969.

[18] Hasanein, H.A., Kazimi, M.S., and Golay, M.W., *Forced Convection In-Tube Steam Condensation in the presence of Non-condensable gasses*, International Journal of Heat and Mass Transfer, Vol. 39, No. 13, pp. 2625-2639, Sept. 1996.

[19] White, F.M., *Fluid Mechanics 3rd Edition*, Pg. 339, McGraw Hill Inc., New York, NY, 1994

[20] Cengel, Y.A., and Boles, M.A., *Thermodynamics: An Engineering Approach, 2nd Edition*, pg. 828, McGraw Hill Inc., New York, NY, 1994.

[21] Ashino, R., Ngase, M., and Vaillancourt, R., *Behind and Beyond the MATLAB ODE Suite,* Computers and Mathematics with Applications, Vol. 40, pp 491-512, 2000.

APPENDIX A

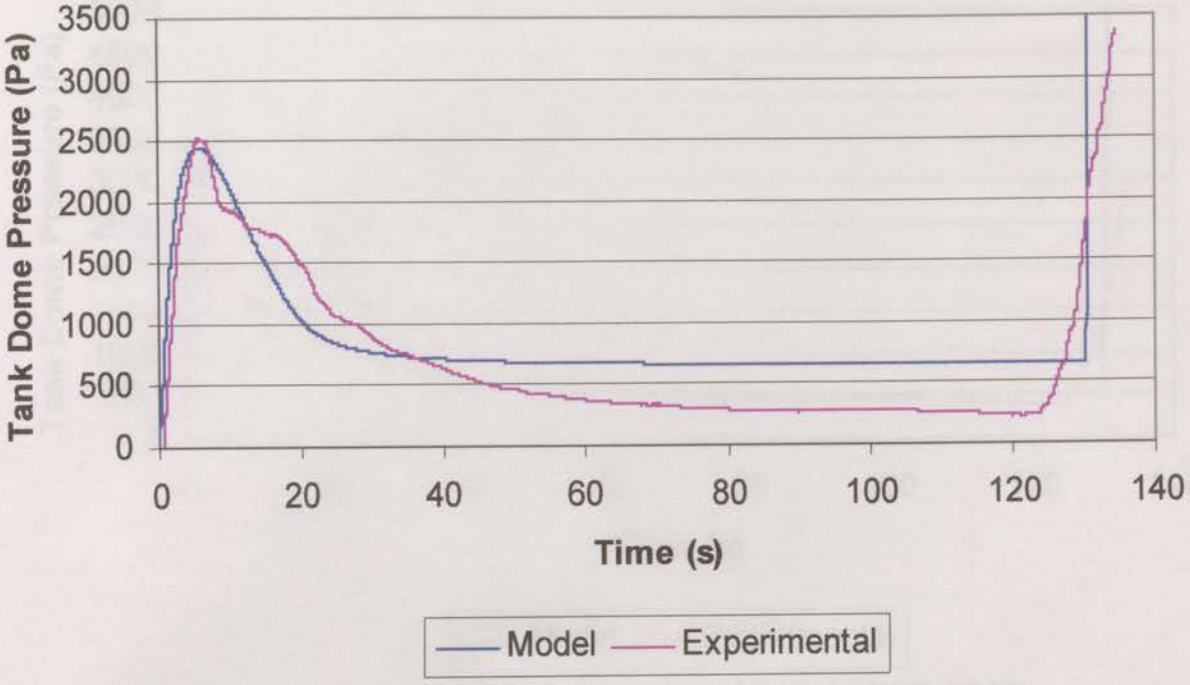

Figure A.1: Tank Dome Pressure, D_{v2}= 9.5 mm, Q_{inL}= 38 L/min, RVP=61 kPa

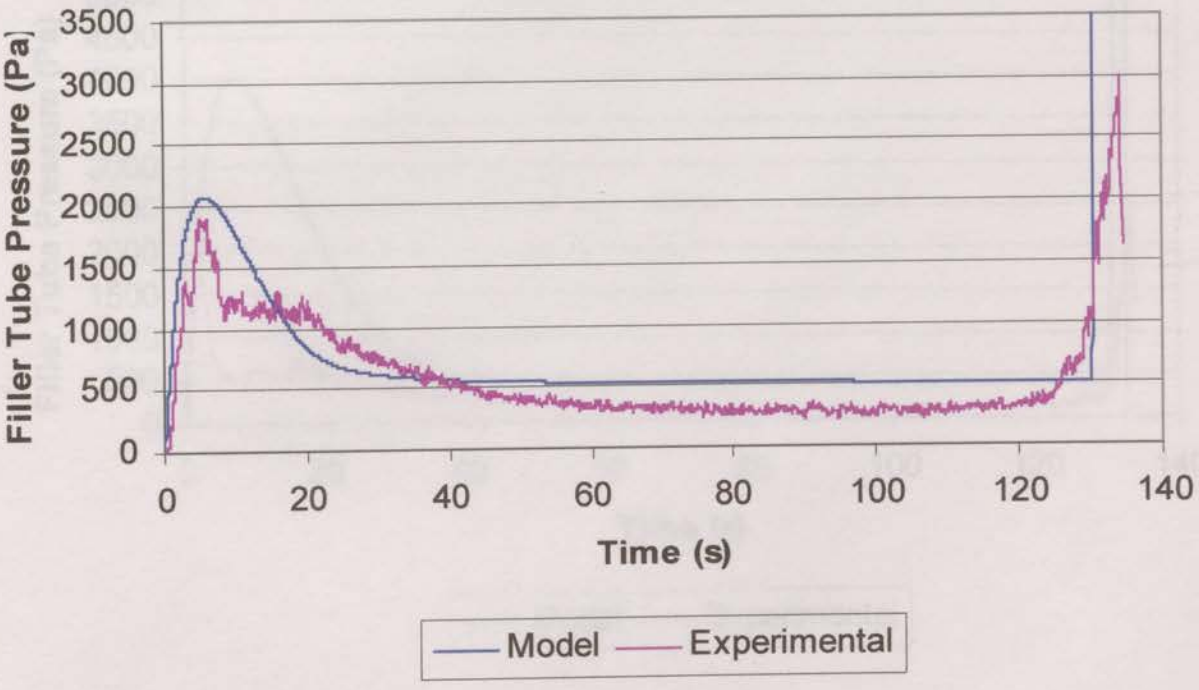

Figure A2: Filler Pipe Pressure, D_{v2}= 9.5 mm, Q_{inL}= 38 L/min, RVP=61 kPa

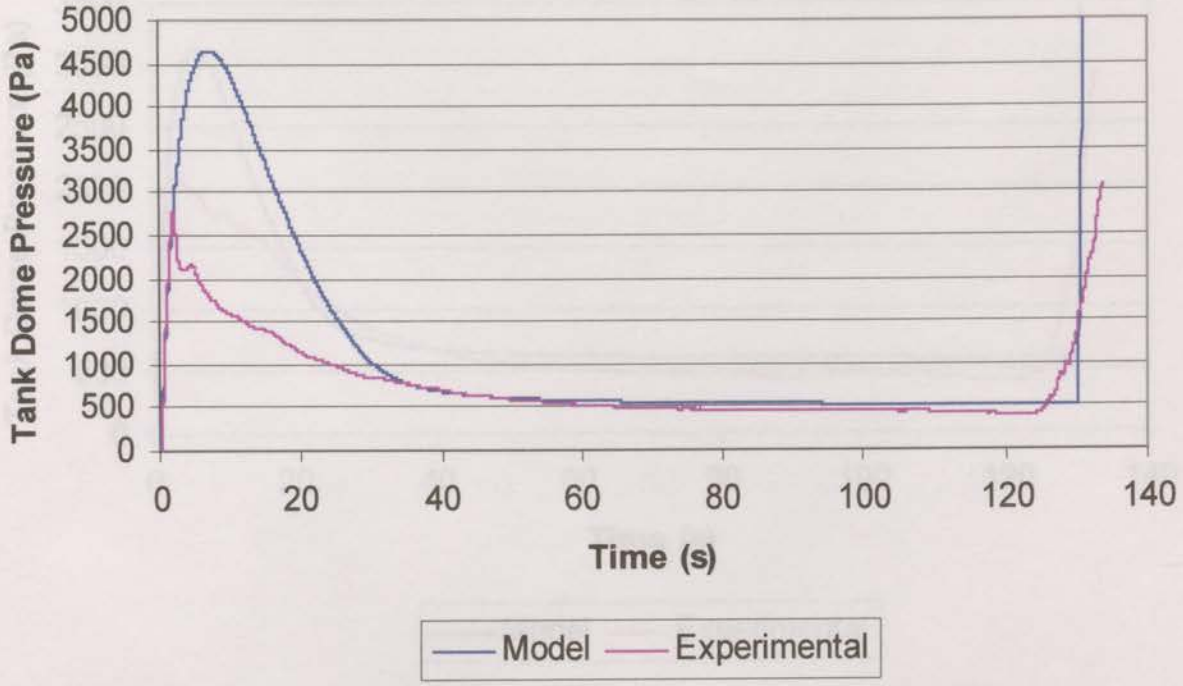

Figure A.3: Tank Dome Pressure, D_{v2}= 9.5 mm, Q_{inL}= 38 L/min, RVP=88 kPa

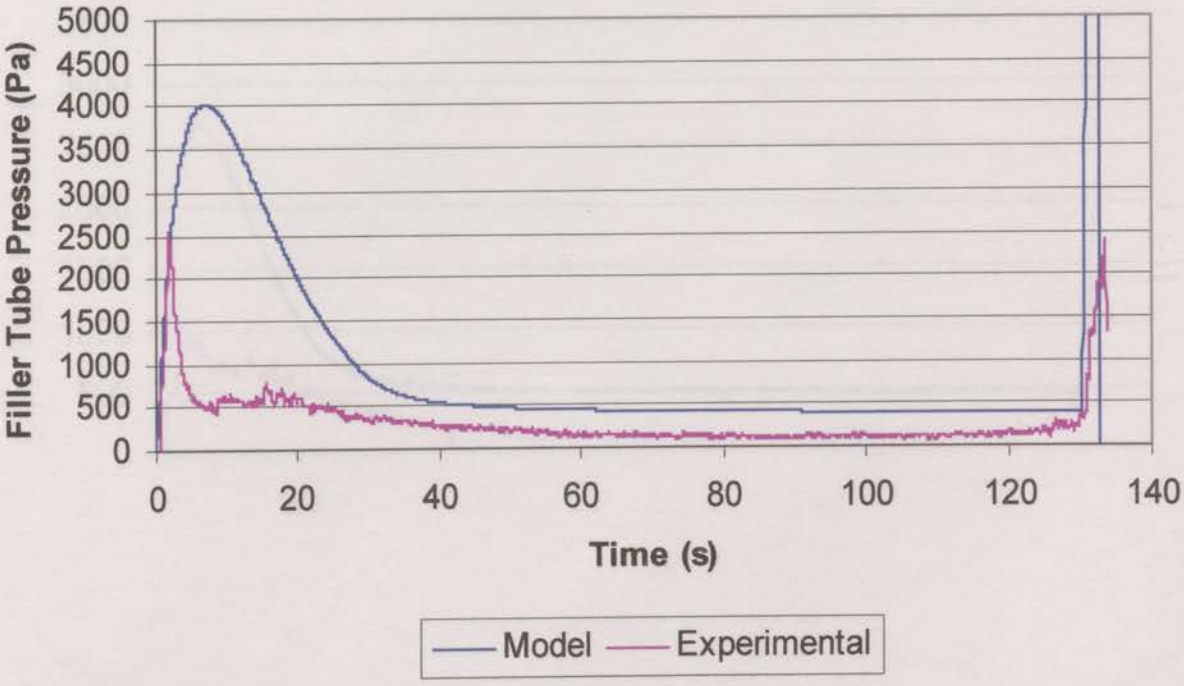

Figure A.4: Filler Pipe Pressure, D_{v2}= 9.5 mm, Q_{inL}= 38 L/min, RVP=88 kPa

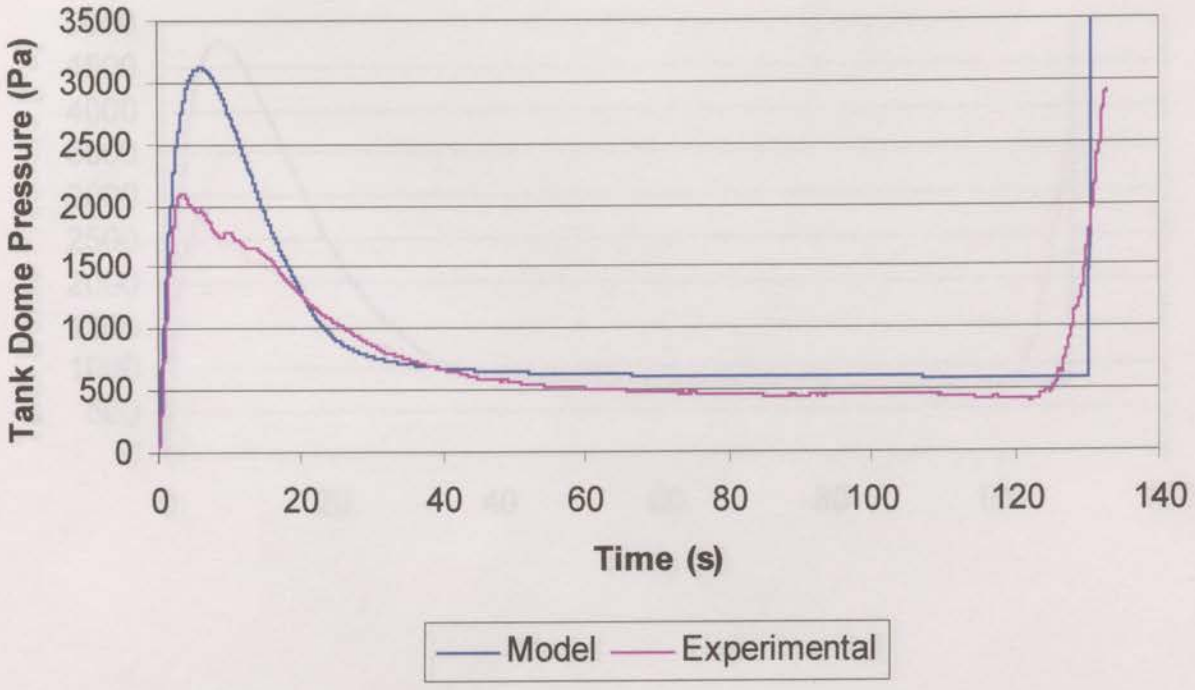

Figure A.5: Tank Dome Pressure, D_{v2}= 9.5 mm, Q_{inL}= 38 L/min, RVP=71 kPa

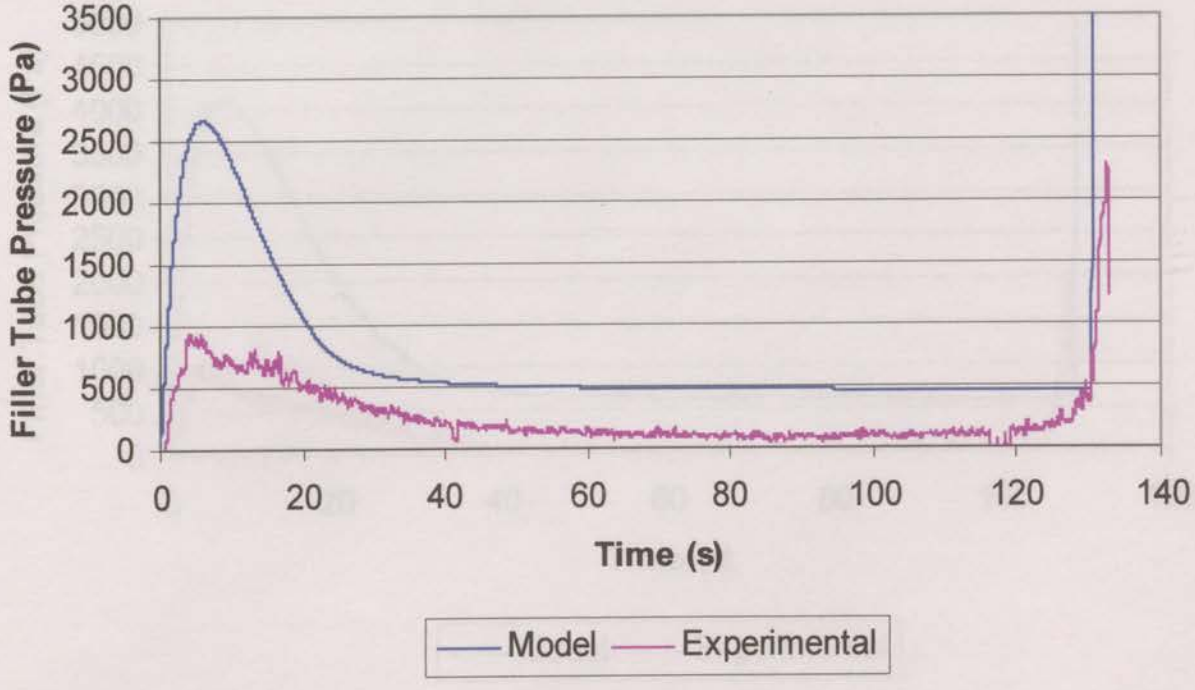

Figure A.6: Filler Pipe Pressure, D_{v2}= 9.5 mm, Q_{inL}= 38 L/min, RVP=71 kPa

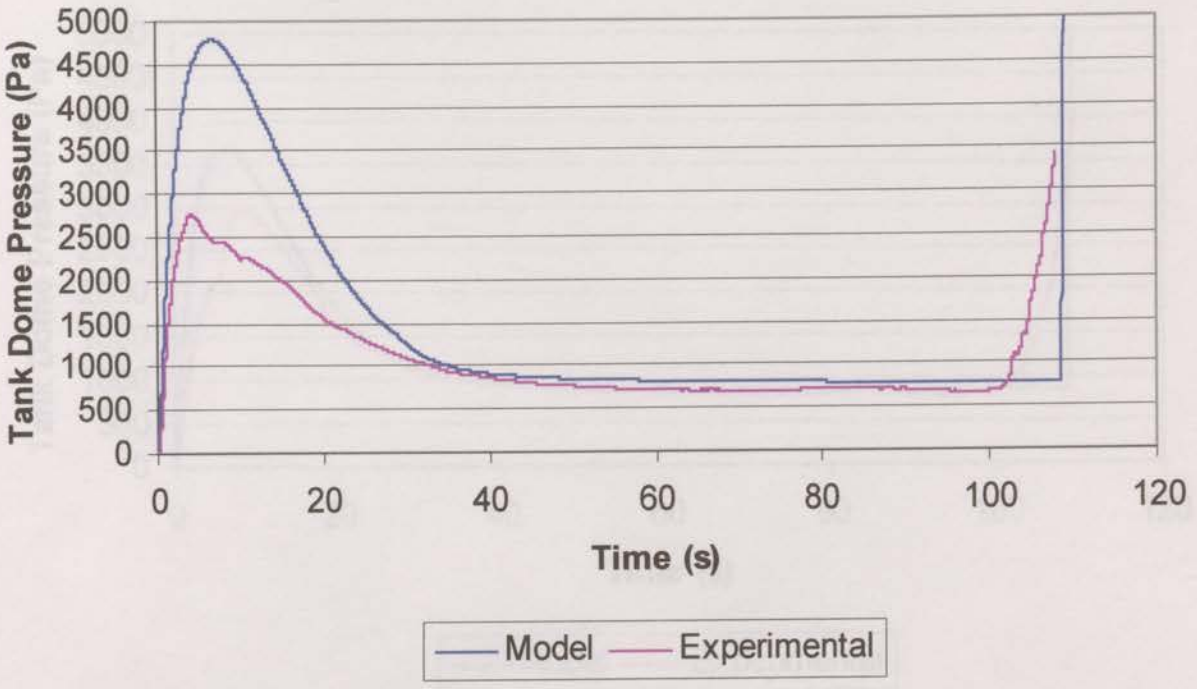

Figure A.7: Tank Dome Pressure, D_{v2}= 9.5 mm, Q_{inL}= 45 L/min, RVP=82 kPa

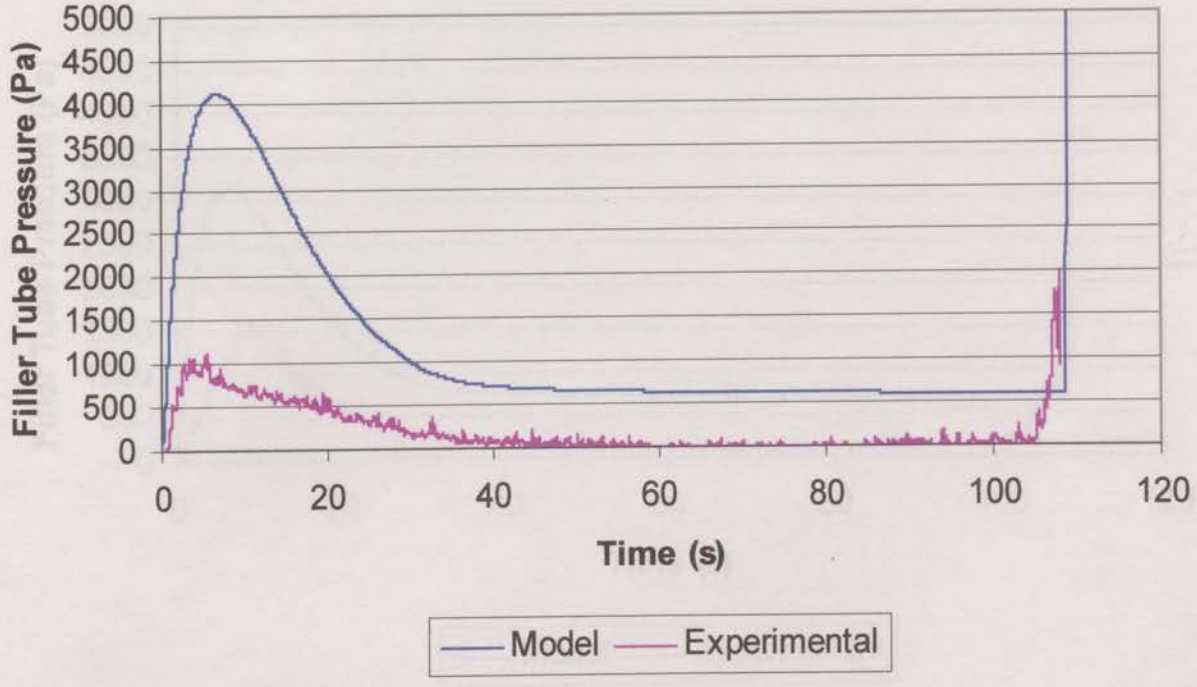

Figure A.8: Filler Pipe Pressure, D_{v2}= 9.5 mm, Q_{inL}= 45 L/min, RVP=82 kPa

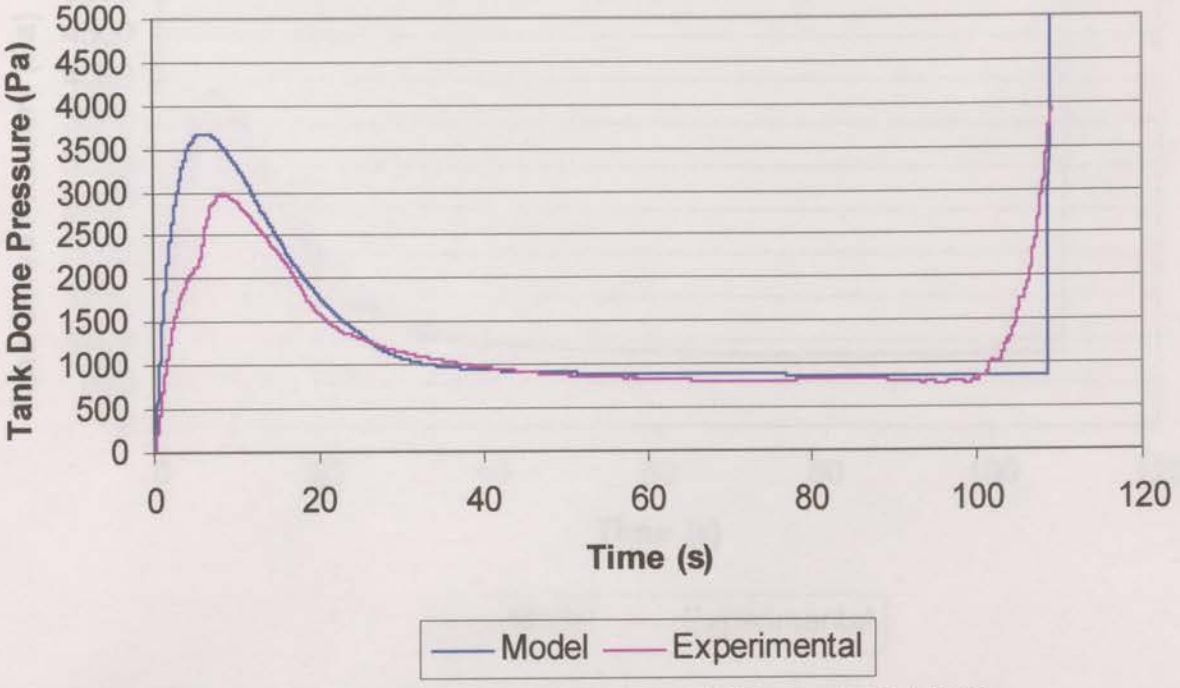

Figure A.9: Tank Dome Pressure, D_{v2}= 9.5 mm, Q_{inL}= 45 L/min, RVP=70 kPa

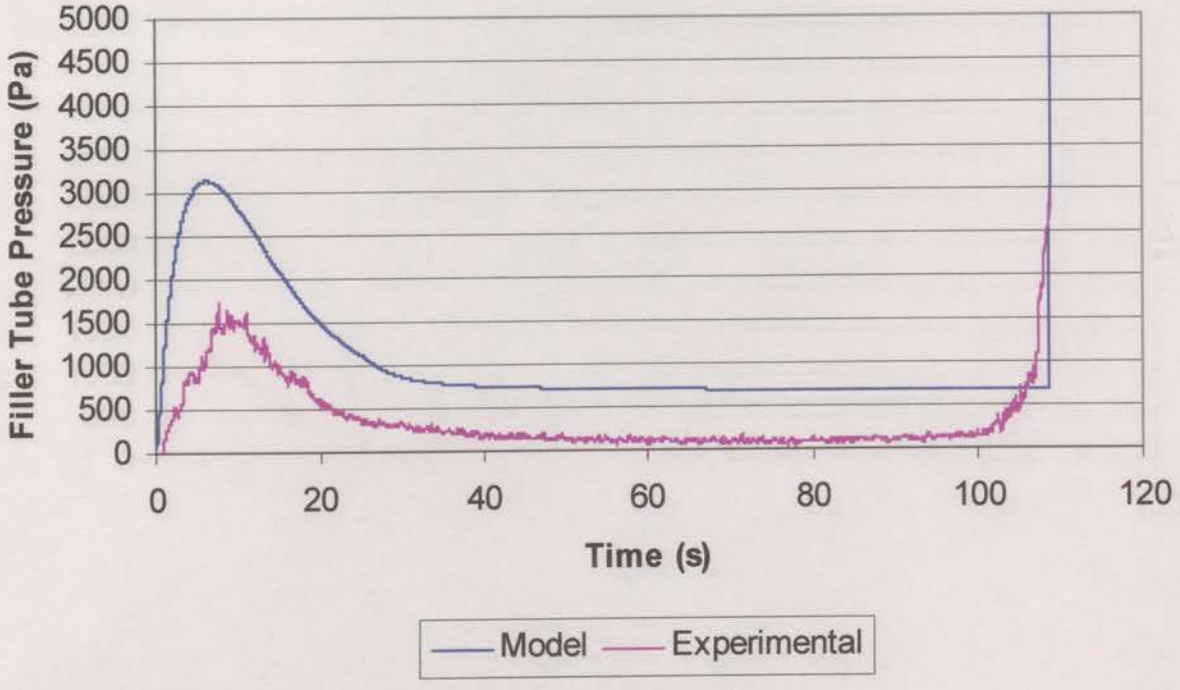

Figure A.10: Filler Pipe Pressure, D_{v2}= 9.5 mm, Q_{inL}= 45 L/min, RVP=70 kPa

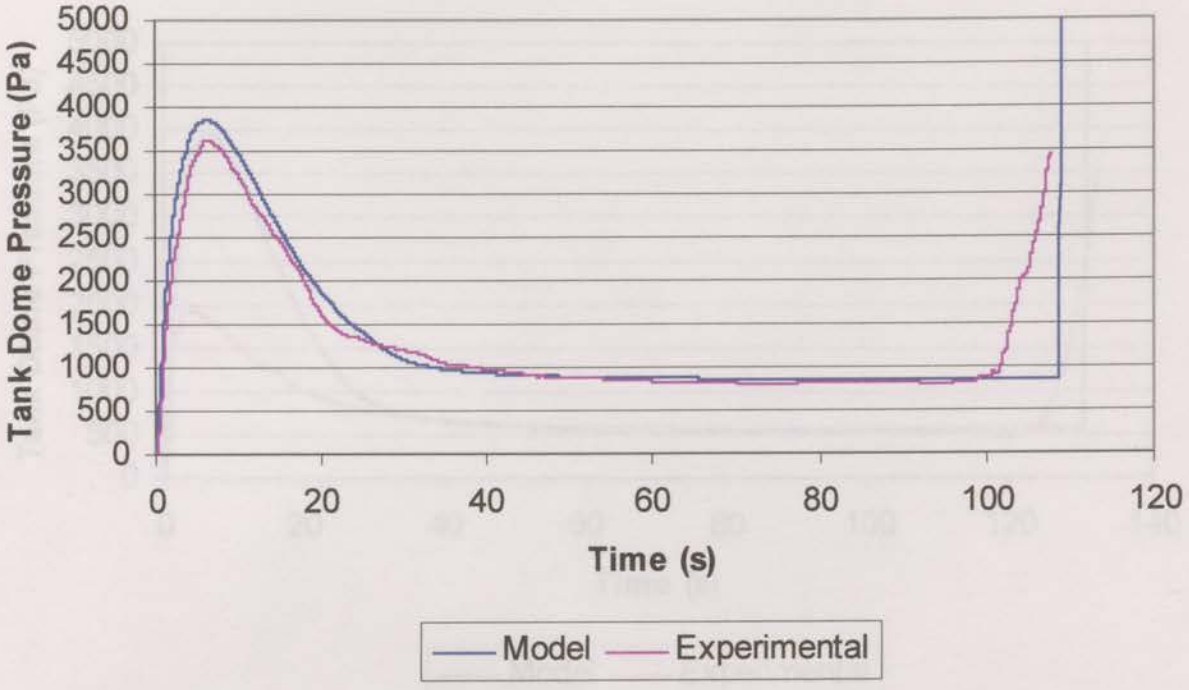

Figure A.11: Tank Dome Pressure, D_{v2}= 9.5 mm, Q_{inL}= 45 L/min, RVP=72 kPa

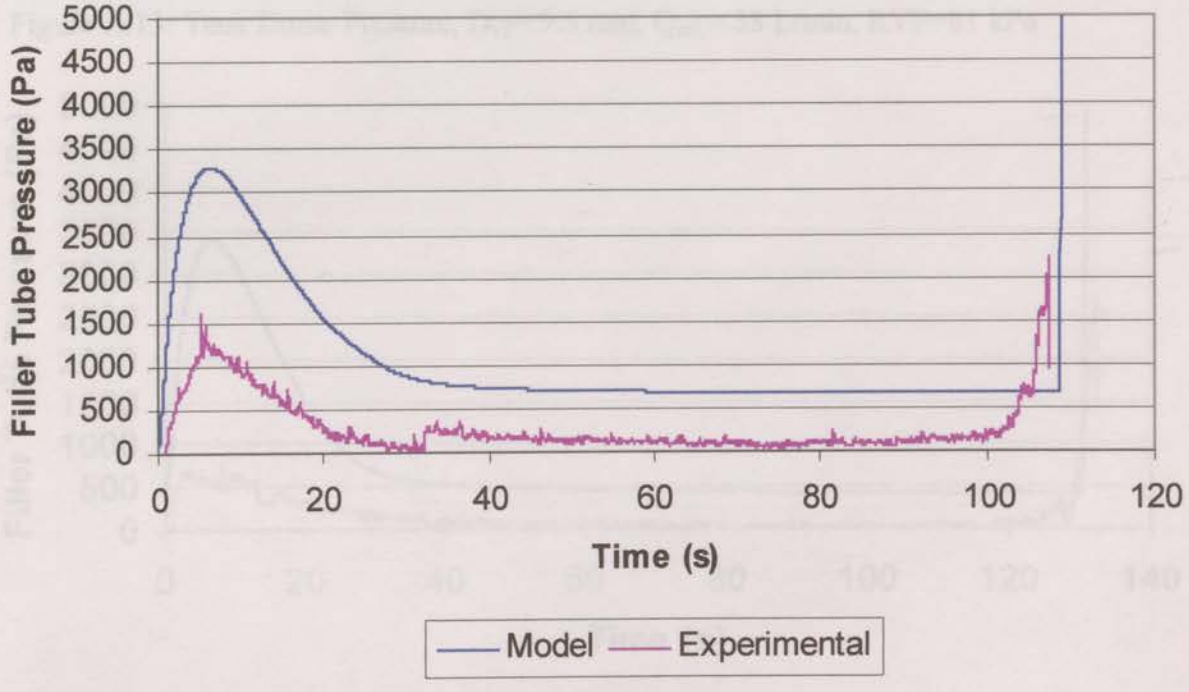

Figure A.12: Filler Pipe Pressure, D_{v2}= 9.5 mm, Q_{inL}= 45 L/min, RVP=72 kPa

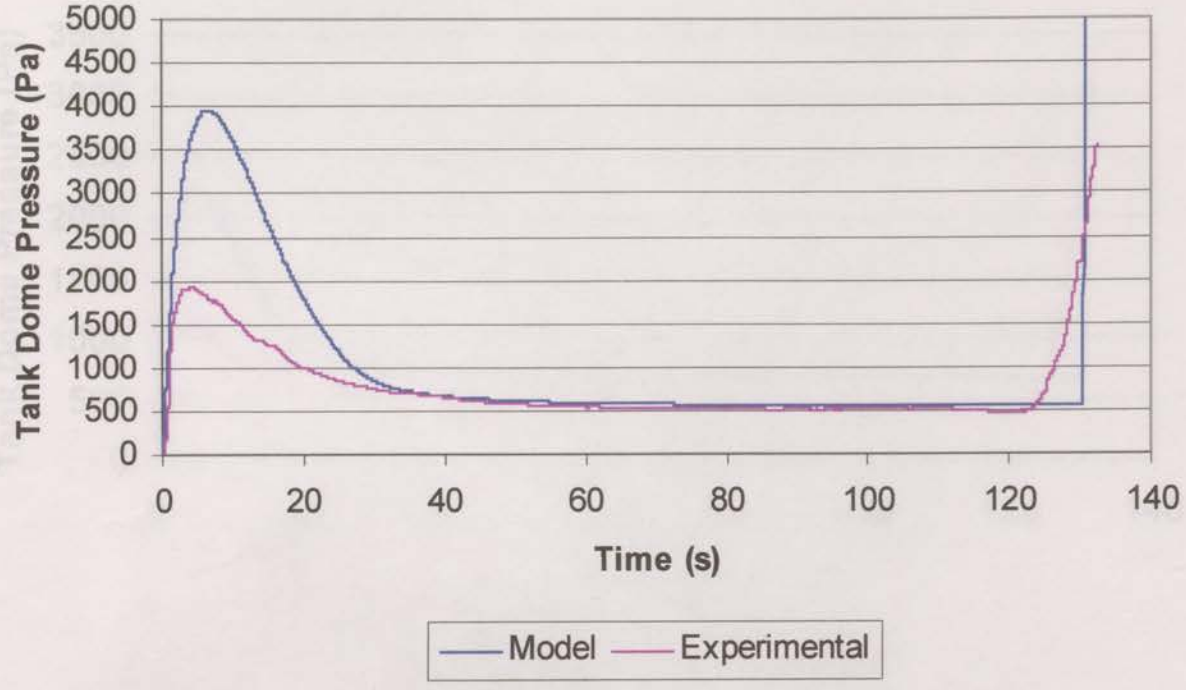

Figure A.13: Tank Dome Pressure, D_{v2}= 9.5 mm, Q_{inL}= 38 L/min, RVP=81 kPa

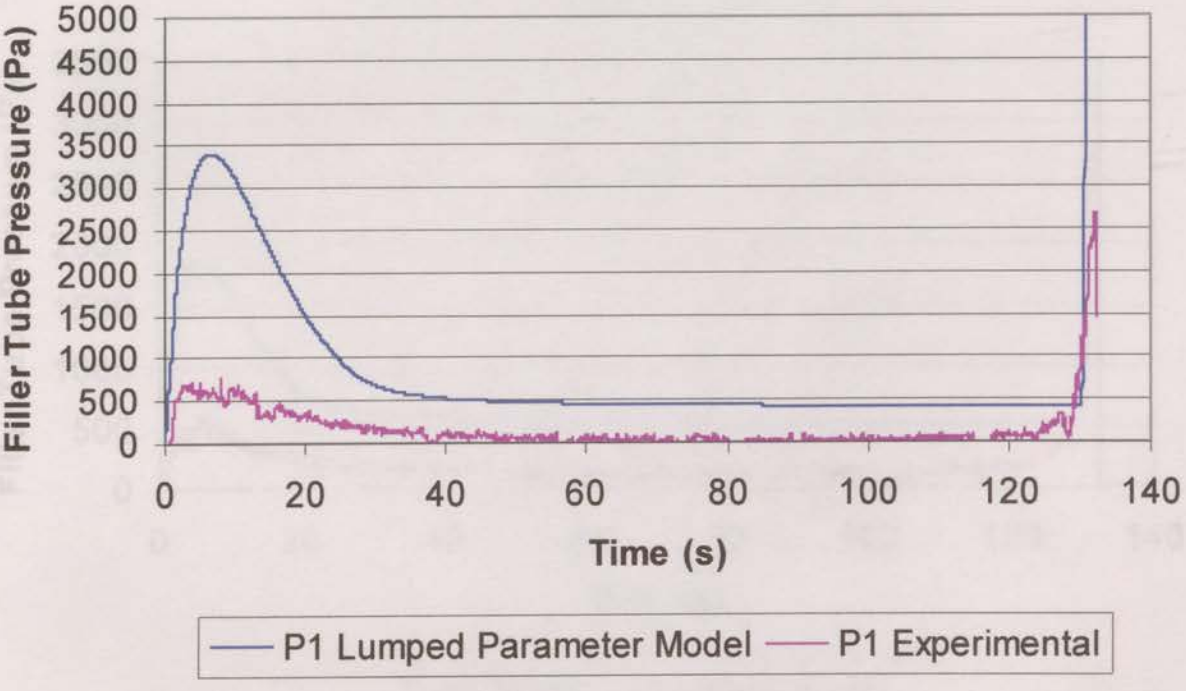

Figure A.14: Filler Pipe Pressure, D_{v2}= 9.5 mm, Q_{inL}= 38 L/min, RVP=81 kPa

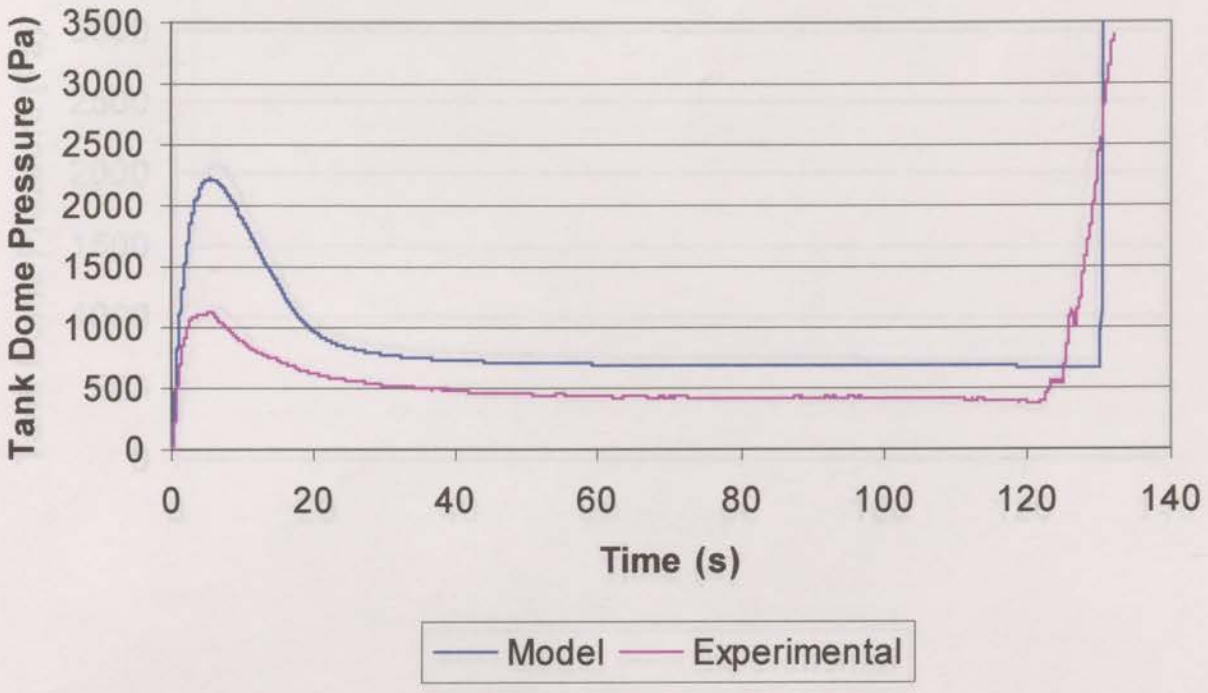

Figure A.15: Tank Dome Pressure, D_{v2}= 9.5 mm, Q_{inL}= 38 L/min, RVP=57 kPa

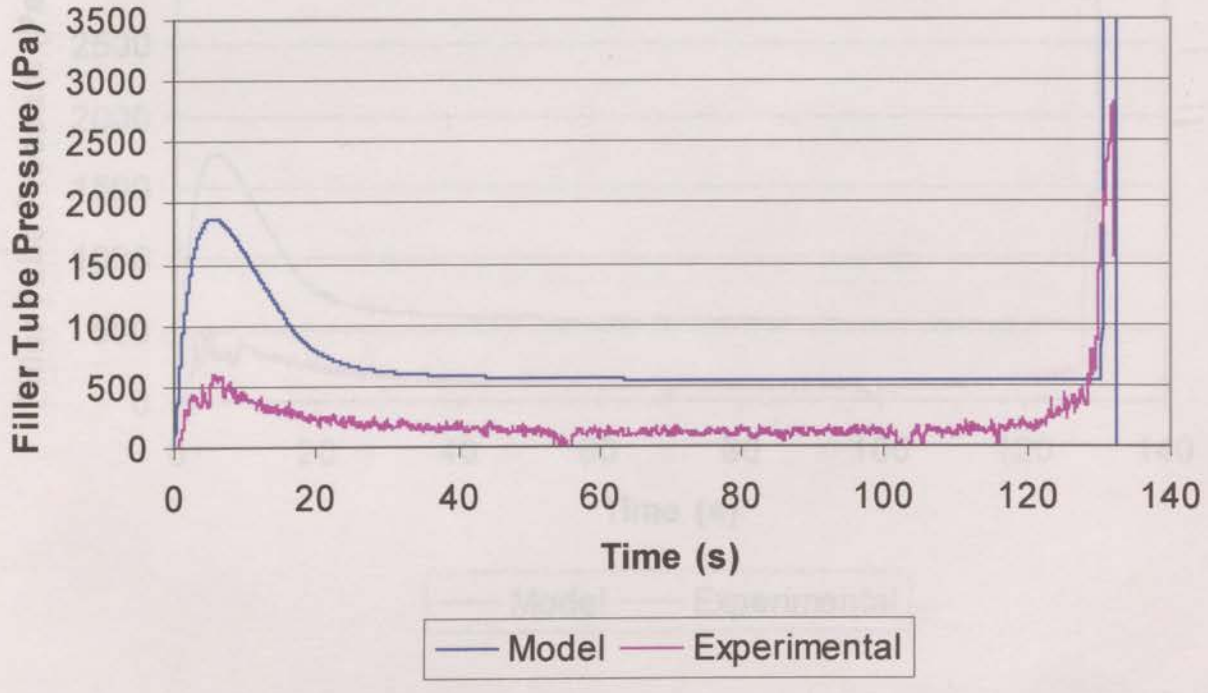

Figure A.16: Filler Pipe Pressure, D_{v2}= 9.5 mm, Q_{inL}= 38 L/min, RVP=57 kPa

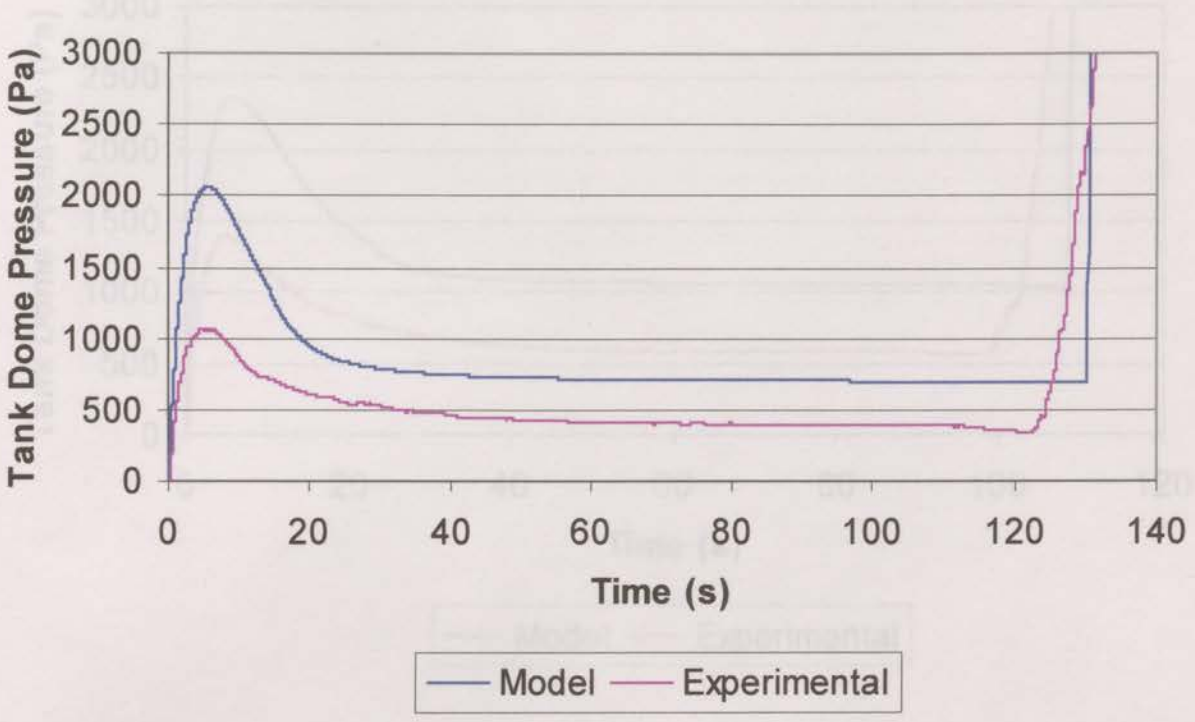

Figure A.17: Tank Dome Pressure, D_{v2}= 9.5 mm, Q_{inL}= 38 L/min, RVP=54 kPa

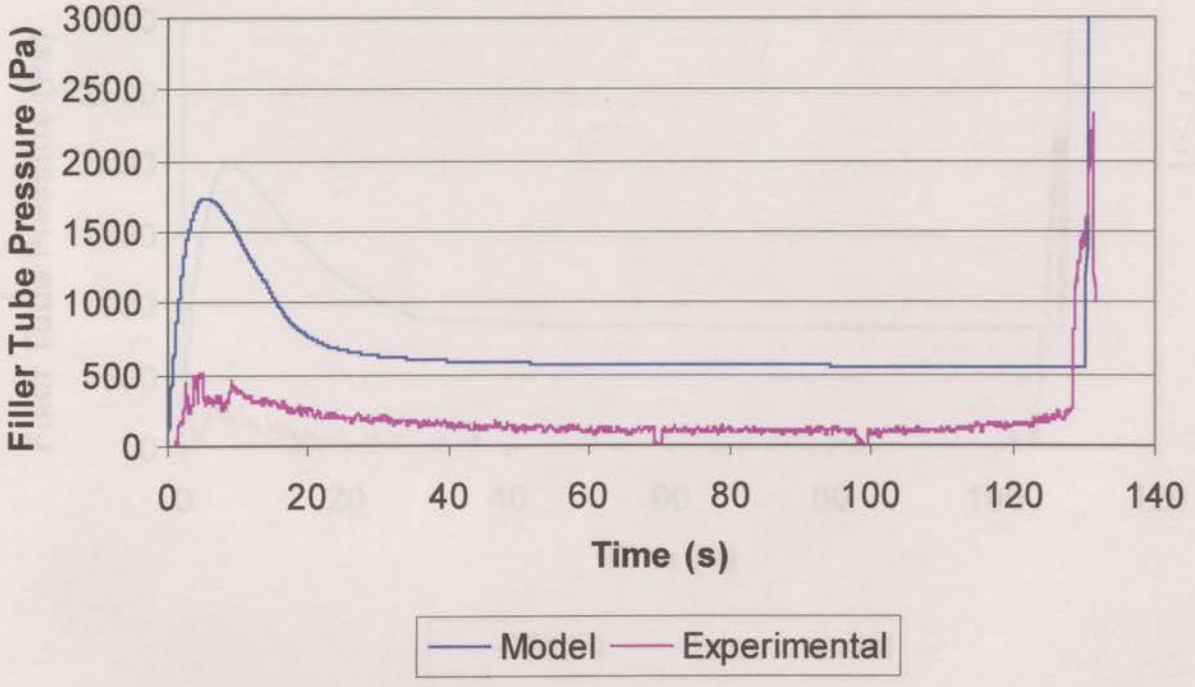

Figure A.18: Filler Pipe Pressure, D_{v2}= 9.5 mm, Q_{inL}= 38 L/min, RVP=54 kPa

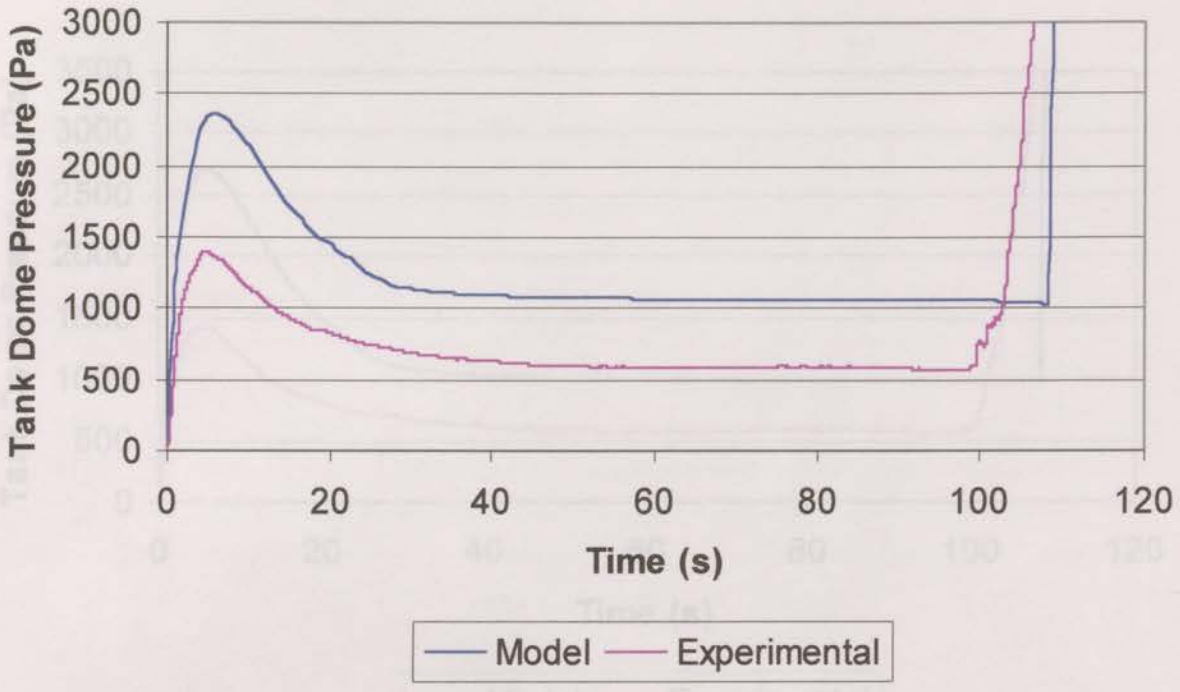

Figure A.19: Tank Dome Pressure, D_{v2}= 9.5 mm, Q_{inL}= 45 L/min, RVP=49 kPa

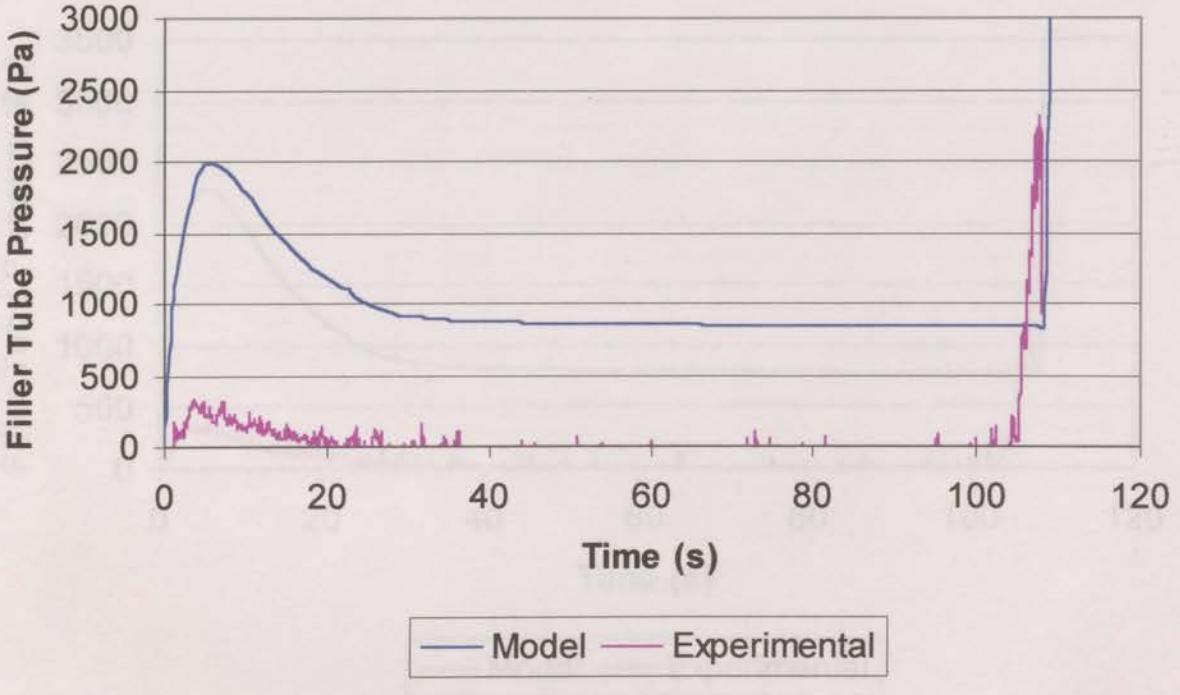

Figure A.20: Filler Pipe Pressure, D_{v2}= 9.5 mm, Q_{inL}= 45 L/min, RVP=49 kPa

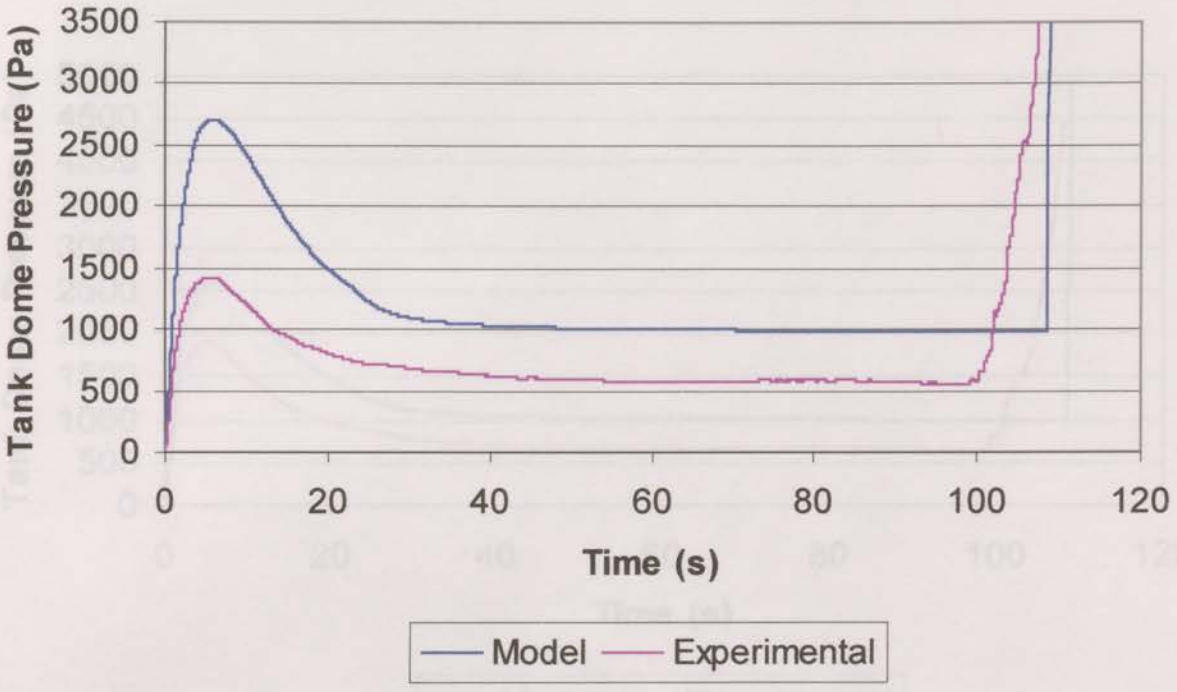

Figure A.21: Tank Dome Pressure, D_{v2}= 9.5 mm, Q_{inL}= 45 L/min, RVP=56 kPa

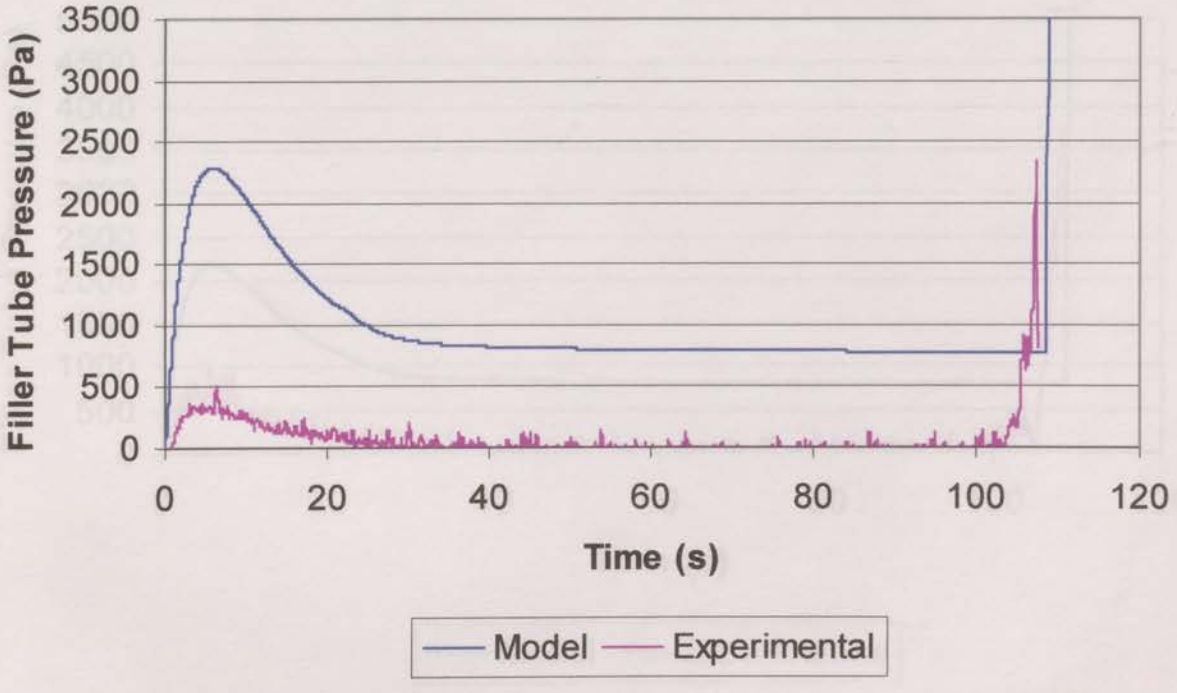

Figure A.22: Filler Pipe Pressure, D_{v2}= 9.5 mm, Q_{inL}= 45 L/min, RVP=56 kPa

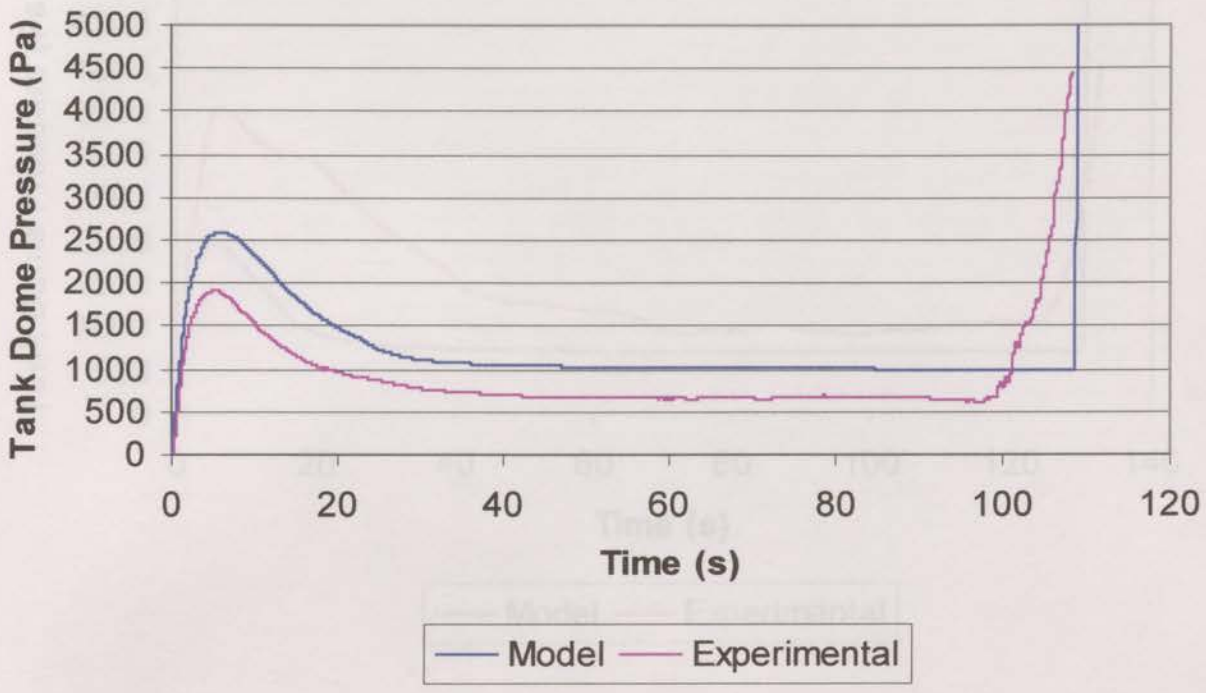

Figure A.23: Tank Dome Pressure, D_{v2}= 9.5 mm, Q_{inL}= 45 L/min, RVP=54 kPa

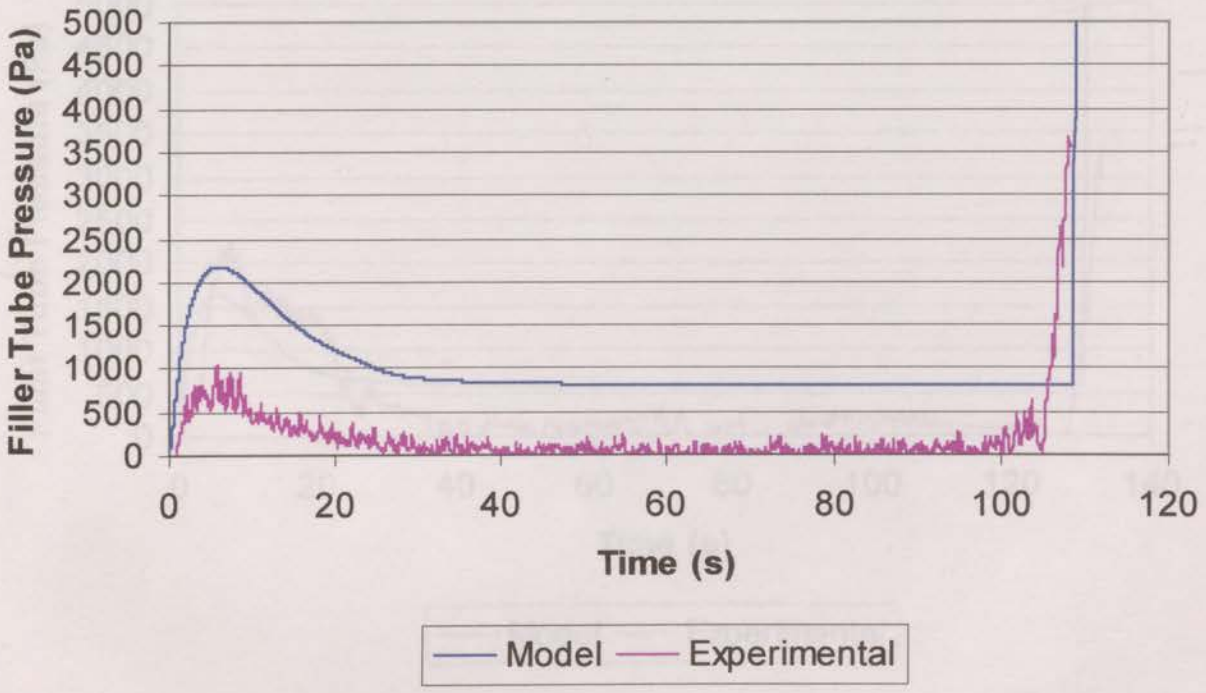

Figure A.24: Filler Pipe Pressure, D_{v2}= 9.5 mm, Q_{inL}= 45 L/min, RVP=54 kPa

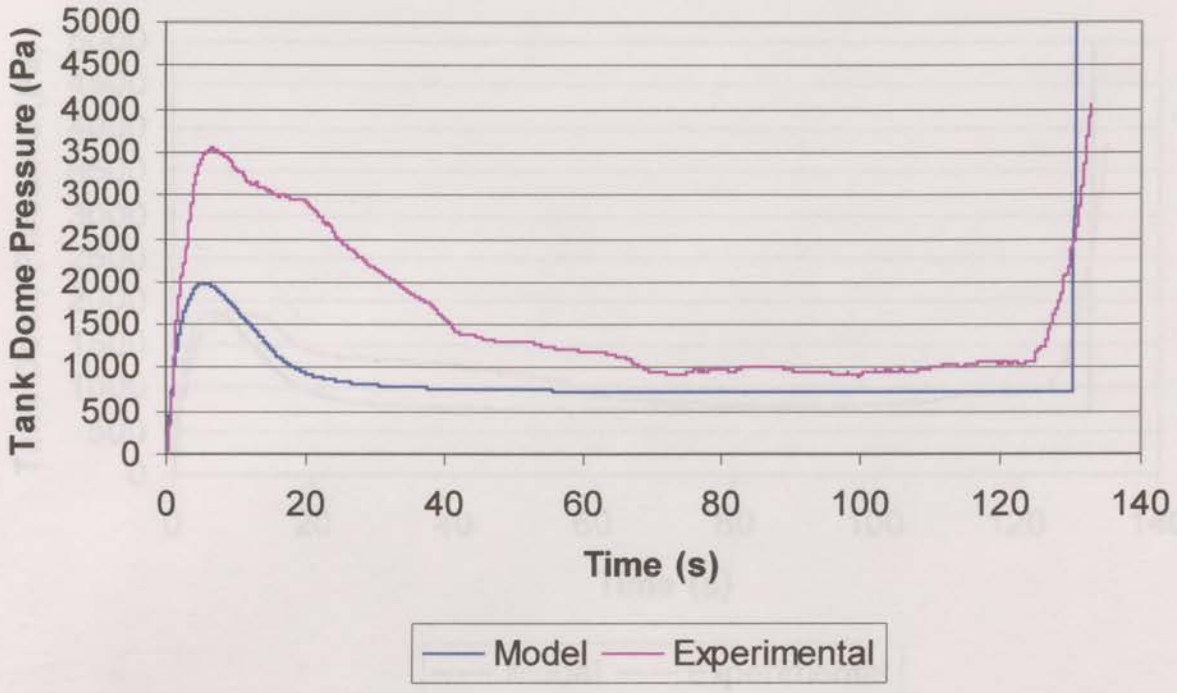

Figure A.25: Tank Dome Pressure, D_{v2}= 6.4 mm, Q_{inL}= 38 L/min, RVP=52 kPa

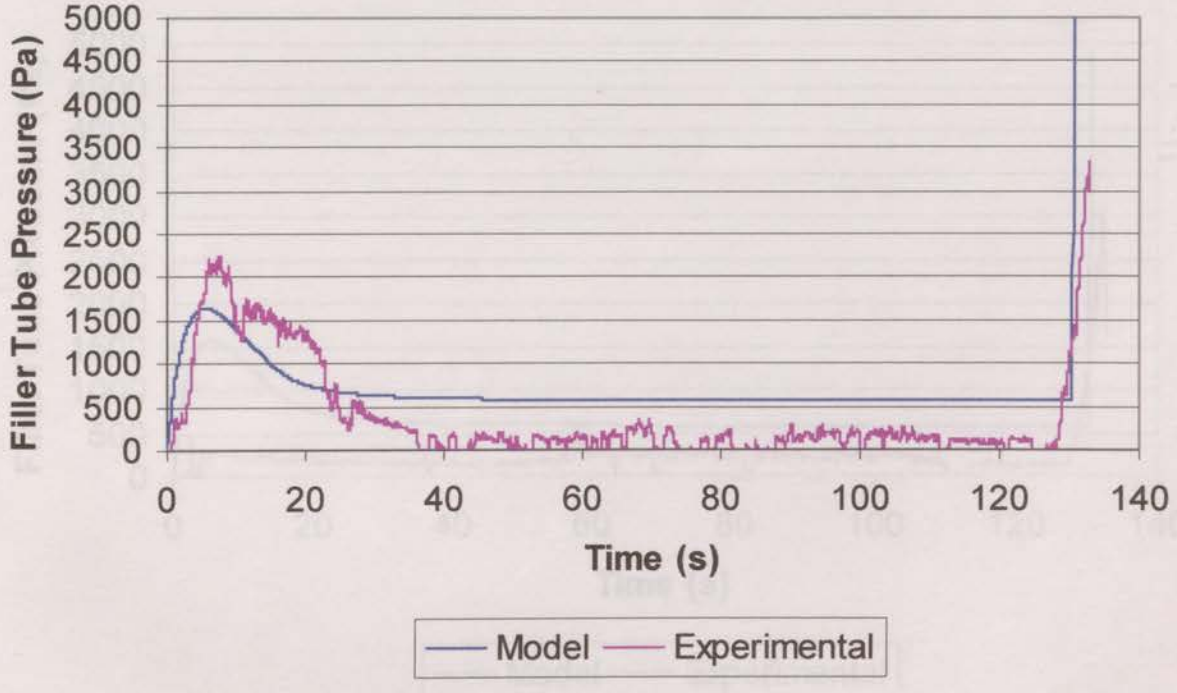

Figure A.26: Filler Pipe Pressure, D_{v2}= 6.4 mm, Q_{inL}= 38 L/min, RVP=52 kPa

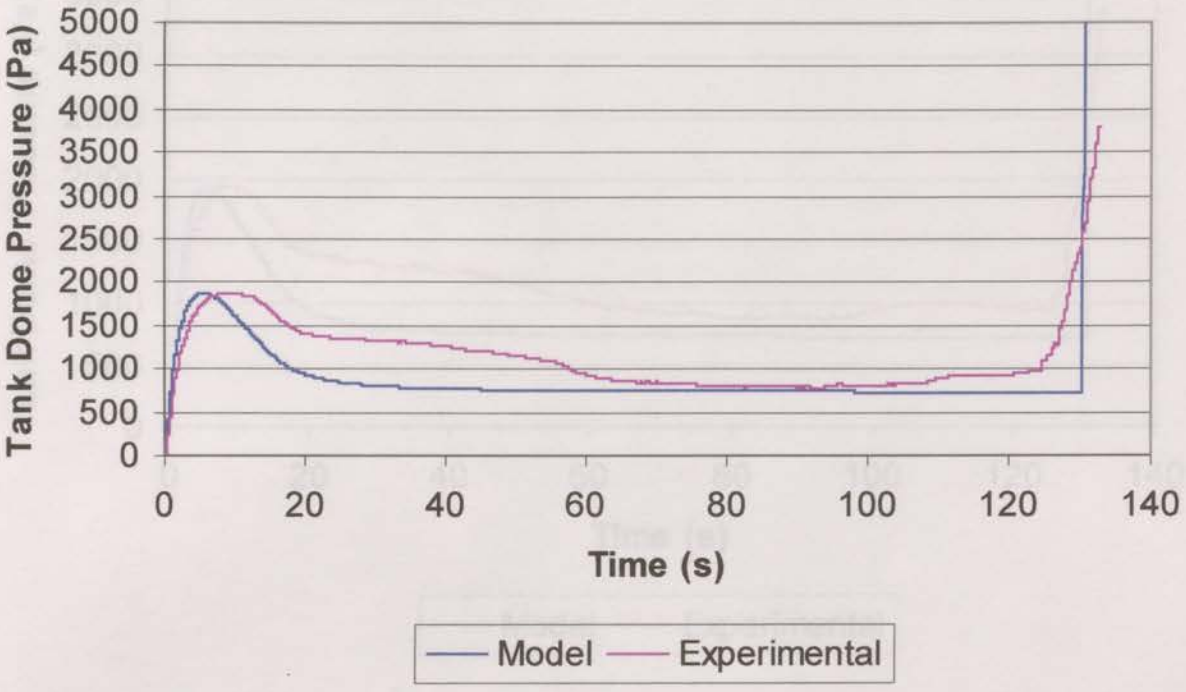

Figure A.27: Tank Dome Pressure, D_{v2}= 6.4 mm, Q_{inL}= 38 L/min, RVP=50 kPa

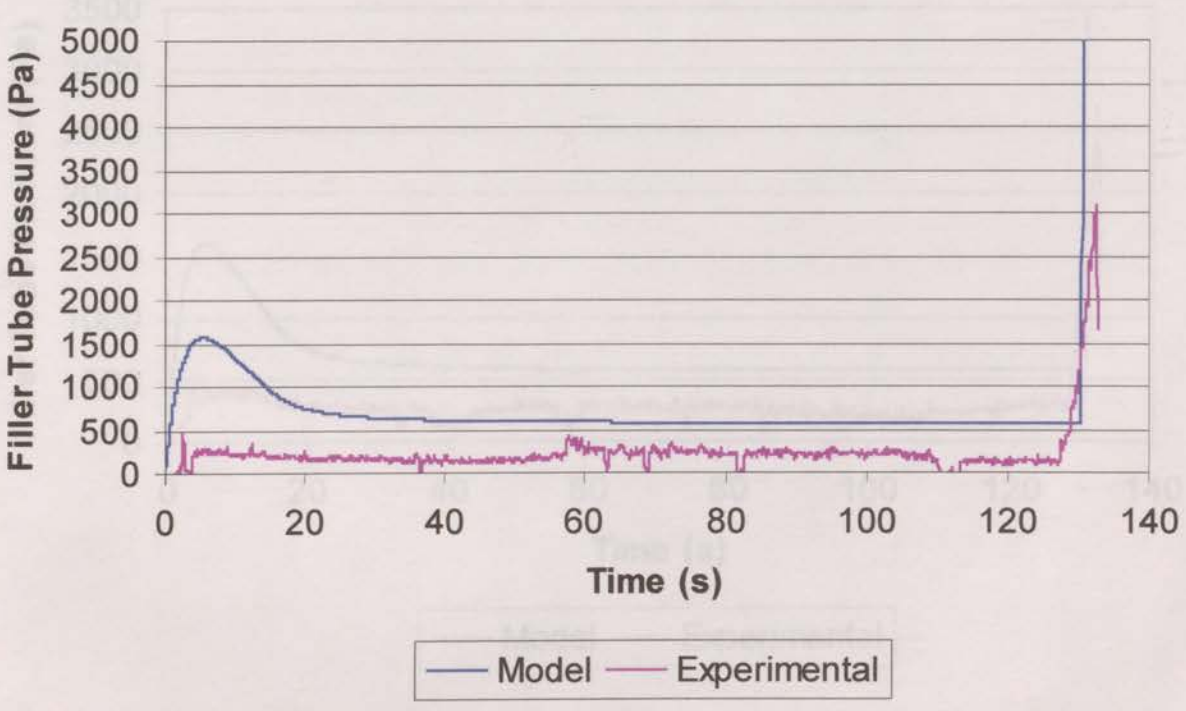

Figure A.28: Filler Pipe Pressure, D_{v2}= 6.4 mm, Q_{inL}= 38 L/min, RVP=50 kPa

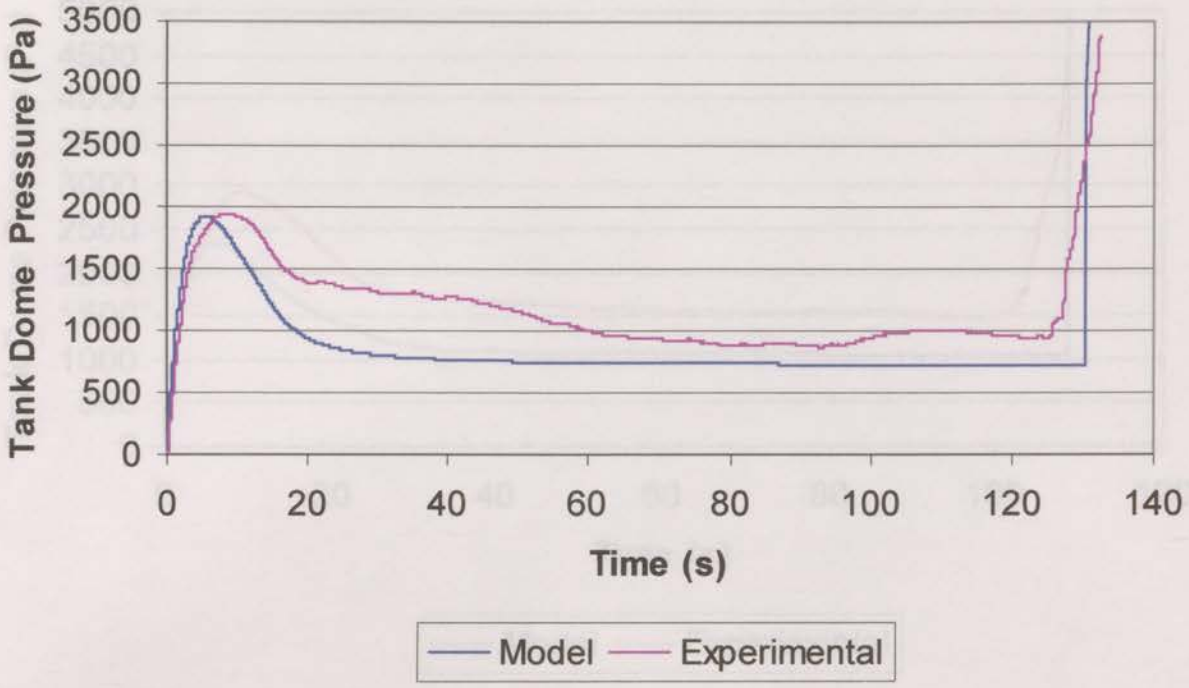

Figure A.29: Tank Dome Pressure, D_{v2}= 6.4 mm, Q_{inL}= 38 L/min, RVP=51 kPa

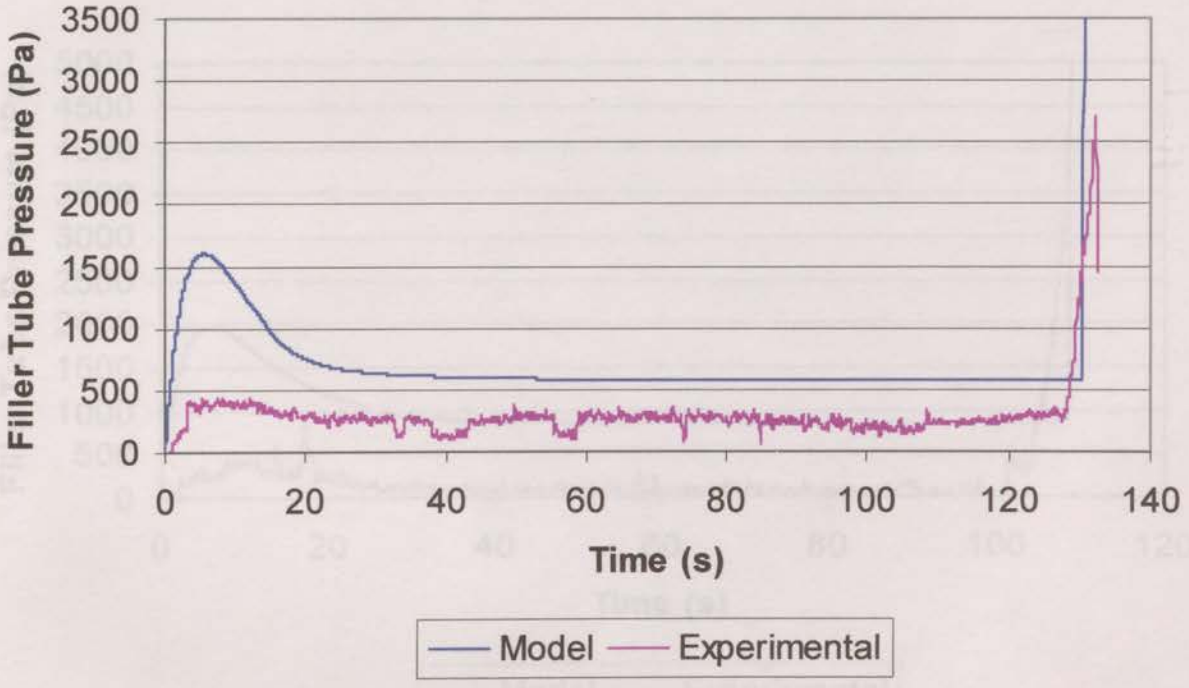

Figure A.30: Filler Pipe Pressure, D_{v2}= 6.4 mm, Q_{inL}= 38 L/min, RVP=51 kPa

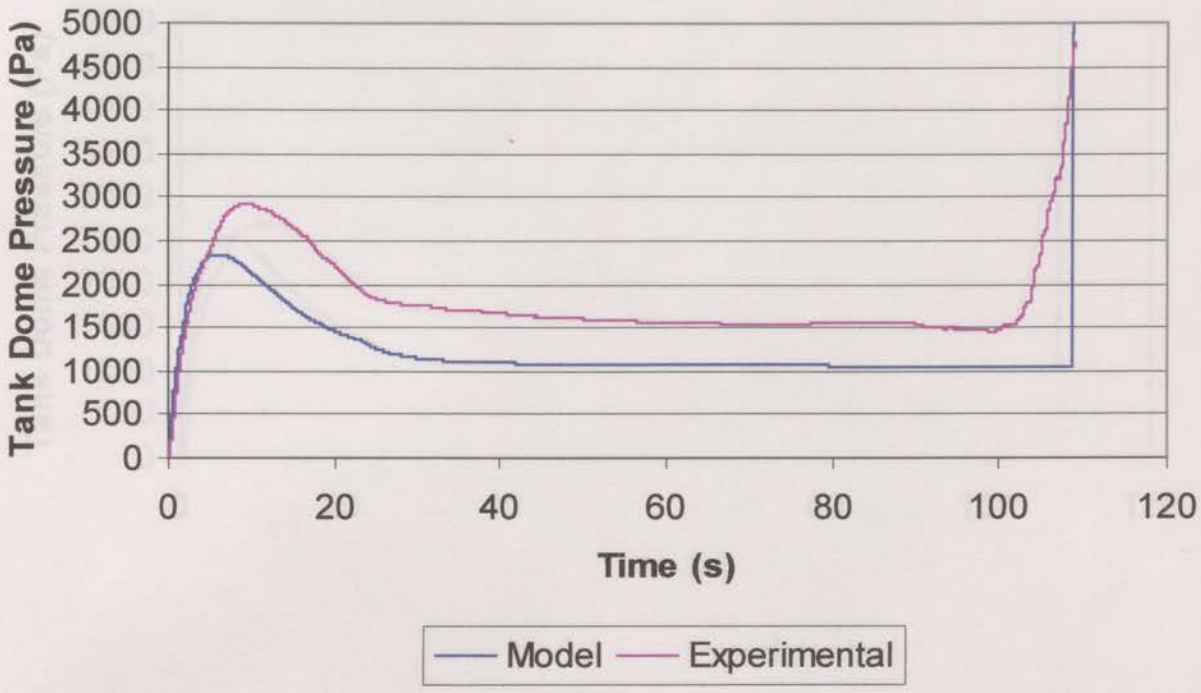

Figure A.31: Tank Dome Pressure, D_{v2}= 6.4 mm, Q_{inL}= 45 L/min, RVP=49 kPa

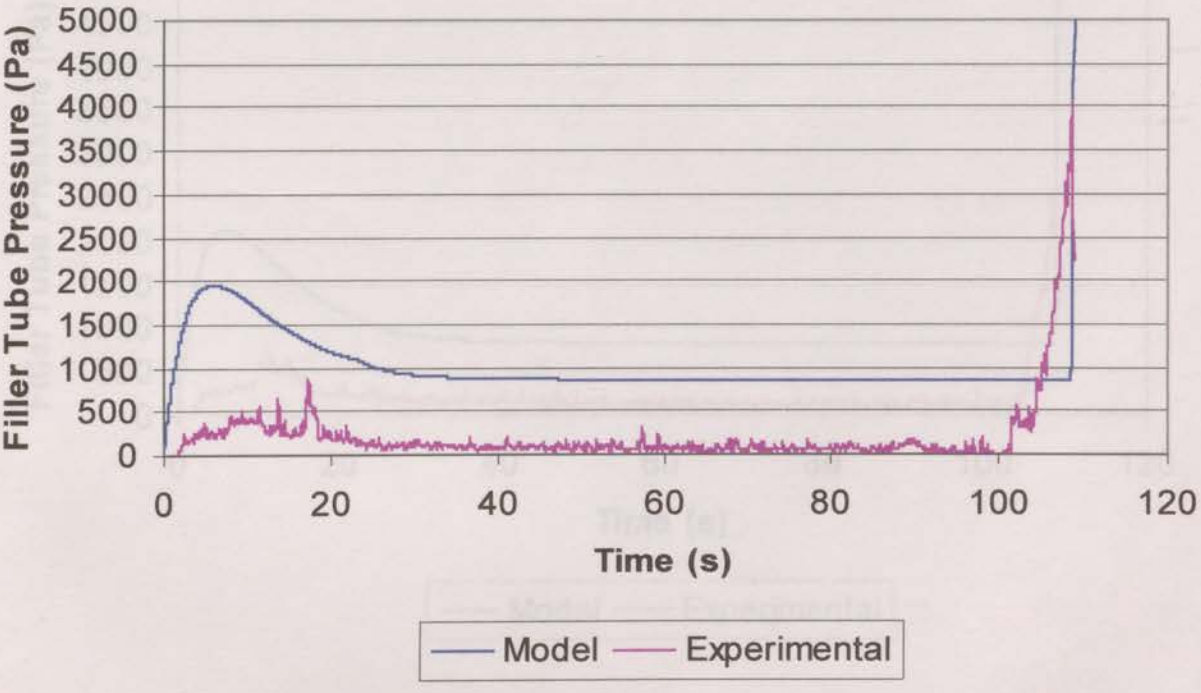

Figure A.32: Filler Pipe Pressure, D_{v2}= 6.4 mm, Q_{inL}= 45 L/min, RVP=49 kPa

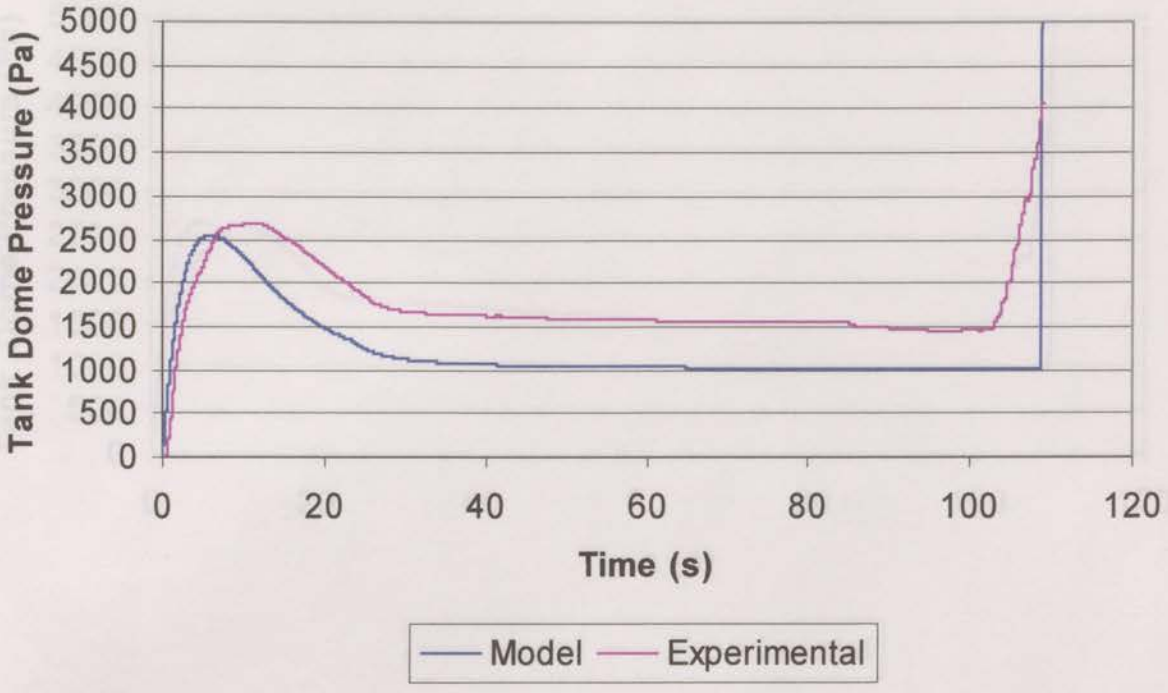

Figure A.33: Tank Dome Pressure, D_{v2}= 6.4 mm, Q_{inL}= 45 L/min, RVP=53 kPa

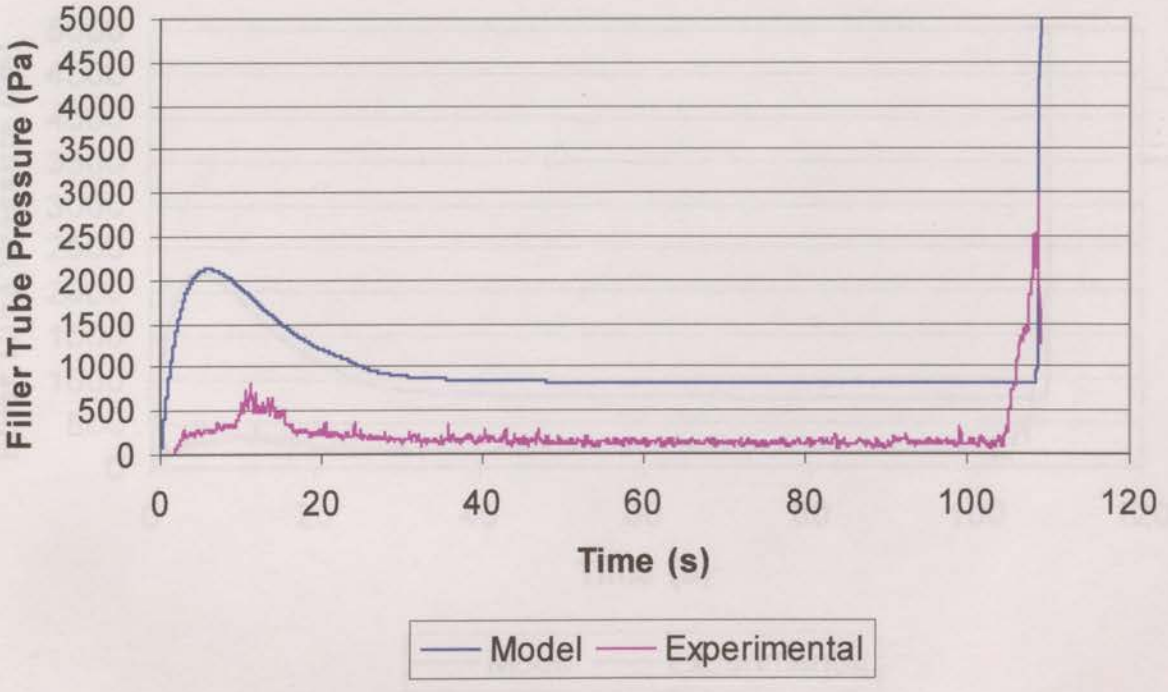

Figure A.34: Filler Pipe Pressure, D_{v2}= 6.4 mm, Q_{inL}= 45 L/min, RVP=53 kPa

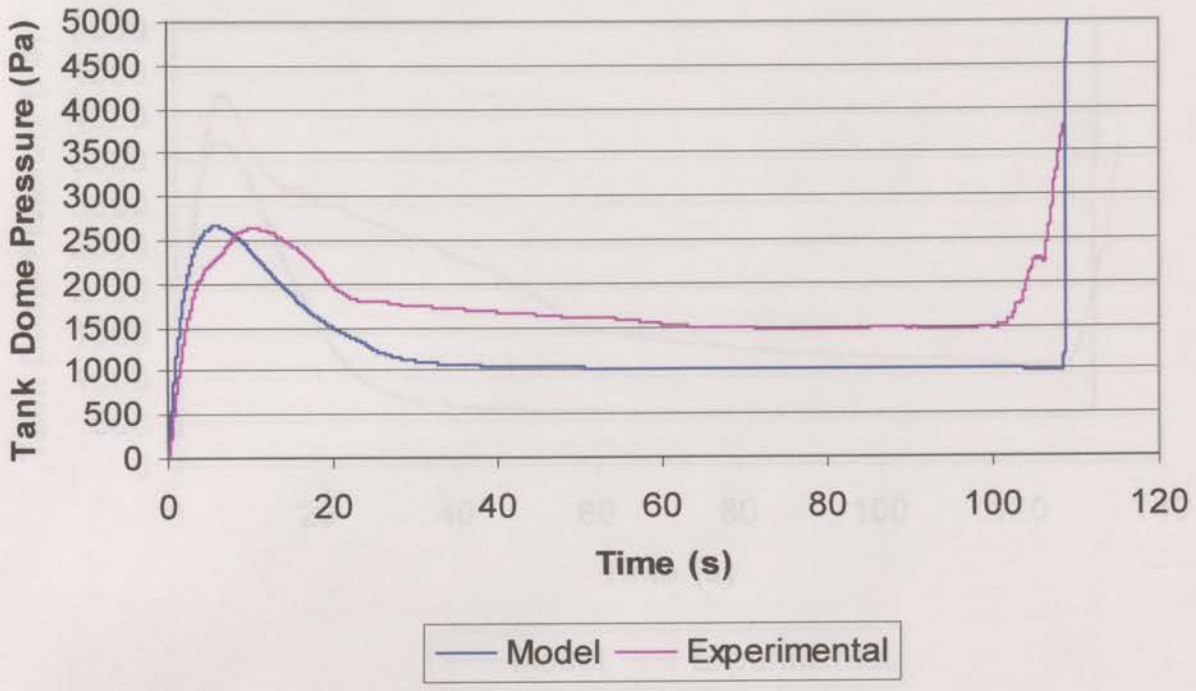

Figure A.35: Tank Dome Pressure, D_{v2}= 6.4 mm, Q_{inL}= 45 L/min, RVP=55 kPa

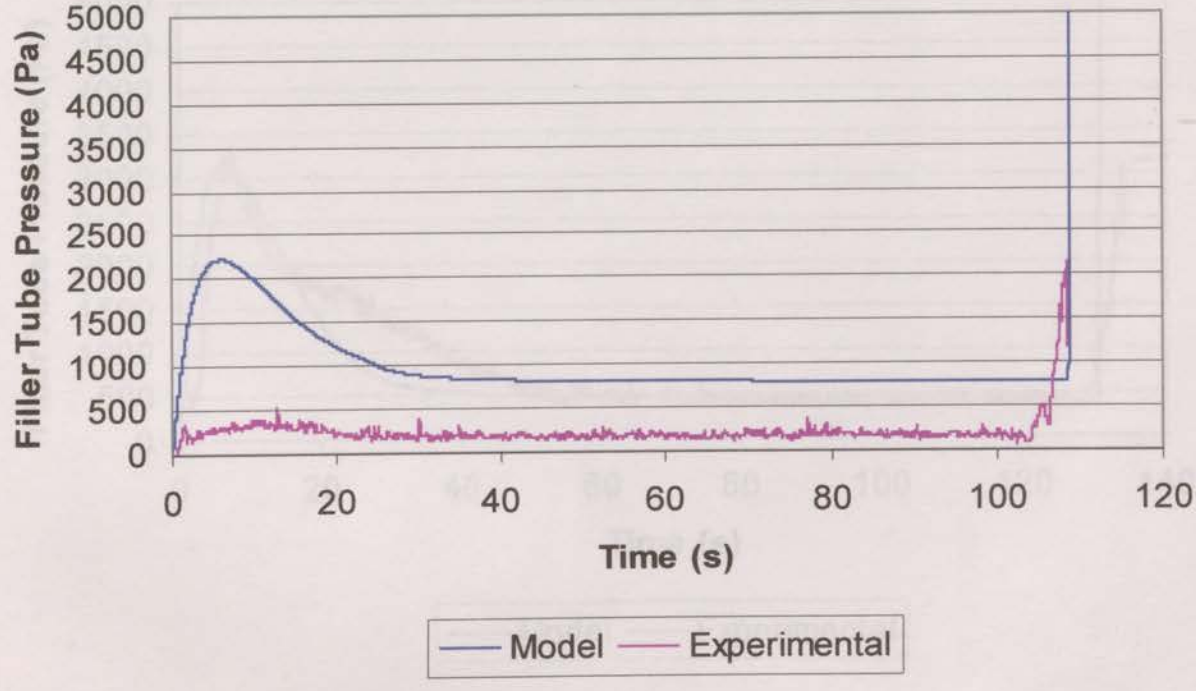

Figure A.36: Filler Pipe Pressure, D_{v2}= 6.4 mm, Q_{inL}= 45 L/min, RVP=55 kPa

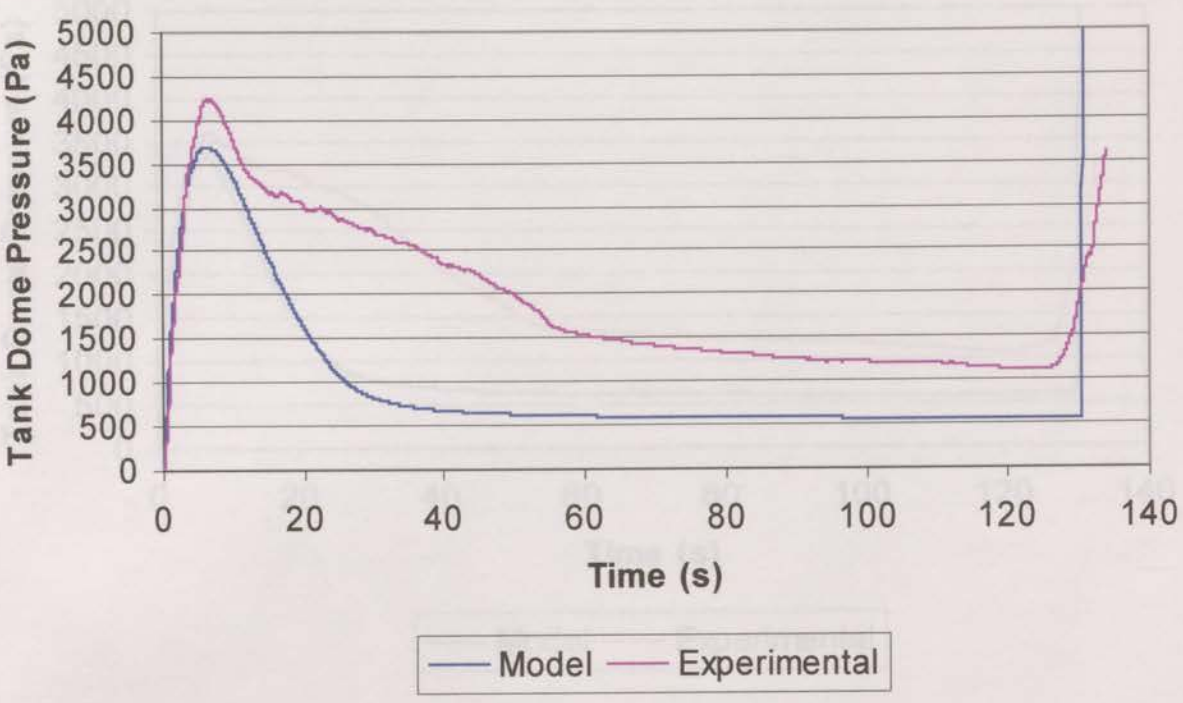

Figure A.37: Tank Dome Pressure, D_{v2}= 6.4 mm, Q_{inL}= 38 L/min, RVP=78 kPa

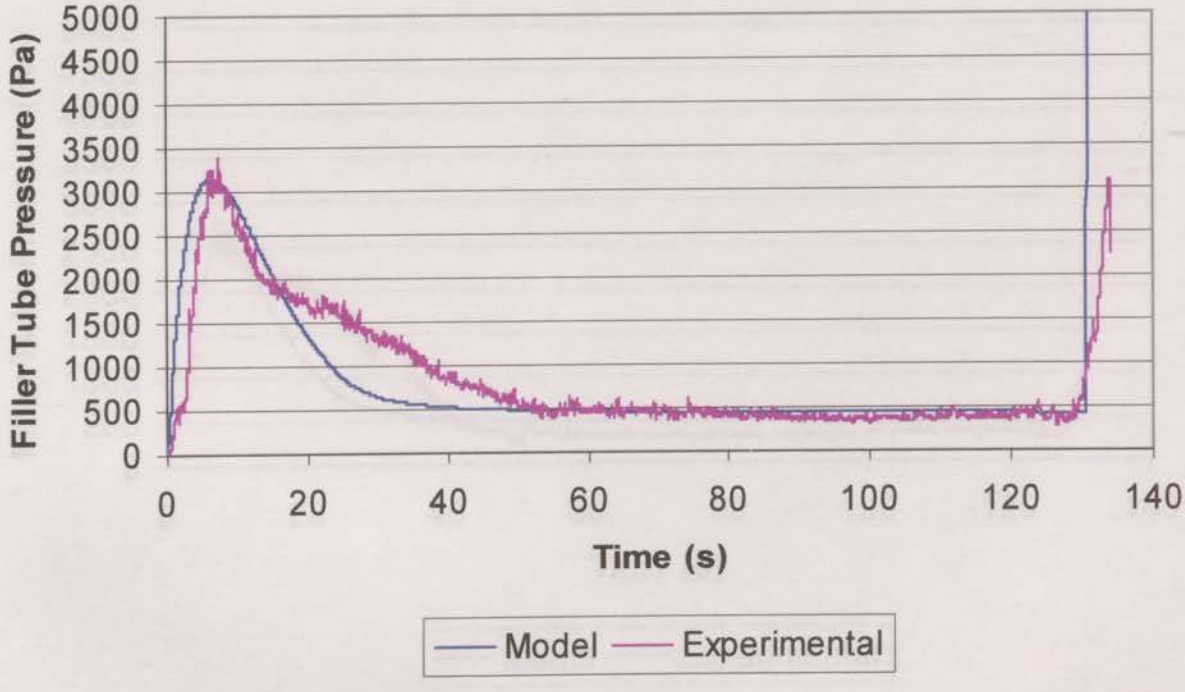

Figure A.38: Filler Pipe Pressure, D_{v2}= 6.4 mm, Q_{inL}= 38 L/min, RVP=78 kPa

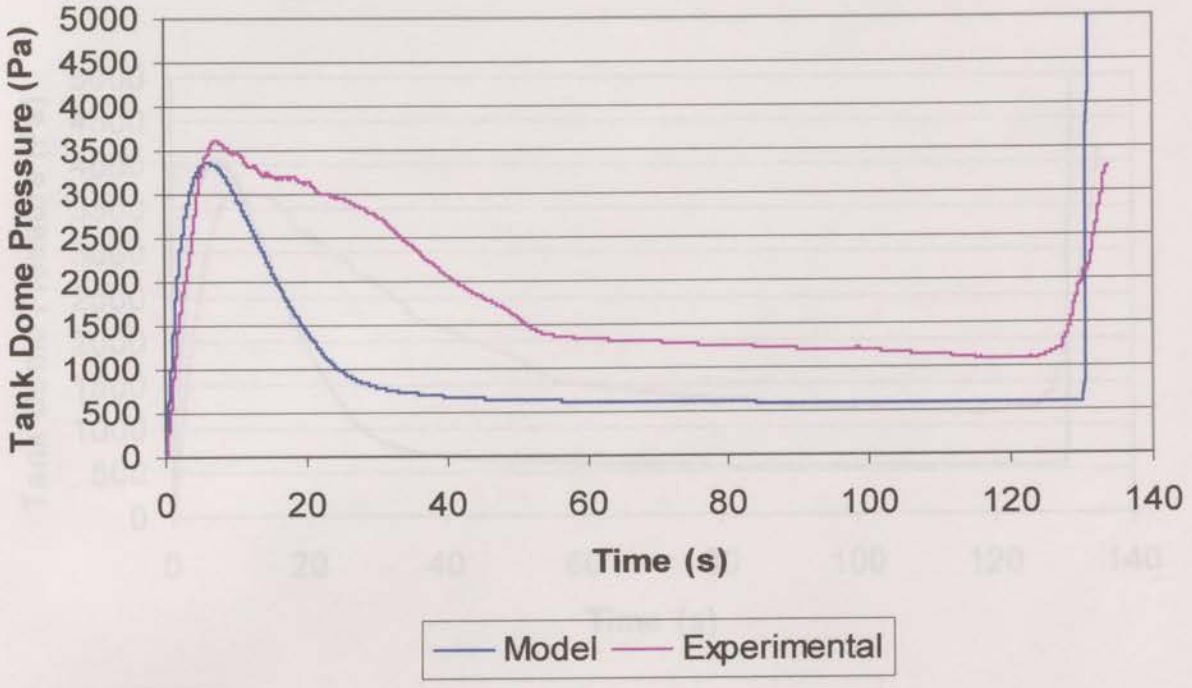

Figure A.39: Tank Dome Pressure, D_{v2}= 6.4 mm, Q_{inL}= 38 L/min, RVP=74 kPa

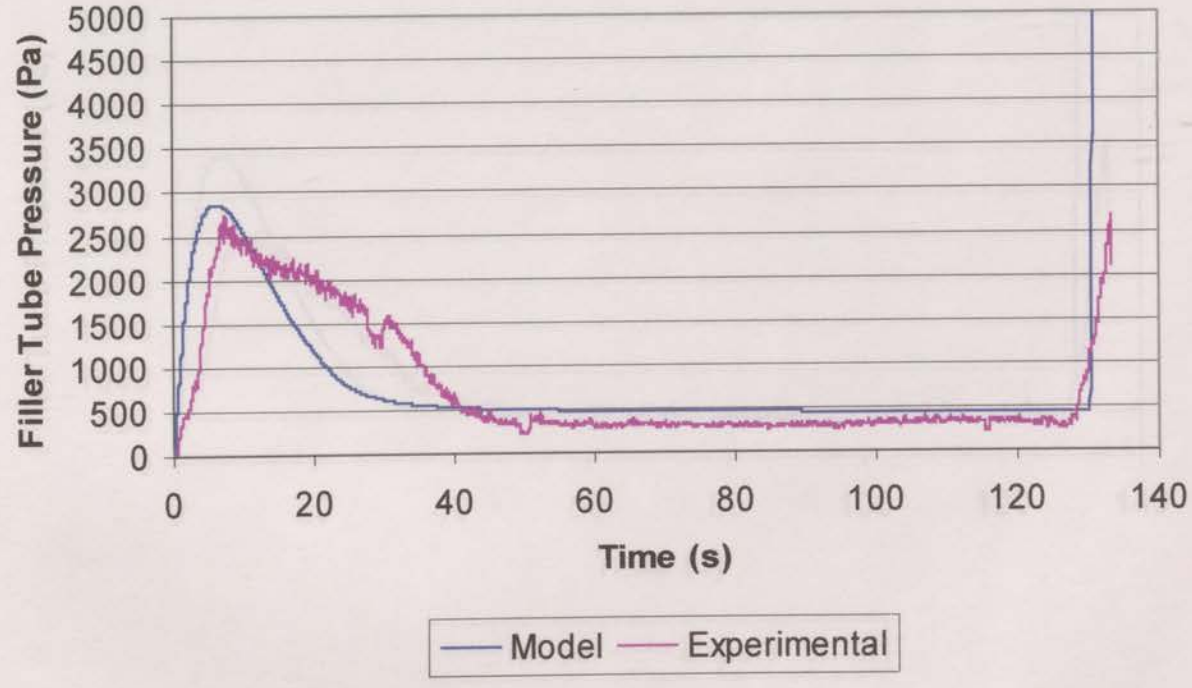

Figure A.40: Filler Pipe Pressure, D_{v2}= 6.4 mm, Q_{inL}= 38 L/min, RVP=74 kPa

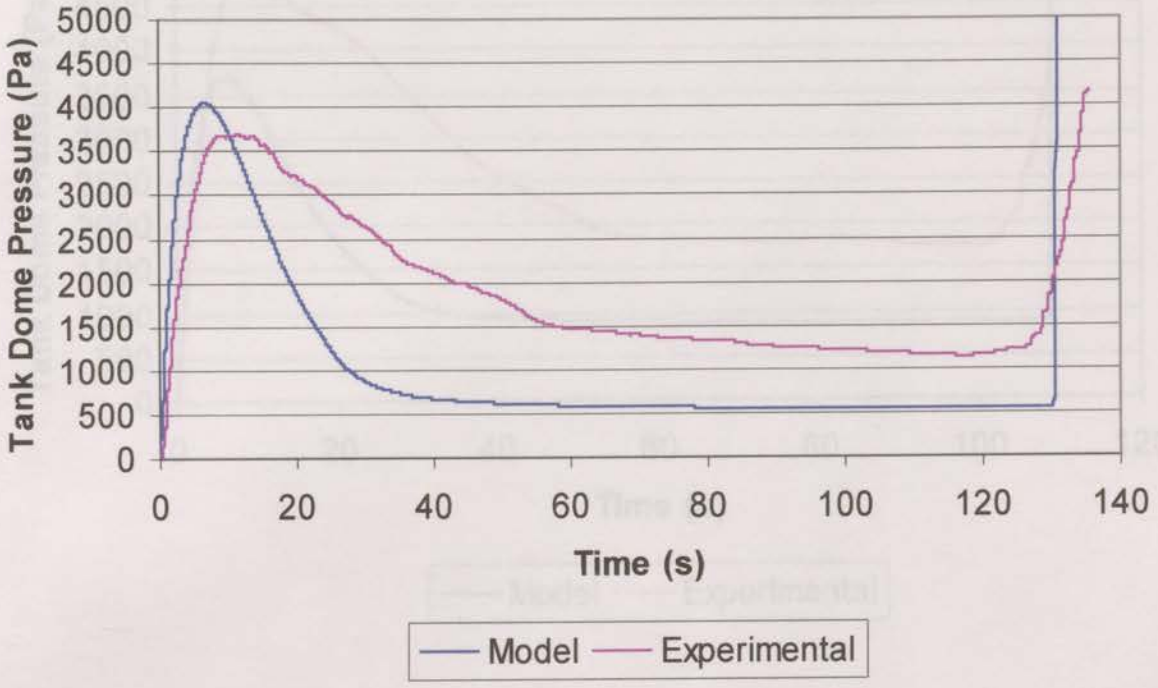

Figure A.41: Tank Dome Pressure, D_{v2}= 6.4 mm, Q_{inL}= 38 L/min, RVP=82 kPa

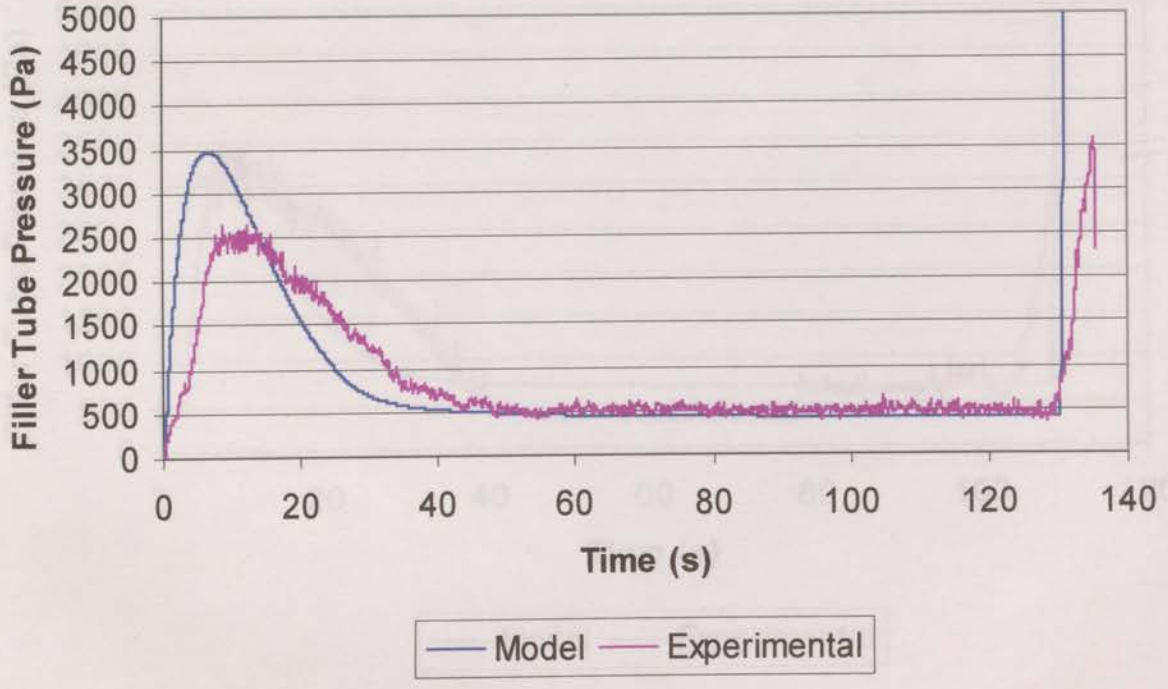

Figure A.42: Filler Pipe Pressure, D_{v2}= 6.4 mm, Q_{inL}= 38 L/min, RVP=82 kPa

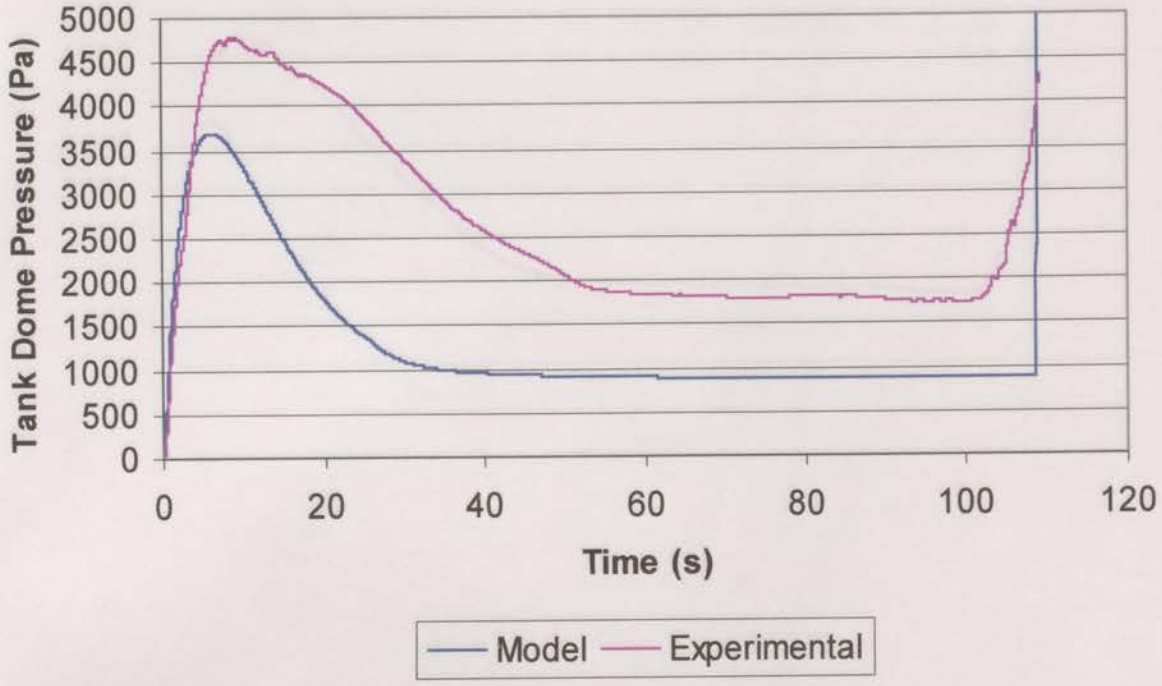

Figure A.43: Tank Dome Pressure: D_{v2}=6.4 mm, Q_{inL}= 45 L/min, RVP=70 kPa

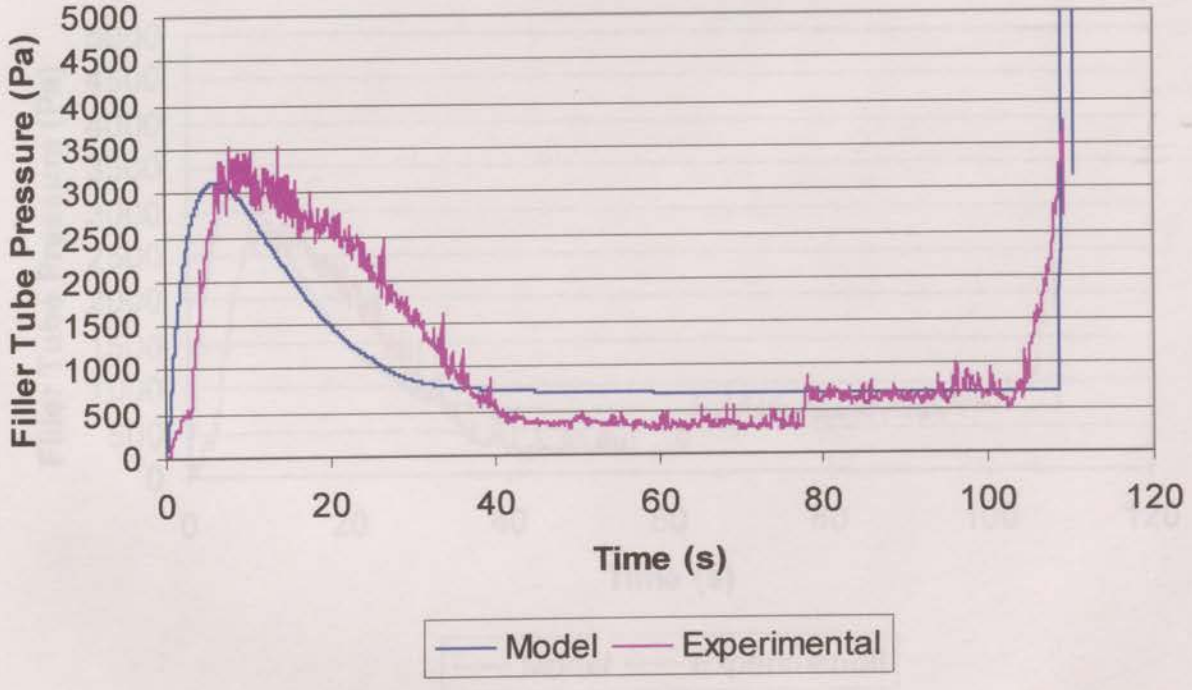

Figure A.44: Filler Pipe Pressure: D_{v2}=6.4 mm, Q_{inL}= 45 L/min, RVP=70 kPa

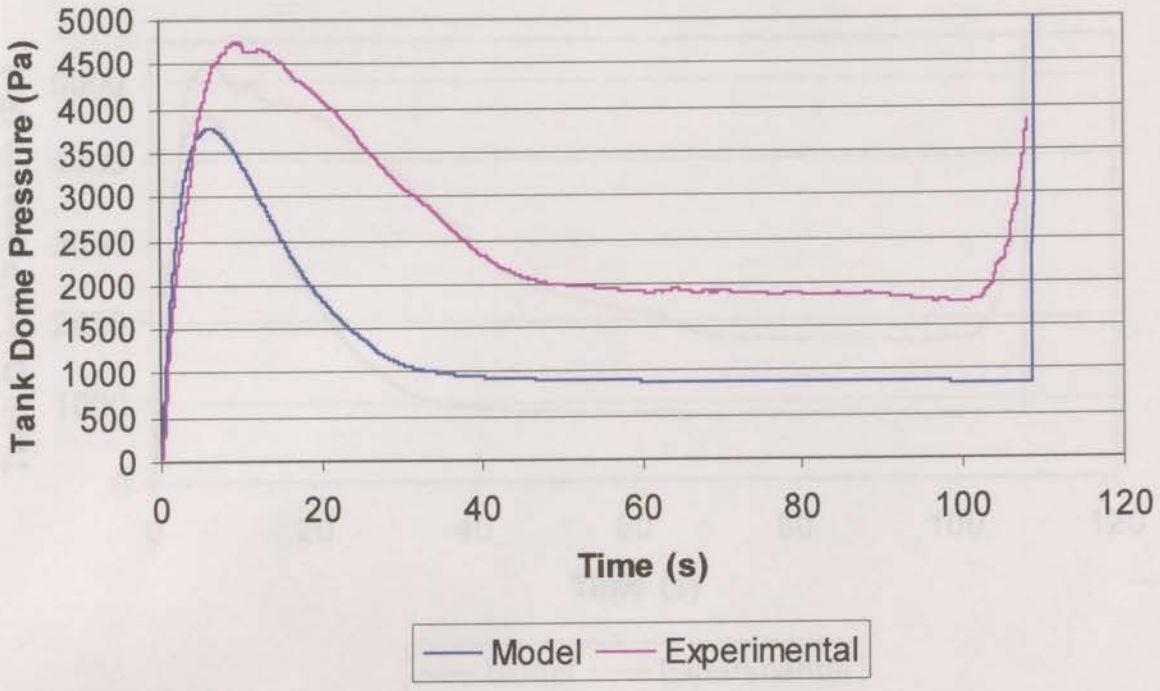

Figure A.45: Tank Dome Pressure: D_{v2}=6.4 mm, Q_{inL}= 45 L/min, RVP=71 kPa

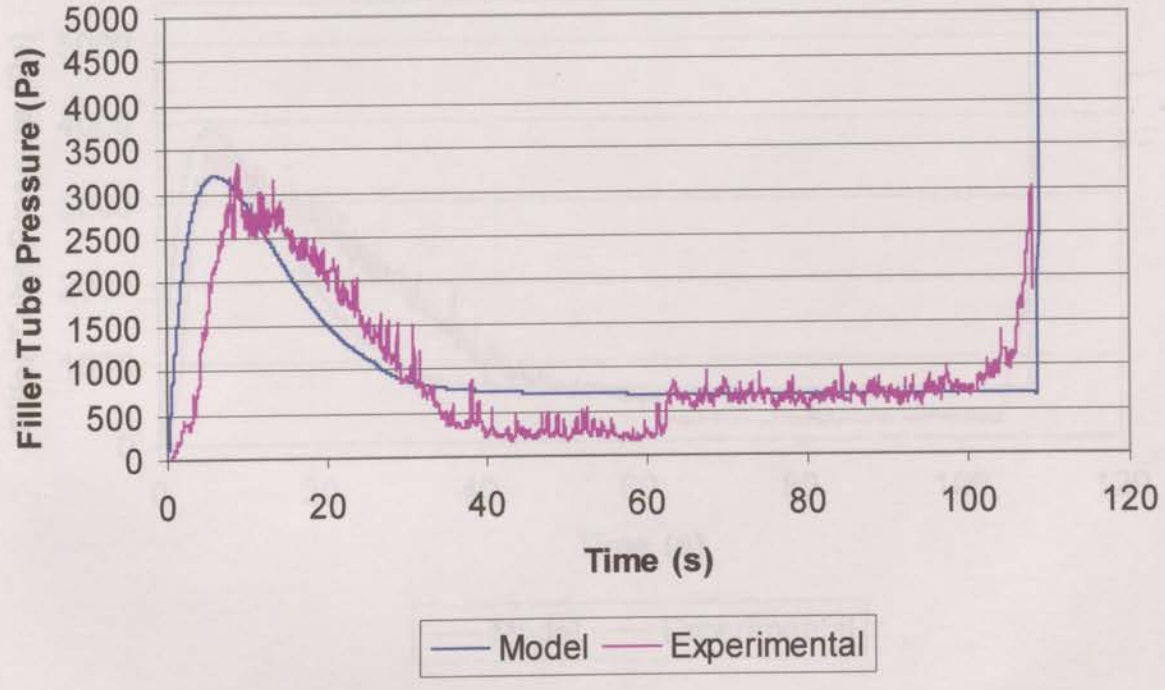

Figure A.46: Filler Pipe Pressure: D_{v2}=6.4 mm, Q_{inL}= 45 L/min, RVP=71 kPa

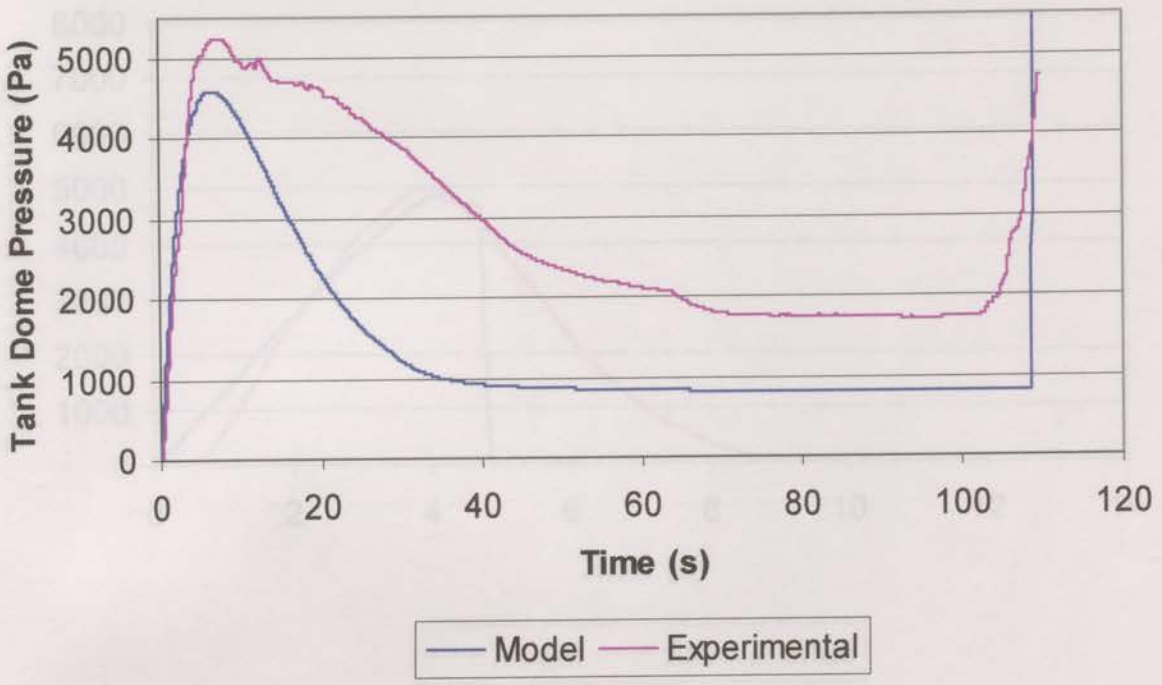

Figure A.47: Tank Dome Pressure: D_{v2}=6.4 mm, Q_{inL}= 45 L/min, RVP=80 kPa

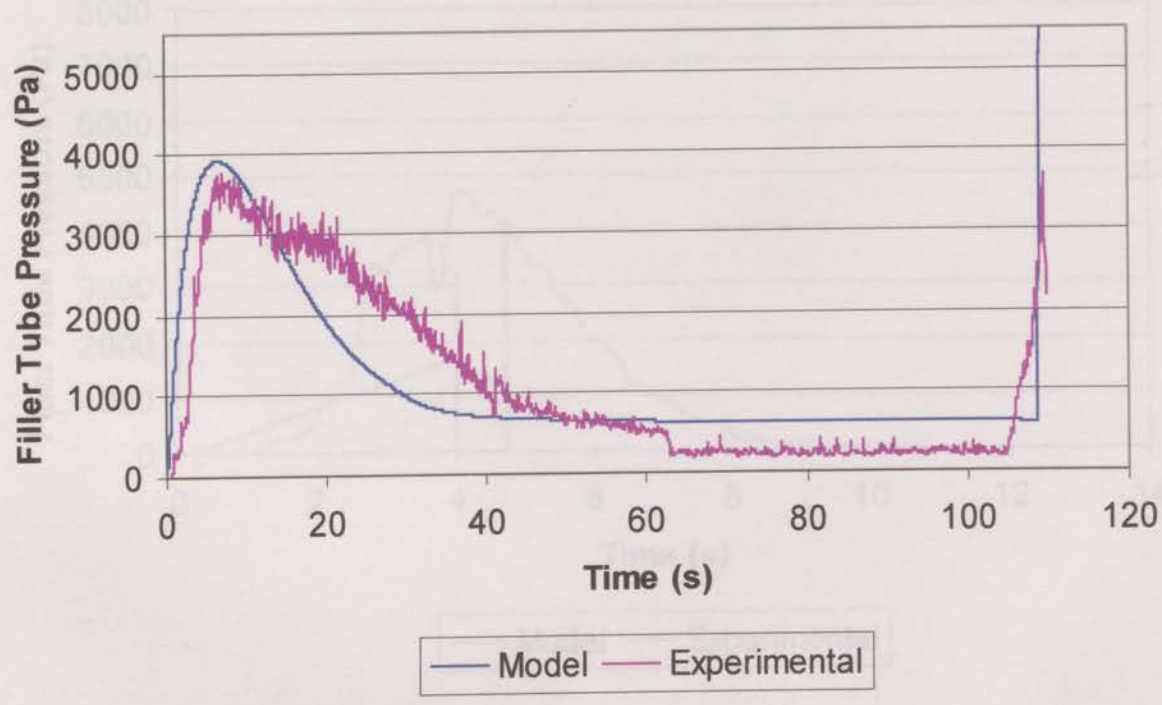

Figure A.48: Filler Pipe Pressure: D_{v2}=6.4 mm, Q_{inL}= 45 L/min, RVP=80 kPa

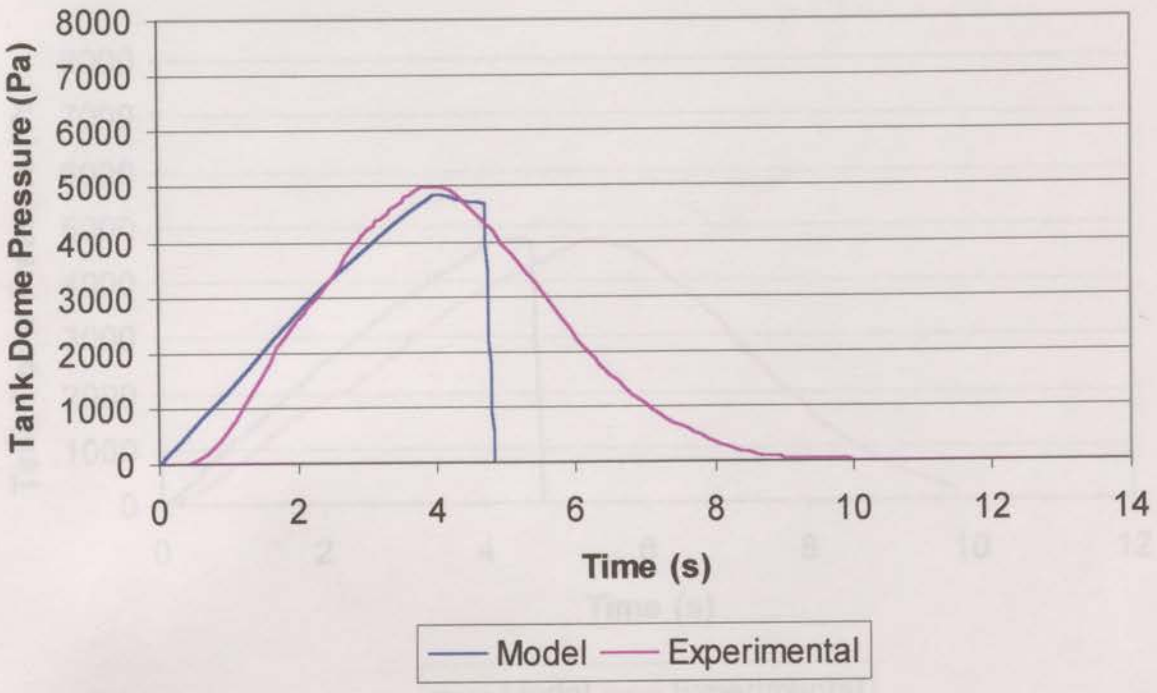

Figure A.49: Tank Dome Pressure: D_{v2}=3.2 mm, Q_{inL}= 38 L/min, RVP=83 kPa

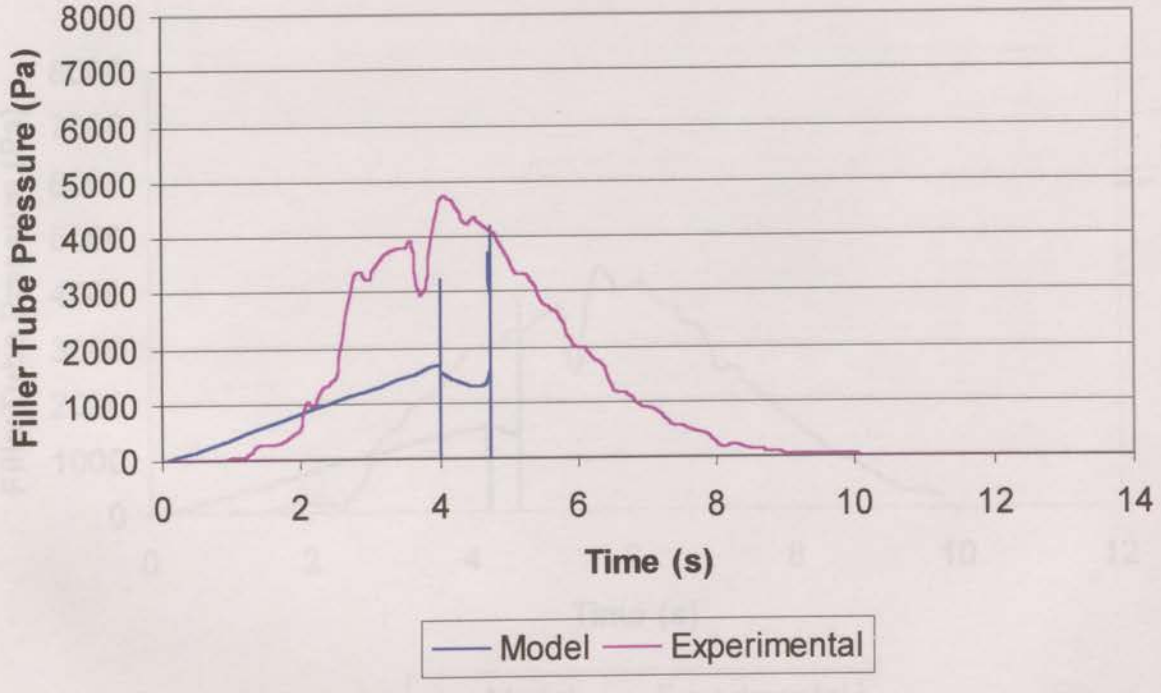

Figure A.50: Filler Pipe Pressure: D_{v2}=3.2 mm, Q_{inL}= 38 L/min, RVP=83 kPa

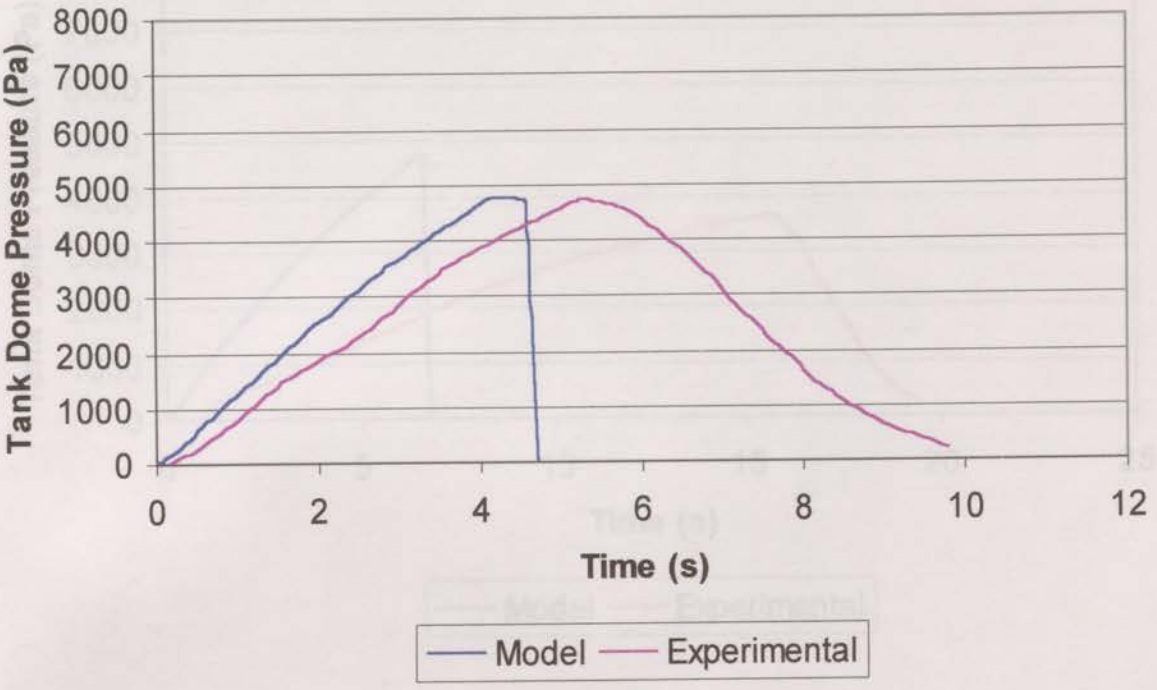

Figure A.51: Tank Dome Pressure: D_{v2}=3.2 mm, Q_{inL}= 38 L/min, RVP=79 kPa

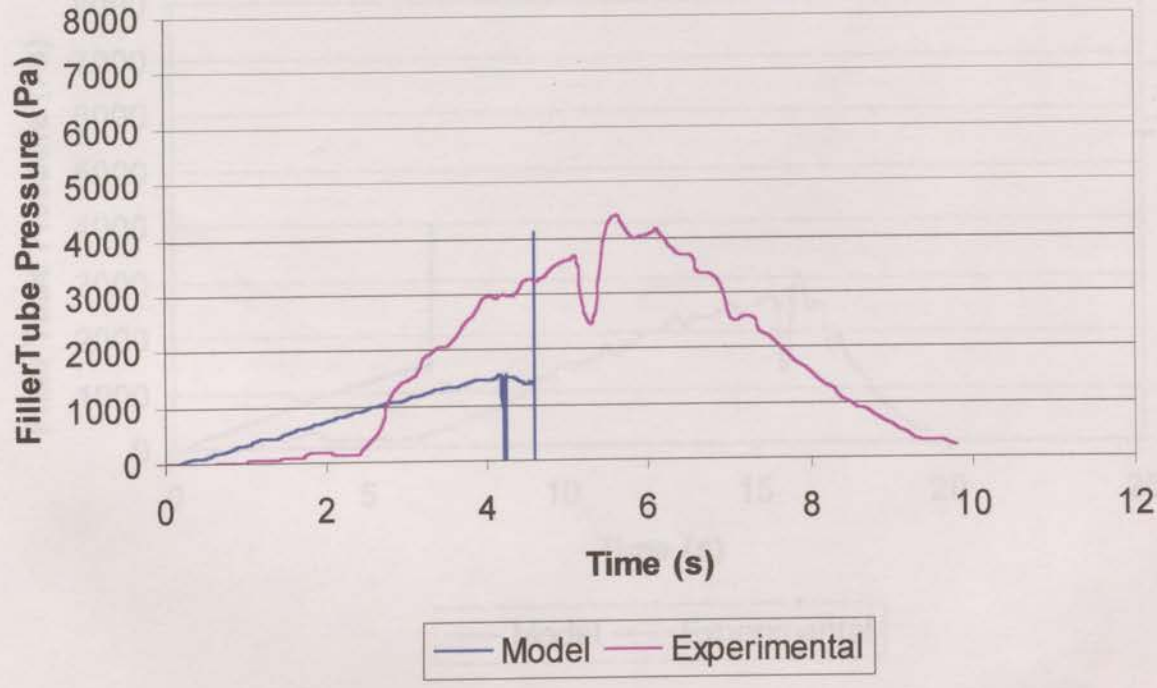

Figure A.52: Filler Pipe Pressure: D_{v2}=3.2 mm, Q_{inL}= 38 L/min, RVP=79 kPa

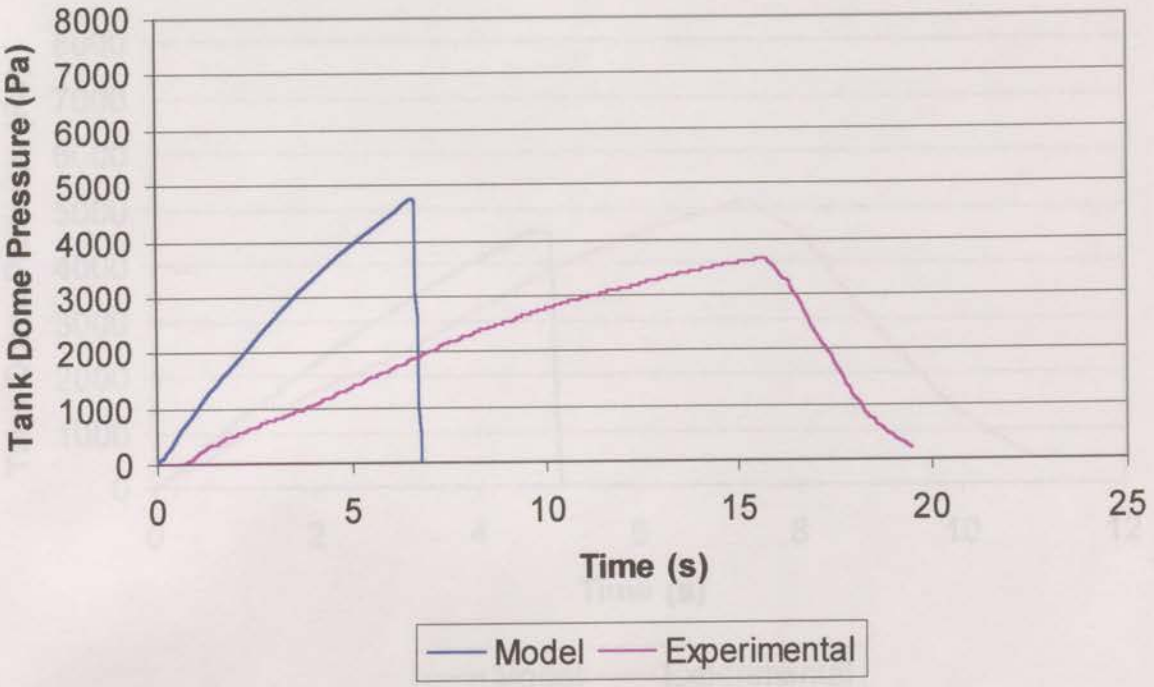

Figure A.53: Tank Dome Pressure: D_{v2}=3.2 mm, Q_{inL}= 38 L/min, RVP=58 kPa

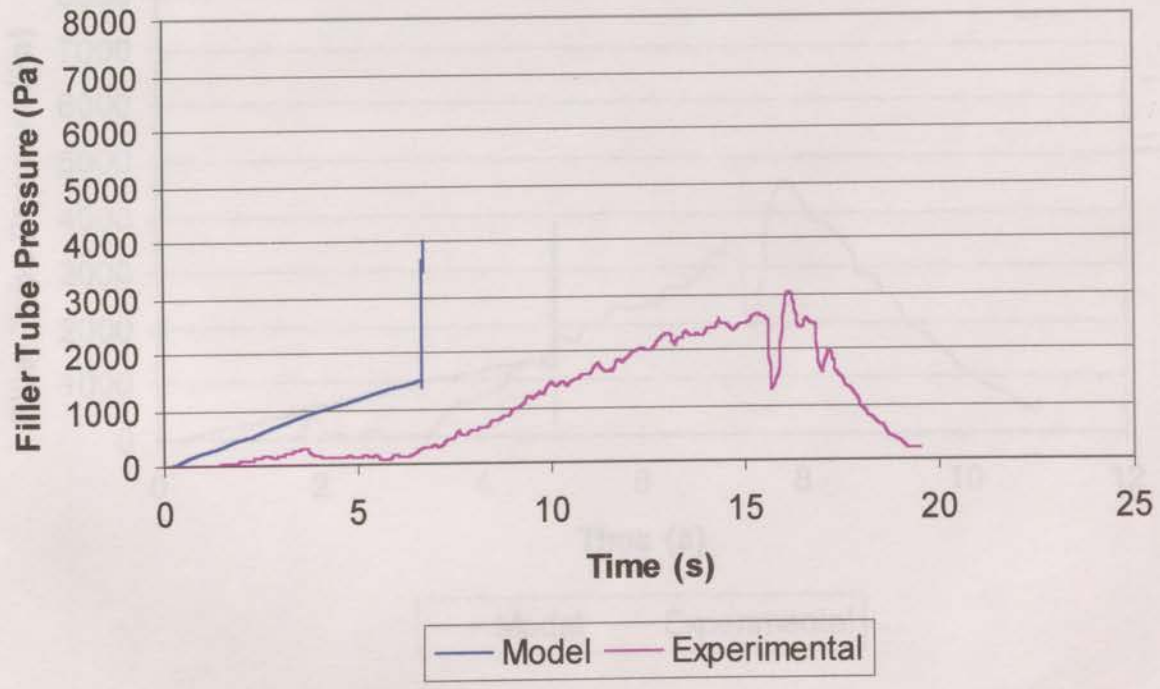

Figure A.54: Filler Pipe Pressure: D_{v2}=3.2 mm, Q_{inL}= 38 L/min, RVP=58 kPa

Figure A.55: Tank Dome Pressure: D_{v2}=3.2 mm, Q_{inL}= 45 L/min, RVP=58 kPa

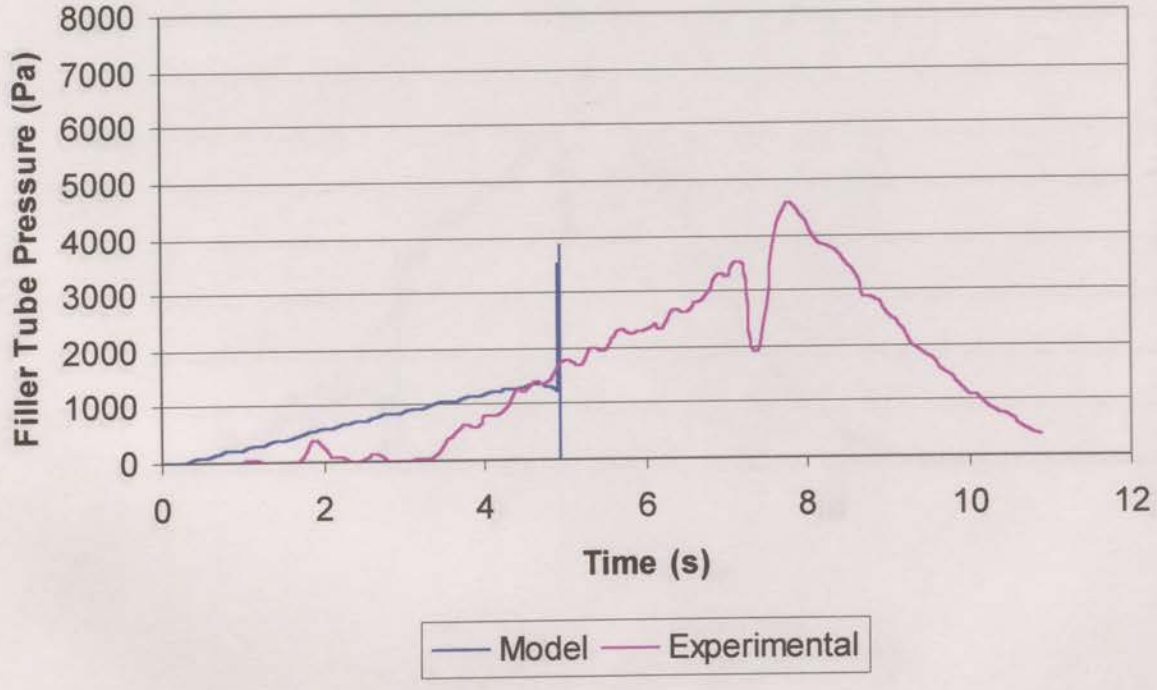

Figure A.56: Filler Pipe Pressure: D_{v2}=3.2 mm, Q_{inL}= 45 L/min, RVP=58 kPa

Figure A.57: Tank Dome Pressure: D_{v2}=3.2 mm, Q_{inL}= 45 L/min, RVP=82 kPa

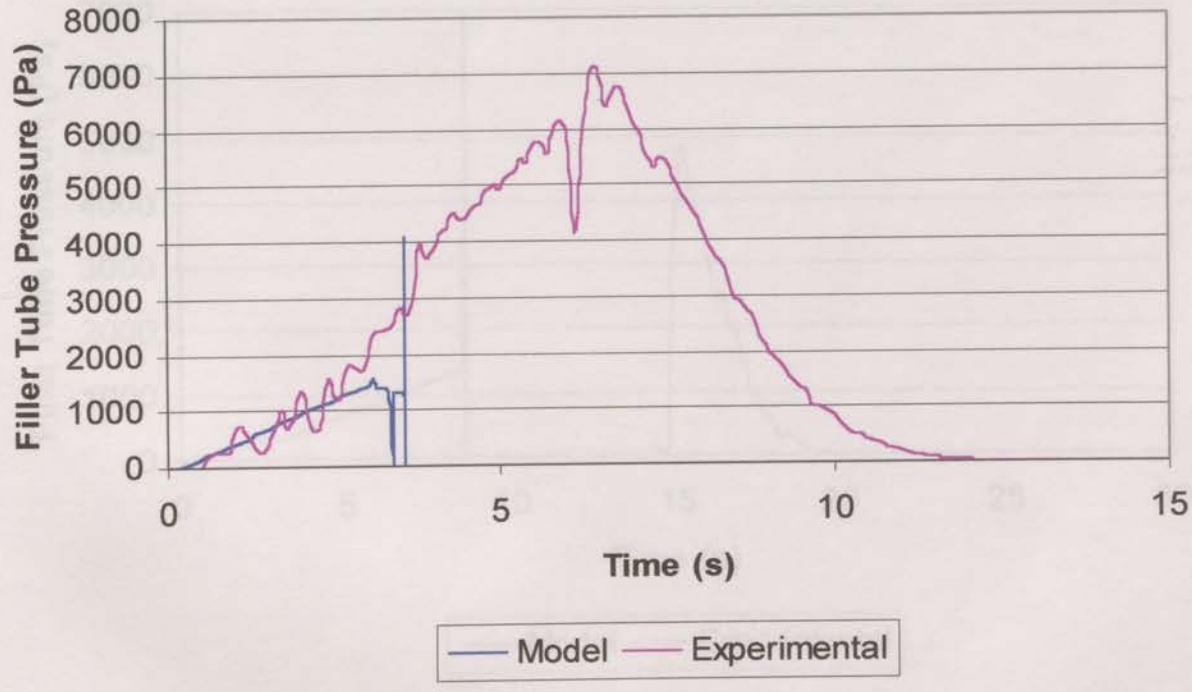

Figure A.58: Filler Pipe Pressure: D_{v2}=3.2 mm, Q_{inL}= 45 L/min, RVP=82 kPa

Figure A.59: Tank Dome Pressure: D_{v2}=3.2 mm, Q_{inL}= 45 L/min, RVP=7 kPa

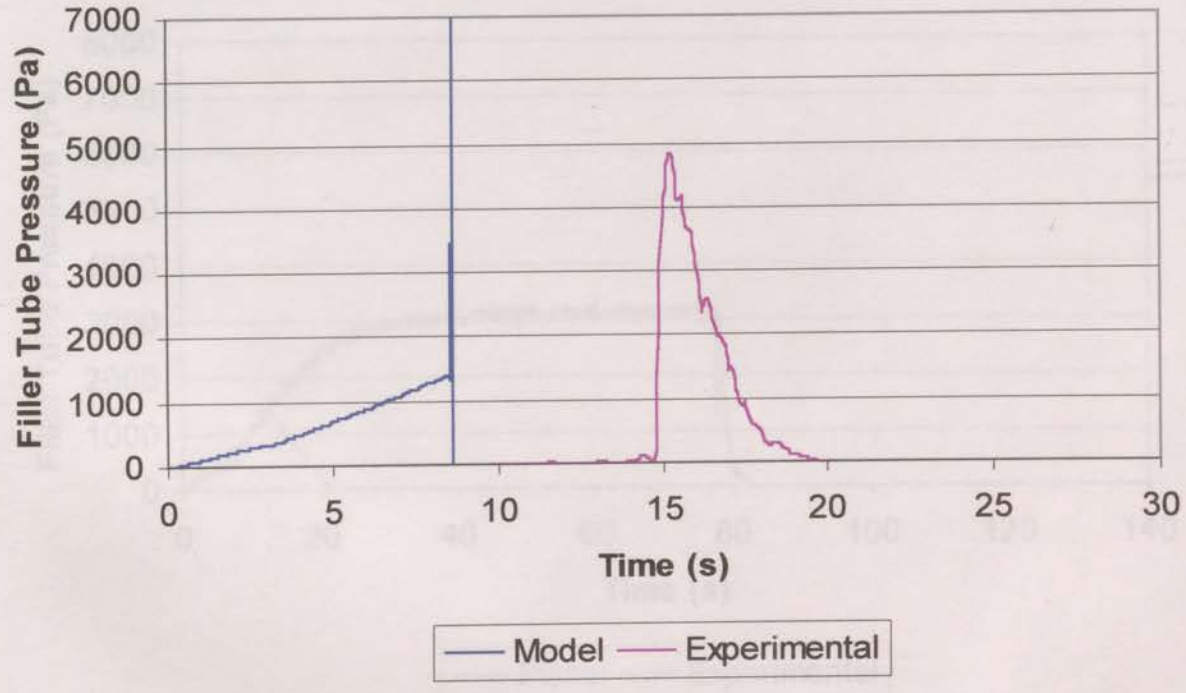

Figure A.60: Filler Tube Pressure: D_{v2}=3.2 mm, Q_{inL}= 45 L/min, RVP=7 kPa

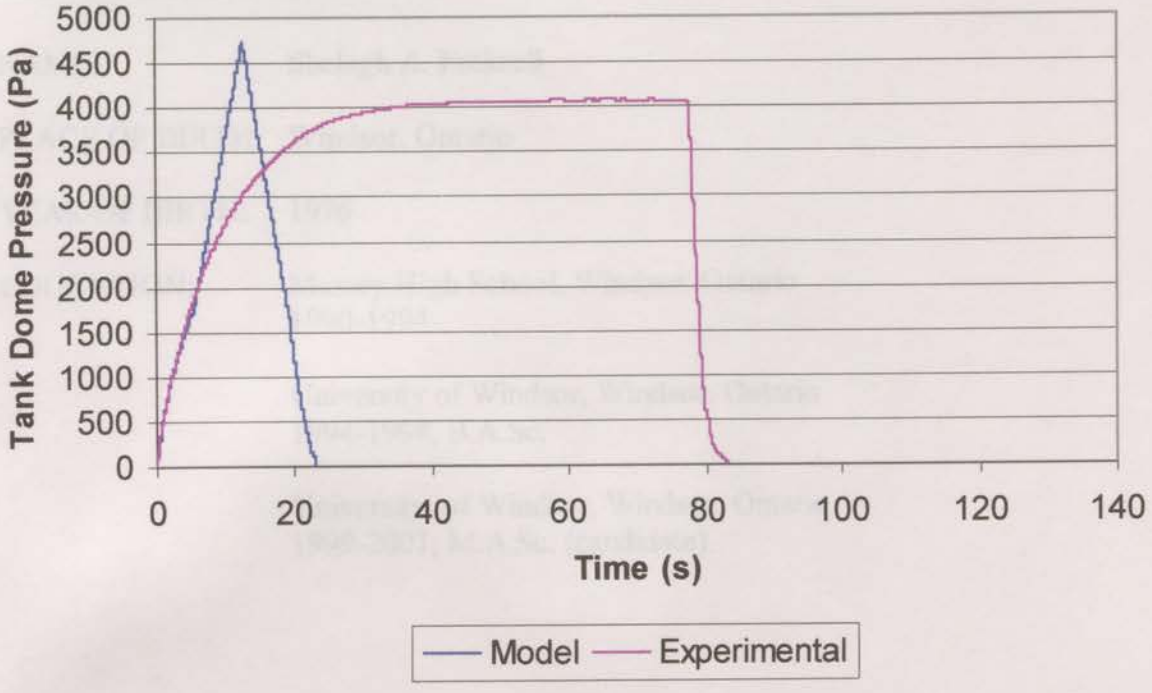

Figure A.61: Tank Dome Pressure: D_{v2}=3.2 mm, Q_{inL}= 38 L/min, RVP=7 kPa

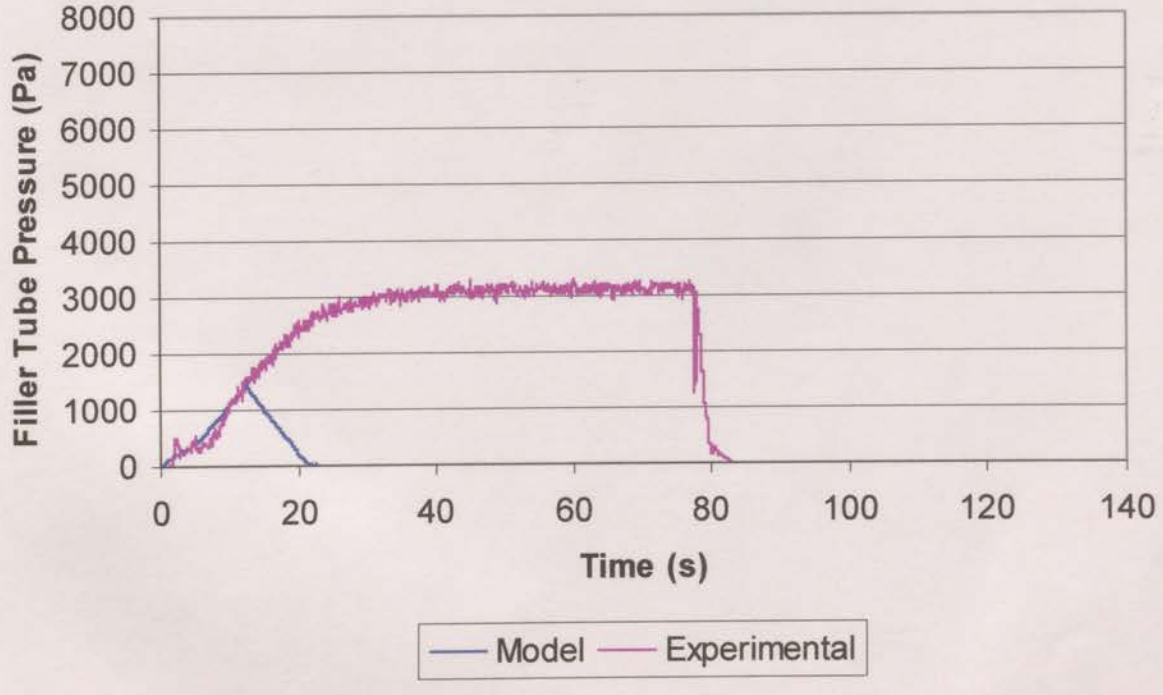

Figure A.62: Filler Tube Pressure: D_{v2}=3.2 mm, Q_{inL}= 38 L/min, RVP=7 kPa

VITA AUCTORIS

NAME: Shelagh A. Fackrell

PLACE OF BIRTH: Windsor, Ontario

YEAR OF BIRTH: 1976

EDUCATION: Massey High School, Windsor, Ontario
1990-1994

University of Windsor, Windsor, Ontario
1994-1998, B.A.Sc.

University of Windsor, Windsor, Ontario
1999-2001, M.A.Sc. (candidate)